UNIVERSITY OF CALIFORNIA

Los Angeles

Understanding the impact of deleterious genetic variation on extinction risk in small populations

A dissertation submitted in partial satisfaction of the

requirements for the degree Doctor of Philosophy

in Biology

by

Christopher C. Kyriazis

2022

ABSTRACT OF THE DISSERTATION

Understanding the impact of deleterious genetic variation on extinction risk in small populations

by

Christopher C. Kyriazis

Doctor of Philosophy in Biology

University of California, Los Angeles, 2022

Professor Kirk Edward Lohmueller, Co-Chair

Professor Robert Wayne, Co-Chair

Deleterious genetic variation is abundant in wild populations and can contribute to extinction when populations become small and isolated. For example, elevated levels of inbreeding in small populations can expose recessive deleterious mutations as homozygous and depress population fitness. Additionally, increased genetic drift in small populations can result in relaxed selection against weakly deleterious mutations, leading to an accumulation of such mutations that can also contribute to fitness declines. Genomic sequencing tools have enabled a proliferation of studies on the threat of deleterious genetic variation in small populations of conservation concern. However, how to best leverage such data to predict extinction risk in these populations remains unclear. My dissertation aims to provide clarity to this issue by leveraging computational genetic simulations in concert with genomic data to better understand the threat that deleterious genetic variation poses to extinction risk. In my first chapter, I used eco-evolutionary simulations to explore the effects of deleterious genetic variation on extinction risk under a variety of

demographic scenarios. These results implicate recessive strongly deleterious mutations as the key drivers of extinction in small populations, as the exposure of such mutations via inbreeding can lead to extinction much faster than the more gradual impacts of weakly deleterious variation. In my second chapter, I applied a similar simulation framework to explore the threat of deleterious genetic variation to extinction risk in the critically endangered vaquita porpoise. My results suggest that the species is genetically well-equipped to recover from a severe bottleneck due to its small historical population size, which implies a low load of recessive strongly deleterious variation that can contribute to future inbreeding depression. In my third chapter, I examined the genomic factors enabling persistence in an isolated population of moose on Isle Royale. My results suggest a role for 'purging' of recessive deleterious mutations during a severe founder event for the population as a key factor resulting in the continued health of the population. Finally, in my fourth chapter, I reviewed simulation-based approaches for quantifying genetic load and predicting extinction risk. Here, I aim to encourage other researchers to also employ simulations in studies of deleterious variation in small populations, providing an overview of the components of a simulation of deleterious genetic variation and the relevant model parameters. Altogether, this dissertation provides novel perspectives and approaches for understanding the risks of extinction due to deleterious genetic variation in wild populations.

The dissertation of Christopher C. Kyriazis is approved.

Howard Bradley Shaffer

Nandita Garud

Kirk Edward Lohmueller, Committee Co-Chair

Robert Wayne, Committee Co-Chair

University of California, Los Angeles

2022

To my family, for their love and support.

Table of Contents

List of Figures

List of Tables

Supplementary Materials

Chapter 3: Genomic underpinnings of population persistence in Isle Royale moose

Chapter3_Supplementary_Information.pdf (File Format .pdf)

Chapter 4: Using computational simulations to quantify genetic load and predict extinction risk

Chapter4_Supplementary_Information.pdf (File Format .pdf)

Acknowledgements

I have so many people to thank for helping me complete this dissertation, it's hard to know where to begin. First and foremost, thank you to my advisors, Kirk Lohmueller and Bob Wayne. Bob, thank you for welcoming me into your lab, challenging me to think big, and supporting my growth as a researcher. I am so very grateful for the broad perspective you provide on science and feel incredibly thankful to have been able to work with you. Kirk, thank you for your never-ending enthusiasm and support, for helping me grow as a scientist in ways I could have never expected, and for your caring guidance through the rollercoaster ride that is a PhD. It's no understatement to say that my PhD would not have been possible without you, and I can't overstate just how big of an influence you have had on my scientific trajectory. Thanks also to my committee members, Nandita Garud and Brad Shaffer, for providing encouragement and valuable insight on my dissertation. Nandita, it's been a joy to see your lab grow since you arrived at UCLA, and I am ever grateful for your feedback and advice. Brad, the seminar course you taught on genetic rescue during my first year was one of the major early influences on my PhD trajectory, and I am very grateful for the discussions we have had on that topic both then and ever since.

I feel deeply grateful to have been surrounded by so many wonderful friends and colleagues during my time at UCLA. First, thanks to members of the Wayne and Lohmueller labs past and present for providing a wonderful environment to do research and many great friendships. Thanks in particular to Bernard Kim and Jacqueline Robinson for being amazing mentors and backpacking buddies, and to Jazlyn, Arun, Jesse, Annabel, Jun, Tina, and Gustavo for being incredible lab mates and friends. I so deeply cherish (and miss) the time we spent at R bar and our many record nights. Thanks also to Meixi, Gabby, Joey, Ana, Daniel, and Miroslava

for being supportive through challenging times and for our many great hikes together. Finally, I am so extremely grateful to my wonderful cohort mates, Mary, Marvin, Ioana, and Ben. Your friendship has been a rock for me throughout the PhD; I can't imagine having done these past five years without you all.

Lastly, I want to express my deep gratitude for my family for their endless love, support, and encouragement during my PhD. Mom and Dad, thank you so much for supporting me on this journey and always taking a sincere interest in my many projects. I know how much education means in our family – from Yiayia wanting so dearly to be able to attend school as a child, to grandpa attending college after retirement. Completing this PhD is as much for them (and you both) as it is for me, and it makes me sad they aren't around to see the fruits of their hard labor. To Will and Mia, thanks for being the best siblings one could ask for and for contributing to a household where we were all able to follow our passions. It's been a joy to grow into our divergent career paths together and support each other along the way.

Chapter 1 is a version of a manuscript that was originally published in *Evolution Letters* ©2021 by John Wiley & Sons, Inc:

Kyriazis, Christopher C., Robert K. Wayne, and Kirk E. Lohmueller. "Strongly deleterious mutations are a primary determinant of extinction risk due to inbreeding depression." *Evolution Letters* 5 (1). https://doi.org/10.1002/evl3.209. Reprinted with permission from *Evolution Letters*.

Acknowledgements. We are grateful to Jacqueline Robinson, Bernard Kim, Brad Shaffer, and members of the Lohmueller and Wayne labs for helpful feedback and ideas. We thank Ben Haller for assistance with SLiM. This research was supported by NIH grant R35GM119856 (to K.E.L.).

Author Contributions. C.C.K. and K.E.L. conceived the project, C.C.K. ran the simulations and analyzed the results, all authors contributed to writing and editing the manuscript.

Chapter 2 is a version of a manuscript that was originally published in *Science* ©2022 by the American Association for the Advancement of Science. Reprinted with permission from the American Association for the Advancement of Science.

Robinson*, Jacqueline A., Christopher C. Kyriazis*, Sergio F. Nigenda-Morales, Annabel C. Beichman, Lorenzo Rojas-Bracho, Kelly M. Robertson, Michael C. Fontaine, Robert K. Wayne, Kirk E. Lohmueller, Barbara L. Taylor, and Phillip A. Morin. 2022. "The critically endangered vaquita is not doomed to extinction by inbreeding depression" *Science* 376 (6593). DOI: 10.1126/science.abm1742 (*: contributed equally)

Acknowledgments. We thank the CanSeq150 project for use of the long-finned pilot whale and Pacific white-sided dolphin genomes. Y. Bukhman generously provided early access to the blue whale genome. We thank J. Mah, P. Nuñez, and M. Lin for providing scripts, and B. Haller for assistance with simulations. We thank the Southwest Fisheries Science Center's Marine Mammal and Sea Turtle Research Collection for use of archival vaquita tissue samples. All samples were imported to the US under appropriate CITES and US Marine Mammal Protection Act permits.

Funding. We thank Frances Gulland, The Marine Mammal Center, and NOAA Fisheries for funding genome resequencing. C.C.K. and K.E.L. were supported by National Institutes of Health (NIH) grant R35GM119856 (to K.E.L.). A.C.B. was supported by the Biological Mechanisms of Healthy Aging Training Program NIH T32AG066574. S.N.M. was supported by the Mexican National Council for Science and Technology (CONACYT) Postdoctoral

Fellowship 724094 and the Mexican Secretariat of Agriculture and Rural Development Postdoctoral Fellowship.

Author contributions. P.A.M., B.L.T., K.E.L., J.A.R., and C.C.K. designed the study. P.A.M., M.C.F., L.R.B. and B.L.T obtained funding. P.A.M., B.L.T., and L.R.B. obtained samples. K.M.R. performed DNA extractions and library preparations. A.C.B., S.F.N.M, J.A.R., and C.C.K. performed analyses. J.A.R. and C.C.K. wrote the manuscript with input from all authors. P.A.M., B.L.T., K.E.L., and R.K.W. supervised the work.

Chapter 3 is a version of a manuscript in revision at *Molecular Biology and Evolution*.

Kyriazis, Christopher C., Annabel C. Beichman, Kristin E. Brzeski, Sarah R. Hoy, Rolf O. Peterson, John A. Vucetich, Leah M. Vucetich, Kirk E. Lohmueller, Robert K. Wayne. 2022. "Genomic underpinnings of population persistence in Isle Royale moose." Preprint: https://doi.org/10.1101/2022.04.15.488504

Acknowledgments. We are grateful to members of the Wayne and Lohmueller labs for helpful input on this work. We thank Michelle Carstensen and the Minnesota Department of Natural Resources for providing tissue samples used in this study. C.C.K. and K.E.L. were supported by National Institutes of Health grant (R35GM119856 to K.E.L.). A.C.B was supported by the National Institutes of Health Biological Mechanisms of Healthy Aging Training Program (T32AG066574). This work was supported by the National Science Foundation (DEB Small Grant #1556705).

Author contributions. C.C.K., R.K.W., and K.E.L. conceived the study. K.E.B., J.A.V., L.M.V., S.R.H. and R.O.P. acquired samples. C.C.K. conducted all analyses with input from A.C.B. and K.E.L. and wrote the manuscript with input from all authors. R.K.W. and K.E.L. jointly supervised this work.

Chapter 4 is a version of a manuscript in preparation for submission to *PNAS.*

Kyriazis, Christopher C., Jacqueline A. Robinson, and Kirk E. Lohmueller. "Using computational simulations to quantify genetic load and predict extinction risk". Preprint: https://doi.org/10.1101/2022.08.12.503792

Acknowledgements. We are grateful to Phil Morin, Annabel Beichman, Robert Wayne, Stella Yuan, and Meixi Lin for comments on the manuscript. C.C.K. and K.E.L. were supported by National Institutes of Health grant (R35GM119856 to K.E.L.).

Author Contributions. C.C.K., J.A.R., and K.E.L. conceived the study. C.C.K. conducted the analyses and wrote the manuscript with input from all authors.

VITA

Christopher C. Kyriazis

EDUCATION:

Bachelor of Science in Biological Sciences, University of Chicago, 2015

PUBLICATIONS:

*denotes co-first authorship
^denotes mentored undergraduate

Preprints and Submitted Manuscripts

11. Wade, EE*^, Kyriazis, CC*, Cavassim, MIA* & KE Lohmueller. Quantifying the fraction of new mutations that are recessive lethal. Preprint: https://doi.org/10.1101/2022.04.22.489225
10. Kyriazis, CC, Beichman, AB, Brzeski, KE, Hoy, SR, Peterson, RO, Vucetch, JA, Vucetch, LM, Lohmueller, KE & RK Wayne. Genomic underpinnings of population persistence in Isle Royale moose. In revision at *Molecular Biology and Evolution.* Preprint: https://doi.org/10.1101/2022.04.15.488504
9. Nigenda-Morales, SF*, Lin, M*, Nuñez-Valencia, PG, Kyriazis, CC, Beichman, AC, Robinson, JA, … Lohmueller, KE, Moreno-Estrada, A, & RK Wayne. 2021. The genomic footprint of whaling and isolation in fin whale populations. In revision at *Nature Communications.*

Published

8. Exposito-Alonso, M, Booker, TA, Czech, L, Fukami, T, Gillespie, L, Hateley, S, Kyriazis, CC, … & E Zess. 2021. Genetic diversity loss in the Anthropocene. *Science*, in press. Preprint: https://doi.org/10.1101/2021.10.13.464000
7. Robinson, JA*, Kyriazis, CC*, Nigenda-Morales, SF, Beichman, AB, Rojas-Bracho, L, Fontaine, M, Robertson, KM, Wayne, RK, Lohmueller, KE, Taylor, BL, & PA Morin, 2022. The critically endangered vaquita is not doomed to extinction by inbreeding depression. *Science*, 639, 635-639.
6. Beichman, AC, Kalhori, P, Kyriazis, CC, DeVries, AA, Nigenda-Morales, S, Koepfli, K, Heckel, G, Schramm, Y, Moreno-Estrada, A, Kennett, DJ, Hylkema, M, Bodkin, J, Lohmueller, KE, & RK Wayne, 2022. Genomic analyses reveal range-wide devastation of sea otter populations. *Molecular Ecology*, in press.
5. Kyriazis, CC, Wayne, RK, & KE Lohmueller, 2021. Strongly deleterious mutations are a primary determinant of extinction risk due to inbreeding depression. *Evolution Letters*, 5, 33-47.
4. Adrion, JR*, Cole, CB*, Dukler, ND*, Galloway, JG*, Gladstein, AL*, Gower, G*, Kyriazis, CC*, Ragsdale, AR*, Tsambos, G*…(17 other co-authors)… Kelleher, J, & AD Kern, 2020. A community-maintained standard library of population genetic models. *eLife,* 9:e54967.

3. Heaney, LR*, Kyriazis, CC*, Balete, DS, Rickart, EA & SJ Steppan, 2018. How small an island? Speciation by endemic mammals on an oceanic Philippine island. *Journal of Biogeography*, 45, 1675-1687.
2. Kyriazis, CC, Alam, B, Wjodyla, M, Hosner, PA, Hackett, SJ, Mays Jr., HL., Heaney, LR & S Reddy, 2018. Colonization and diversification of the White-browed Shortwing in the Philippines. *Molecular Phylogenetics and Evolution,* 121, 121-131.
1. Kyriazis, CC, Bates, JM & LR Heaney, 2017. Dynamics of genetic and morphological diversification in an incipient intra-island radiation of Philippine rodents (Muridae: *Bullimus*). *Journal of Biogeography*, 44, 2585-2594.

SELECTED PRESENTATIONS:

Aug. 2022	Conference talk, Society of Marine Mammalogy
July 2022	Conference talk, SMBE Graduate Student Excellence Symposium
June 2022	Department Seminar, UCLA Department of Ecology and Evolutionary Biology
July 2021	Invited seminar (via Zoom), Exposito-Alonso lab, Carnegie Department of Plant Biology, Stanford University.
June 2021	Conference talk, Virtual Evolution 2021
Nov. 2019	Invited seminar, Stanford University Center for Evolutionary and Human Genetics. Palo Alto, CA.
June 2019	Conference talk, SSE Hamilton Award Competition. Evolution Meetings, Providence, RI.
Aug. 2017	Conference talk, American Ornithological Society Meeting. East Lansing, MI.
June 2016	Conference talk, American Society of Mammalogists Meeting. Minneapolis, MN.

SELECTED AWARDS AND HONORS:

July 2022	SMBE Graduate Student Excellence Award Finalist ($500)
June 2022	UCLA EEB Scherbaum Research Award ($200)
July 2021	UCLA Graduate Research Grant ($1,000)
June 2020	UCLA Graduate Research Grant ($1,500)
June 2020	Young Investigator Award, Society for Molecular Biology and Evolution (conference cancelled due to COVID-19)
June 2019	UCLA Graduate Research Grant ($2,000)
June 2019	Hamilton Award Finalist, Society for the Study of Evolution ($500)
May 2018	UCLA Graduate Research Grant ($1,100)
2017-2019	UCLA Dean's Scholar ($14,500)
Summer 2014	Field Museum NSF REU Summer Research Grant ($7,500)
2011-2015	Dean's List, University of Chicago

Chapter 1: Strongly deleterious mutations are a primary determinant of extinction risk due to inbreeding depression

Originally published in *Evolution Letters*

Supplementary materials available online from *Evolution Letters*:

https://onlinelibrary.wiley.com/doi/full/10.1002/evl3.209

Abstract

Human-driven habitat fragmentation and loss have led to a proliferation of small and isolated plant and animal populations with high risk of extinction. One of the main threats to extinction in these populations is inbreeding depression, which is primarily caused by recessive deleterious mutations becoming homozygous due to inbreeding. The typical approach for managing these populations is to maintain high genetic diversity, increasingly by translocating individuals from large populations to initiate a 'genetic rescue.' However, the limitations of this approach have recently been highlighted by the demise of the gray wolf population on Isle Royale, which declined to the brink of extinction soon after the arrival of a migrant from the large mainland wolf population. Here, we use a novel population genetic simulation framework to investigate the role of genetic diversity, deleterious variation, and demographic history in mediating extinction risk due to inbreeding depression in small populations. We show that, under realistic models of dominance, large populations harbor high levels of recessive strongly deleterious variation due to these mutations being hidden from selection in the heterozygous state. As a result, when large populations contract, they experience a substantially elevated risk of extinction after these strongly deleterious mutations are exposed by inbreeding. Moreover, we demonstrate that, although genetic rescue is broadly effective as a means to reduce extinction risk, its effectiveness can be greatly increased by drawing migrants from small or moderate-sized

source populations rather than large source populations due smaller populations harboring lower levels of recessive strongly deleterious variation. Our findings challenge the traditional conservation paradigm that focuses on maximizing genetic diversity in small populations in favor of a view that emphasizes minimizing strongly deleterious variation. These insights have important implications for managing small and isolated populations in the increasingly fragmented landscape of the Anthropocene.

Introduction

The prevailing paradigm in conservation biology prioritizes the maintenance of high genetic diversity in small populations threatened with extinction due to inbreeding depression (Caughley 1994; Spielman et al. 2004). Under this paradigm, genetic diversity is considered one of the primary determinants of fitness (Allendorf and Leary 1986; Reed and Frankham 2003), and the harmful effects of inbreeding are thought to be minimized by maintaining genetic diversity. However, this thinking is challenged by the observation that some species, such as the Channel island fox, can persist at small population size with extremely low genetic diversity and show no signs of inbreeding depression (Robinson et al. 2016; Robinson et al. 2018). This example and other similar studies suggest that, rather than being mediated by high genetic diversity, the persistence of small populations may instead be enabled by the purging of strongly deleterious mutations (Laws and Jamieson 2011; Xue et al. 2015; Hedrick and Garcia-Dorado 2016; Robinson et al. 2016; Robinson et al. 2018; Van Der Valk et al. 2019; Grossen et al. 2020). In this study, we investigate how genetic diversity, deleterious variation, and demographic history influence extinction risk due to inbreeding depression using ecologically-realistic population genetic simulations. Our results demonstrate the central role of strongly deleterious variation in determining extinction risk due to inbreeding depression in small and isolated populations, and highlight the counterintuitive effects of strategies aimed at maintaining high genetic diversity. We argue that, in cases where populations are destined to remain small and isolated with high levels of inbreeding, management strategies should aim to minimize strongly deleterious variation rather than maximize genetic diversity.

The motivating example for our simulations is the gray wolf population on Isle Royale, an island in Lake Superior that has long served as a natural laboratory in ecology and conservation biology (Mech 1966; Peterson et al. 1984; Wayne et al. 1991; McLaren and Peterson 1994). Following 70 years of near-complete isolation at a size of ~10-50 individuals, the population was driven to the brink of extinction by severe inbreeding depression, with just two individuals remaining in 2018 (Hedrick et al. 2019; Robinson et al. 2019). Recent findings have suggested that the collapse of the population may have been prompted by the introduction of high levels of recessive strongly deleterious variation by a migrant individual who arrived from the mainland in 1997 (Adams et al. 2011; Hedrick et al. 2014; Hedrick et al. 2019; Robinson et al. 2019). The high reproductive output of this individual on the island (34 offspring) led to intensive subsequent inbreeding in the population, driving these strongly deleterious mutations to high frequency and leading to severe inbreeding depression and ultimately the collapse of the population.

The example of the Isle Royale wolf population, though extreme, highlighted the potentially negative effects of founding or rescuing small populations with individuals from large and genetically-diverse populations. An alternative approach for genetic rescue or reintroduction initiatives could instead target historically-smaller populations where strongly deleterious mutations have been purged, or screen populations for individuals with low levels of strongly deleterious variation. The growing evidence for purging in wild populations (e.g., Xue et al. 2015; Robinson et al. 2018; Grossen et al. 2020) suggests that this approach may be effective as a means to decrease the severity of inbreeding depression in small populations at high risk of extinction. Given the ongoing reintroduction of wolves to Isle Royale, and the increasing

necessity of reintroduction and genetic rescue more broadly (Whiteley et al. 2015; Frankham et al. 2017; Bell et al. 2019), such an approach could have wide-ranging implications for the conservation of small populations at risk.

The applicability of population genetic models to understanding extinction has historically been limited by unrealistic assumptions that often ignore stochastic ecological factors and rarely consider both weakly and strongly deleterious mutations (Lande 1994; Lynch et al. 1995; O'Grady et al. 2006; Caballero et al. 2017). Here, we use a novel population genetic simulation framework that combines realistic models of population dynamics with exome-scale genetic variation (Haller and Messer 2019) to assess how genetic diversity, deleterious variation, and demographic history influence extinction risk in small populations. Our simulations aim to capture the ecological factors that may contribute to extinction in small populations, such as those observed in the Isle Royale wolf population, by incorporating the effects of demographic and environmental stochasticity, as well as natural catastrophes. Coupled with these stochastic population dynamics, we model a genome with parameters reflecting that of a canine exome, which accumulates neutral and deleterious mutations from an empirically-estimated distribution of fitness effects (Kim et al. 2017). Although our model is motivated by the Isle Royale wolf population, it is also intended to capture the dynamics of many other classic examples of population decline, inbreeding depression, and genetic rescue, such as Scandinavian wolves (Åkesson et al. 2016), Florida panthers (Johnson et al. 2010), and bighorn sheep (Hogg et al. 2006). Here, we focus on rapid contractions from large historical populations to very small populations, as these populations experience especially high risk of extinction due to inbreeding depression.

Methods

Overview of the SLiM non-Wright-Fisher model

We conducted non-Wright-Fisher (nonWF) simulations using SLiM 3 (Haller and Messer 2019). The impetus for this model was to allow for more ecologically-realistic population genetic simulations by relaxing many of the restrictive assumptions of the Wright-Fisher model (Haller and Messer 2019). Such assumptions include non-overlapping generations and a fixed population size that is not influenced by fitness, both of which are unrealistic when trying to model the extinction of a population due to genetic factors.

Instead, the SLiM nonWF approach models population size (N) as an emergent property of individual absolute (rather than relative) fitness and a user-defined carrying capacity (K). Thus, if individual fitness declines, a population experiences extinction through a biologically realistic process (a fitness-driven reduction in population size). Further, the model includes overlapping generations, such that individuals with high fitness can survive and reproduce for multiple generations. At the start of each generation, each individual randomly mates with another individual in the population, with one offspring resulting from each mating. At the end of each generation, individuals die with a probability given by their absolute fitness (ranging from 0 to 1), which is rescaled by the ratio of K/N to model the effects of density dependence. Thus, the carrying capacity here does not directly determine the simulated population size, but rather it indirectly influences it through its impact on individual fitness and viability selection. For the sake of both tractability and generality, we assume a hermaphroditic random mating population.

A discussion of how the carrying capacity of a SLiM nonWF model is related to its Wright-Fisher effective population size is provided in the Supplementary Methods.

Demographic scenarios

To obtain a baseline understanding for how ancestral demography influences extinction risk in small populations, we first explored a 'population contraction' scenario with our simulations (Figure 1.1A). Here, we modeled an instantaneous contraction from a large 'ancestral population' ($K_{ancestral} \in \{1{,}000, 5{,}000, 10{,}000, 15{,}000\}$) to a small 'endangered population' ($K_{endangered} \in \{25, 50\}$) (Figure 1.1A). This contraction scenario could represent the isolation of a population with historical connectivity (e.g., the Florida panther population) or alternatively the founding of an isolated population through migration or translocation (e.g., the initial founding of the Isle Royale wolf population). For each contraction event, we randomly sampled $K_{endangered}$ number of individuals from the ancestral population to seed the endangered population after a burn-in of $10*K_{ancestral}$ generations. All simulations were run until the endangered population went extinct. To examine the effects of a more gradual contraction, we also explored a scenario where an ancestral population with carrying capacity 10,000 first contracted to an intermediate carrying capacity of 1,000 for 200 generations, and finally an endangered carrying capacity of 25. We ran 25 simulation replicates for each combination of ancestral and endangered carrying capacities.

We next explored a 'genetic rescue' scenario, which similarly consisted of a population contraction from a large ancestral population to a small endangered population (Figure 1.1B). Here, however, we fixed the ancestral carrying capacity to 10,000, and again explored two endangered carrying capacities of 25 and 50. Prior to the contraction, we split off the following

source populations for genetic rescue: 1) a large population remaining at the ancestral size (K=10,000); 2) a moderate-sized population with long-term isolation (K=1,000 for 1,000 generations); 3) a small population with relatively recent isolation (K=100 for 100 generations); and 4) a very small population with very recent isolation (K=25 for 10 generations). These source population demographic histories were set to reflect a range of biologically-relevant scenarios (i.e., large and outbred populations, populations with moderate size and long-term isolation, smaller populations that have been more recently isolated) as well as provide a range of source population levels of genetic diversity and strongly deleterious variation to examine how these factors influence the efficacy of genetic rescue. Genetic rescue was initiated by translocating five randomly-selected individuals from the source population after the endangered population decreased in size to five or fewer individuals for the case when $K_{endangered}$=25, and 15 or fewer individuals for the case when $K_{endangered}$=50. Importantly, the exact number of generations of isolation for these source populations depended on the number of generations before translocation, which varied for each simulation replicate depending on the stochastic trajectory of the endangered population. For these simulations, we ran 50 replicates for simulations with $K_{endangered}$=25 and 25 replicates for simulations with $K_{endangered}$=50.

To further explore the dynamics of our genetic rescue scenario, we ran several additional simulations, here with endangered carrying capacity fixed to 25. First, to investigate the impact of selecting individuals for translocation to either maximize genetic diversity or minimize strongly deleterious variation, we ran simulations (50 replicates) were we picked selected five migrants from the K=10,000 source population with either the highest heterozygosity or fewest number of strongly deleterious alleles (where strongly deleterious mutations were defined to be

those mutations with $s < -0.01$). We also explored scenarios with varying numbers of migrants (1, 5, or 10) with the number of translocations fixed to one, as well as varying the number of translocations (1, 2, or 5) with the number of migrants fixed to five. Here, we ran 25 replicates for each parameter combination. All simulations were run until the endangered population went extinct.

Stochastic population dynamics

To capture the non-genetic factors that can contribute to extinction in small populations (Caughley 1994), our model includes three sources of ecological stochasticity. First, demographic stochasticity was modelled using the built-in mechanics of the SLiM nonWF model, in which survival from one generation to the next is determined by a Bernoulli trial with the probability of survival determined by the absolute fitness of an individual scaled by K/N (Haller and Messer 2019). Next, we incorporated the effects of environmental stochasticity in our simulations by modelling the carrying capacity of the endangered population as an Ornstein-Uhlenbeck process, in which the carrying capacity in a generation is given by:

$$\log(K(t+1)) = (1-\phi)K_{endangered} + \phi\log(K(t)) + w(0,\sigma)$$

where $\phi = 0.9$, $K_{endangered} \in \{25,50\}$ and $\sigma = \log_{10}(1.3)$ (Figure S1-1). The values of ϕ and σ were set arbitrarily to model environmental stochasticity with a moderate amount of variation and a high degree of auto-correlation. Finally, we modelled the effects of random natural catastrophes in our simulations by drawing a probability of mortality due to a catastrophe each generation from a beta distribution with $\alpha = 0.5$ and $\beta = 8$ (Figure S1-1). In each generation, deaths due to a

catastrophe are then determined by the outcome of a Bernoulli trial for each individual with the probability given by the beta distribution. Environmental stochasticity and natural catastrophes were only modelled in the small endangered population. Importantly, these stochastic ecological effects rarely lead to extinction in the endangered population in the absence of deleterious variation (8/25 simulation replicates with neutral mutations extinct within 10,000 generations at $K_{endangered} = 25$, and none extinct for $K_{endangered} = 50$).

Genomic parameters

We set the genomic parameters in our simulations to model the exome of a wolf-like organism. To do this, each diploid individual in our simulation has 20,000 genes of length 1500 bp, which occur on 38 autosomes with the number of genes on each chromosome determined by the ratios observed in the dog genome (Lindblad-Toh et al. 2005). Recombination between these genes occurs at a rate of 1×10^{-3}, with no recombination within genes and free recombination between chromosomes. These genes accumulate neutral and deleterious mutations at a rate of 1×10^{-8} per site, with the ratio of deleterious to neutral mutations set to 2.31:1 (Huber et al. 2017; Kim et al. 2017). The selection coefficients for these deleterious mutations were drawn from a distribution of fitness effects (DFE) estimated from a large sample of humans (Kim et al. 2017; see Supplementary Methods for additional details).

We initially set the dominance coefficients for our simulations according to the following *hs* relationship from Henn et al. 2016, based on results from Agrawal and Whitlock 2011:

$$h(s) = \frac{1/2}{(1+7071.07 \times s)}$$

This *hs* relationship intends to capture the pattern evident in empirical data that the dominance coefficient of a mutation tends to be inversely related to its selection coefficient, such that the most strongly deleterious mutations are highly recessive (Simmons and Crow 1977; Agrawal and Whitlock 2011; Huber et al. 2018). However, we found that simulations with this *hs* relationship in SLiM were extremely computationally intensive, such that we were only able to obtain results for simulations with the smallest ancestral carrying capacities of 1,000 and 5,000 (see Supplementary Methods for further discussion).

To overcome these computational limitations for realistic models of dominance, we instead implemented an approach assuming that weakly/moderately deleterious mutations ($s \geq -0.01$) were partially recessive (h=0.25) and strongly deleterious mutations ($s < -0.01$) were fully recessive (h=0). The aim of this approach (hereafter referred to as our "*hmix*" model) was to capture the key feature of the *hs* relationship that more deleterious mutations tend to be more recessive, with the dominance coefficients for these two classes of mutations reflecting their mean dominance coefficient under the *hs* relationship (Figure S1-2). Given our finding that the behavior of this model is extremely similar to that of the *hs* relationship (see Results), we used the *hmix* model for all simulations except where otherwise noted. More details on how the *hmix* model was implemented in SLiM is provided in the Supplementary Methods.

To further explore the impact of dominance coefficients, we also ran simulations where we varied the dominance coefficient for all mutations ($h \in \{0, 0.01, 0.05, 0.2, 0.5\}$). In addition, we explored the impact of decreasing the number of sites in which fully recessive (h=0) deleterious mutations can occur (i.e., the mutational target size) by varying the number of genes in our

simulations ($g \in \{1{,}000, 5{,}000, 10{,}000, 15{,}000, 20{,}000\}$). These simulations were run solely under the 'population contraction' demographic scenario with $K_{ancestral} \in \{1{,}000, 5{,}000, 10{,}000, 15{,}000\}$ and $K_{endangered} = 25$. We ran 25 replicates for each of these simulations, terminating the simulation when the endangered population went extinct.

During the simulations, we kept track of several summaries of the state of the population. These include the population's mean heterozygosity, mean inbreeding coefficient (F_{ROH}), the mean fitness, and the average number of deleterious alleles per individual binned into weakly ($-0.001 < s \leq -0.00001$), moderately ($-0.01 < s \leq -0.001$), strongly ($s < -0.01$), and very strongly ($s < -0.05$) deleterious classes. Fitness was calculated multiplicatively across sites. Here, we restricted F_{ROH} to include only runs of homozygosity greater than 1 Mb to capture inbreeding due to mating between close relatives. These statistics were calculated from a sample of 30 individuals every 1000 generations during the burn-in and every generation following the contraction.

Burn-in conditions for the simulations

Our simulations during the burn-in retained fixed mutations and did not model reverse mutation. Retaining fixed mutations during the burn-in was important to ensure that weakly deleterious mutations that drifted to fixation contribute to absolute fitness. However, one consequence of retaining fixed mutations is that there is no mutation-selection-drift equilibrium in the ancestral population since weakly deleterious mutations continue to accumulate as fixations even after heterozygosity of segregating variation has leveled off (Figure S1-3). As a result, fitness during the burn-in also never reaches equilibrium, but instead declines gradually as weakly deleterious mutations are fixed. Although fixation of weakly deleterious mutations occurs at a rate that is

inverse to population size (i.e., much faster in smaller populations), we found that this effect is cancelled out when the length of the burn-in is proportional to the population's carrying capacity (i.e., 10*K, leading to a much shorter burn-in for smaller populations), resulting in the same pre-contraction fitness regardless of population size (Figure S1-4a). To explore the impact of these proportional burn-ins, we ran simulations under an *hmix* model of dominance in which all burn-ins were run for 30,000 generations, regardless of the ancestral size. This led to a notable reduction in pre-contraction fitness for the K=1,000 population, and a slight increase in fitness for the larger populations (Figure S1-4). However, there were no qualitative differences in extinction times relative to when proportional burn-ins were used (Figure S1-4C), suggesting that extinction dynamics are governed more by the numbers of recessive strongly deleterious alleles in these populations rather than their pre-bottleneck fitness. This finding is further supported by our simulation results that demonstrate that strongly deleterious mutations are a far more important determinant of extinction times compared to weakly or moderately deleterious mutations (see Results).

Results

Population contraction simulations under the hmix model

Our population contraction simulations demonstrate that, although larger populations have higher genetic diversity (Figure 1.2A), they also harbor higher levels of strongly deleterious variation (Figure 1.2B). Consequently, we observe a strong effect of ancestral demography on time to extinction following a population contraction, with populations that were historically large experiencing more rapid extinction (Figure 1.2C). For example, given an endangered carrying capacity of 25, a population with an ancestral carrying capacity of 1,000 will go extinct

in 474 generations on average, whereas a population with an ancestral carrying capacity of 15,000 will do so in 70 generations on average (Figure 1.2C). When modelling a more gradual contraction from an ancestral carrying capacity of 10,000, we found that extinction times were slightly increased relative to the instantaneous contraction scenario (Figure S1-5), suggesting that more gradual contractions can facilitate purging and ultimately decrease extinction risk.

Examination of individual simulation replicates provides insight into the dynamics of extinction in these populations (Figures 3A and S6). Endangered populations with an ancestral carrying capacity of 1,000 contain fewer strongly deleterious mutations, translating to a decreased severity of inbreeding depression and ultimately longer persistence (Figures 3A and S6). This decreased severity of inbreeding depression allows these populations to become highly inbred ($F_{ROH} \approx 1$) well before going extinct (Figures 3A and S6). By contrast, endangered populations with a larger ancestral carrying capacity of 15,000 have much higher levels of recessive strongly deleterious variation due to these mutations being hidden from selection in the ancestral population, resulting in a more rapid loss of fitness as these populations become inbred (Figures 3B and S6). As a result, these populations typically go extinct well before F_{ROH} approaches one (Figures 3B and S6). These populations also lose fitness due to increased genetic drift and inbreeding among more distant relatives, which is not captured by our definition of F_{ROH}.

Following contraction, the ability of the endangered population to purge its load of recessive deleterious mutations also depended on stochastic ecological factors. For example, when the carrying capacity of the endangered population was by chance higher due to environmental stochasticity, natural selection was most effective at removing strongly deleterious alleles,

translating to longer persistence (Figures 3 and S6). By contrast, when the carrying capacity of the endangered population was low soon after contraction, purging tended to be less effective, resulting in more rapid extinction (Figures 3 and S6). However, in both cases, purging was also counteracted by continual input of strongly deleterious alleles by mutation, which eventually contributed to population extinction. Overall, these various sources of genetic and ecological stochasticity together resulted in highly variable extinction times for any given parameter settings, highlighting the important role of random events in determining whether a small population can persist.

Our simulations also demonstrate the importance of increasing the carrying capacity of the endangered population as a means to ensure population persistence. Larger endangered populations (K=50) were better able to purge recessive deleterious mutations following the contraction, resulting in much longer persistence (Figure S1-7). Moreover, larger populations were less impacted by stochastic ecological factors, which also contributed to increased time to extinction. Nevertheless, extinction times for these larger endangered populations still depended strongly on the ancestral carrying capacity (Figure S1-7), demonstrating the importance of considering both recent and historical demography when assessing extinction risk.

Results under varying genomic parameters

We next explored the sensitivity of our results to the genomic parameters assumed in our model. In particular, we focus on the impact of dominance coefficients, as previous work has suggested that the extent to which strongly deleterious mutations accumulate at higher frequencies in larger populations depends strongly on the assumed dominance coefficients (Nei 1968; Hedrick 2002;

Hedrick and Garcia-Dorado 2016). Under the most realistic model of an *hs* relationship, we found that strongly deleterious mutations do accumulate at much higher frequencies in larger populations, leading to much faster extinction following contraction (Figure 1.4). However, we also found that simulations with an *hs* relationship in SLiM were extremely computationally intensive, such that we were unable to obtain results for the larger ancestral carrying capacities of 10,000 and 15,000 (see Supplementary Methods). Nevertheless, these results demonstrate a strong concordance between the *hs* relationship and our *hmix* model, suggesting that our *hmix* model captures the key features of the *hs* relationship (Figures 4 and S2).

When assuming a single dominance coefficient for all mutations, our results demonstrate a range of outcomes that depended on the assumed dominance coefficient. Specifically, when assuming h=0 or 0.01, we again find that larger populations harbor higher levels of strongly deleterious variation, with similar patterns to the *hs* relationship or *hmix* model (Figure 1.4). However, this effect is greatly diminished when mutations are only partially recessive (h=0.05 or 0.2), and is nonexistent when mutations are additive (h=0.5), as expected (Figure 1.4). Notably, although the average dominance coefficient under our assumed *hs* relationship is approximately 0.2, our results with h=0.2 are dramatically different from those under the *hs* relationship (Figure 1.4).

To further investigate the importance of strongly vs weakly/moderately deleterious mutations in our *hmix* model, we ran simulations where we truncated our DFE to only permit strongly deleterious ($s < -0.01$ and h=0) or weakly/moderately deleterious mutations ($s \geq -0.01$ and h=0.25) to enter the population. More specifically, in the case of permitting only strongly deleterious mutations, we allowed any mutation with $s < -0.01$ to enter the population as normal,

however mutations with $s \geq -0.01$ instead became neutral mutations. Here, our results for simulations that only included strongly deleterious mutations were notably similar to the full *hmix* model, with extinction times that depended strongly on ancestral demography (Figure S1-8). By contrast, results for simulations that only included weakly/moderately deleterious mutations were dramatically different from the full model, and had greatly increased extinction times (Figure S1-8). Given that strongly deleterious mutations constitute only ~25% of all new deleterious mutations under our assumed DFE (Kim et al. 2017), these results demonstrate their disproportionate impact on extinction risk relative to the effects of more weakly or moderately deleterious mutations.

As a final way of exploring the impact of recessive deleterious mutations, we also conducted simulations where we decreased the target size for deleterious mutations assuming h=0. The motivation for these simulations was to test whether we would still observe an impact of ancestral demography on extinction times when lowering the number of genes that could accumulate fully recessive deleterious mutations. To do this, we decreased the number of genes (g) in our simulations from 20,000 to $g \in \{1{,}000, 5{,}000, 10{,}000, \text{and } 15{,}000\}$. Here, we observed that the effect of ancestral demography is still present, though greatly diminished, with as few as 1,000 genes, and remains substantial with as few as 5,000 genes (Figure S1-9).

Genetic rescue simulations

We next explored how demography and strongly deleterious variation impact the effectiveness of genetic rescue assuming the *hmix* model of dominance. Here, we quantify the effectiveness of genetic rescue as the extent to which the introduction of migrants to the endangered population

increased extinction times. When translocating five migrants from one of four source populations (Figure 1.5A-B) to an endangered population with K=25, we found that all source populations led to increases in time to extinction relative to a no-rescue scenario (Figure 1.5C). Importantly, however, we found that the magnitude of increase in time to extinction was highly dependent on source population demography and levels of strongly deleterious variation. For example, whereas genetic rescue from the large source population (K=10,000) led to a notable increase in mean time to extinction of 16% (one-tailed t-test p=0.159), rescue from the moderate-sized source population resulted in a much more dramatic increase of 130% (p=1.75e-7; Figure 1.5C). Genetic rescue from small and moderately-inbred populations (mean $F < 0.1$; Figure S1-10) also resulted in increases in mean time to extinction that were at least as great as that of the large source population (63% increase for K=100 [p=0.00132], 13% increase for K=25 [p=0.224]) (Figure 1.5C). We observed similar patterns when conducting simulations with a larger endangered population (K=50) (Figure S1-11), though the beneficial effects of genetic rescue were somewhat diminished, likely due to the larger recipient population size when translocation was initiated ($N \leq 15$) as well as the greater efficacy of purging within the larger recipient population.

Examination of individual simulation replicates again offers insight into the factors driving extinction in these populations (Figures 6 and S12). In all simulated scenarios, we observed a large increase in fitness immediately following the introduction of migrants (Figures 6, S12-13), likely due to the high strength of heterosis (masking of fixed recessive deleterious alleles) following initial admixture. In most cases, these increases in fitness led to population growth, though the extent to which population sizes increased was strongly influenced by environmental

stochasticity (Figures 6 and S12). Soon after genetic rescue, however, the resumption of inbreeding again led to a decline in fitness (Figures 6 and S12). Here, the rate of fitness decline was determined by the levels of strongly deleterious variation in the migrant individuals and their descendants. For example, when translocation occurred from a large source population (K=10,000), levels of strongly deleterious variation remained high after genetic rescue, eventually resulting in severe inbreeding depression once inbreeding resumed (Figure 1.6). By contrast, when the moderate-sized source population was used (K=1,000), levels of strongly deleterious variation dramatically decreased following genetic rescue, greatly decreasing the severity of inbreeding depression in future generations (Figure 1.6).

These results demonstrate that, although the larger source populations have higher fitness and genetic diversity, they also harbor a high number of heterozygous recessive strongly deleterious mutations (Figures 5 and S10). These mutations are quickly made homozygous by inbreeding in the endangered population following translocation, exacerbating the severity of inbreeding depression and eventually contributing to extinction. In support of this interpretation, we found that time to extinction following genetic rescue is predicted by the average number of strongly deleterious alleles per individual in the source population when examining all source populations simultaneously (Figure 1.5D). By contrast, we found that average source population heterozygosity was not very predictive of time to extinction, where in fact we observed a slight negative correlation due to the fact that source populations with higher genetic diversity also tend to harbor higher levels of recessive strongly deleterious variation (Figure 1.5E). We obtained similar results when restricting this analysis to the K=25 source population, the source population for which there was the highest variability in strongly deleterious variation and

genetic diversity (Figure S1-14). However, in this case, we do see a strong negative correlation between genetic diversity and extinction times, which is likely driven by heterozygosity being correlated with strongly deleterious variation at this intra-population scale.

Our finding that source population levels of strongly deleterious variation predict the efficacy of genetic rescue suggests that genome-wide levels of deleterious variation could be used to select individuals for genetic rescue. We explored the efficacy of this strategy by selecting the individuals with the fewest strongly deleterious alleles ($s < -0.01$) from the large source population (K=10,000) for rescue. This approach resulted in an increase in mean time to extinction of 74% (p=1.15e-4) compared to the non-rescue scenario, a 49% increase relative to randomly selecting individuals from the large source population (Figure 1.5F). By contrast, when individuals with the highest genome-wide heterozygosity were selected, we observed an increase in time to extinction that was no greater than when individuals were selected at random (p=0.148; Figure 1.5F). These results further support the causal relationship between strongly deleterious variation and extinction risk due to inbreeding depression, as well as the lack of this relationship between heterozygosity and extinction risk.

Lastly, we explored the effects of varying the number of migrants (1, 5, or 10) as well as the number of translocation events (1, 2, or 5), focusing on the K=10,000 and K=1,000 source populations. These simulations show persistent increases in time to extinction with increasing number of translocations regardless of the source population (Figure S1-15), suggesting that the efficacy of genetic rescue does not diminish with each additional migration event. When varying the number of migrants, we found that extinction times increased slightly in the case where

migrants were drawn from the K=1,000 source population, but did not increase when drawing migrants from the K=10,000 source population (Figure S1-15).

Discussion

Our simulations demonstrate the central importance of demographic history and recessive strongly deleterious mutations in determining the risk of extinction due to inbreeding depression in small and isolated populations. We find that populations that were historically large have a much higher risk of extinction following a population contraction compared to historically-smaller populations (Figure 1.2). These findings may be counterintuitive given the thinking that small populations should be less fit due to an accumulation of weakly deleterious alleles (Kimura et al. 1963; Lynch and Gabriel 1990; Lynch et al. 1995; Battaillon and Kirkpatrick 2000). The key insight that our simulations highlight is that larger ancestral populations harbor more recessive strongly deleterious mutations (Figure 1.2), due to these mutations being hidden from purifying selection as heterozygotes. The exposure of these mutations as homozygous by inbreeding in small populations can lead to dramatic reductions in fitness and drive rapid extinction, well before 'mutational meltdown' due to an accumulation of weakly deleterious mutations can occur (Lynch and Gabriel 1990; Lynch et al. 1995). By demonstrating that this effect is sufficient to ultimately drive extinction on short timescales, our simulations illustrate the importance of recessive deleterious variation as the primary mechanism of inbreeding depression (Charlesworth and Willis 2009; Hedrick and Garcia-Dorado 2016).

Although the insight that strongly deleterious mutations that are fully recessive can accumulate at greater frequencies in larger populations has been noted elsewhere (Nei 1968; Battaillon and

Kirkpatrick 2000; Hedrick 2002; Hedrick and Garcia-Dorado 2016; Szpiech et al. 2019), our results add to this work by demonstrating that that these effects persist under realistic genomic parameters and models of dominance, including both an *hs* relationship and our *hmix* model (Figure 1.4). This result is due to the fact that strongly deleterious mutations under these models tend to be highly recessive (Simmons and Crow 1977; Agrawal and Whitlock 2011; Huber et al. 2018), and are therefore hidden from purifying selection when present as heterozygotes in large populations Moreover, when examining models with a single dominance coefficient for all mutations, we find that our results with fully recessive mutations (h=0 or 0.01) are highly similar to those under more realistic models of dominance, whereas the impact of ancestral demography is greatly diminished with partially recessive (h=0.05 or 0.2) mutations and nonexistent with additive (h=0.5) mutations (Figure 1.4). The transition in this behavior has previously been explored using analytical models, where it was similarly shown that the impact of population size on levels of strongly deleterious variation greatly diminishes as h approaches 0.05 (Hedrick 2002; Hedrick and Garcia-Dorado 2016)

While the mean dominance coefficient under our assumed *hs* relationship is ~0.2, this model showed very different extinction dynamics compared to the model assuming h=0.2 for all mutations (Figure 1.4). This result suggests that the key factor mediating extinction dynamics is the presence of highly recessive strongly deleterious mutations, rather than the overall mean dominance coefficient. In support of this interpretation, we show that simulations that only include the fraction of mutations that are strongly deleterious and fully recessive (h=0) exhibit extinction times that are highly similar to those under an *hs* relationship or *hmix* model, whereas simulations that only include the fraction of mutations that are weakly or moderately deleterious

and partially recessive (h=0.25) have much longer extinction times that depend only minimally on ancestral demography (Figure S1-8). This result is especially striking when considering that strongly deleterious mutations comprise only ~25% of the overall number of deleterious mutations under our assumed DFE (Kim et al. 2017). Taken together, these results further bolster our conclusion that strongly deleterious mutations are the primary determinant of extinction risk due to inbreeding depression in small populations. The extent to which these dynamics may be relevant for a given species, however, will depend on their distribution of selection and dominance coefficients, and specifically the extent to which there exists a substantial fraction of mutations that are highly recessive and strongly deleterious. Although these parameters remain poorly known for the vast majority of organisms, highly recessive strongly deleterious mutations are commonly observed across disparate taxa (e.g., Simmons and Crow 1977; McCune et al. 2002), suggesting that their influence on extinction may be widespread. However, these dynamics may prove to be most relevant to mammals and other vertebrates with high levels of "organismal complexity", which has been demonstrated to result in a higher fraction of strongly deleterious mutations (Huber et al. 2017).

The considerable influence of ancestral demography that our simulations reveal has important implications for predicting the threat of extinction due to inbreeding depression in wild populations. Quantifying inbreeding depression in the wild and predicting the threat it poses to extinction remains a major challenge in conservation biology, and the reasons why some small populations suffer from inbreeding depression and others do not is often unclear (Hedrick and Garcia-Dorado 2016). Our simulations suggest that these differences may be determined in large part by the ancestral demography of a species. Consequently, we suggest that information on

ancestral demography, which is increasingly becoming accessible using genomic data (Beichman et al. 2018), should be more widely incorporated into extinction risk predictions. In particular, given that nearly all threatened populations have recently undergone reductions in size due to anthropogenic pressures, these results suggest that their continued persistence may depend crucially on their ancestral demography and load of recessive strongly deleterious mutations. In addition, our results also suggest that island populations that have historically been small may in fact have reduced extinction risk due to inbreeding depression as a result of to their high isolation and smaller population size, which may have facilitated purging of recessive strongly deleterious mutations (Laws and Jamieson 2011; Robinson et al. 2018). However, our simulations also reveal that the fate of small populations is highly stochastic, and that even under the same ecological and genetic parameters, time to extinction can vary substantially (Figures 2 and 4). Thus, predictions of extinction risk for any wild population should necessarily be accompanied by a high degree of uncertainty.

Our results also provide insight on how best to conduct genetic rescue, which is becoming increasingly necessary for maintaining small and isolated populations under growing anthropogenic pressures (Whiteley et al. 2015; Hedrick and Garcia-Dorado 2016; Frankham et al. 2017; Bell et al. 2019). Consistent with many other studies (e.g., Hogg et al. 2006; Johnson et al. 2010; Frankham 2015; Åkesson et al. 2016), our simulations highlight the beneficial effects of genetic rescue, supporting recent calls for its more widespread application (Whiteley et al. 2015; Frankham et al. 2017; Bell et al. 2019). However, in stark contrast to existing recommendations (Pickup et al. 2012; Whiteley et al. 2015), we found that targeting large source populations with high genetic diversity was among the least effective genetic rescue strategies

(Figures 5 and S11). Instead, our results demonstrate that the effectiveness of genetic rescue can potentially be maximized by drawing migrants from moderate-sized source populations (Figures 5 and S11). These source populations are ideal due to being small enough to purge strongly deleterious recessive mutations, but not so small that they accumulate a substantial load of fixed weakly deleterious mutations. Finally, our results demonstrate that even small and somewhat inbred populations (mean $F < 0.1$) can also serve as effective source populations (Figures 5C and S10), as other studies have shown (S. Heber et al. 2012; Sol Heber et al. 2012). Our results do not suggest, however, that inbred populations will always serve as more effective source populations than outbred populations, or that highly inbred source populations are likely to be effective, as has been recently claimed (Ralls et al. 2020). Rather, our results demonstrate that source populations that are only slightly inbred (mean $F_{ROH} \sim 0.06$) may be comparable in their effectiveness to large source populations, though both are likely to be less effective than purged source populations with long-term moderate size.

A key factor accounting for the differences between our results and previous experimental and empirical studies examining source population effectiveness (Pickup et al. 2012; Frankham 2015) is a difference of temporal scale. Specifically, existing studies rarely examine the consequences of gene flow beyond the F1 generation, whereas our simulation framework enables tracking these dynamics over the longer term. Previous research has shown that, during the generations immediately following genetic rescue, fitness increases are likely to be greatest when migrants are sourced from larger source populations (Pickup et al. 2012; Frankham 2015). Indeed, our results agree with these findings, and demonstrate greater fitness increases during the F1 generation when drawing migrants from larger source populations (Figure S1-13). Where our

results differ, however, is in the generations well after F1, after the initial strong heterosis is diminished and inbreeding resumes. Here, we find that using smaller source populations with decreased levels of strongly deleterious variation can lower the severity of inbreeding depression and increases population persistence (Figure 1.6). This result emphasizes the importance of evaluating genetic rescue outcomes over the longer term, since the dynamics in the generations immediately following genetic rescue might differ greatly from those several generations later, as was so dramatically demonstrated by the Isle Royale wolf population.

Although our results suggest that large populations may not be ideal source populations for genetic rescue, we demonstrate that the effectiveness of this strategy can be greatly increased when individuals are screened for low levels of strongly deleterious variation (Figure 1.5F). However, applications of such approach may remain limited by our ability to accurately predict the fitness consequences of individual mutations, which remains a major challenge even in humans (Eilbeck et al. 2017). Our results also demonstrate that repeated genetic rescue from large or moderate-sized source populations can result in persistent beneficial effects (Figure S1-15), highlighting the efficacy of this strategy for populations that are destined to remain small and isolated. One inevitable consequence of this or any other genetic rescue strategy, however, is a loss of native ancestry (Johnson et al. 2010; Adams et al. 2011; Harris et al. 2019), which can potentially swamp out locally adapted alleles (though see Fitzpatrick et al. 2020). Although we do not track levels of admixture in our simulations, it is probable that the post-rescue populations are composed of highly admixed individuals (Harris et al. 2019).

In addition to providing guidelines for how to best conduct genetic rescue, our results also have implications for understanding the mechanisms underlying genetic rescue. Two mechanisms have generally been proposed for genetic rescue: heterosis (masking of fixed recessive deleterious mutations) and adaptive evolution (increases in fitness due to selection on new alleles) (Whiteley et al. 2015). By demonstrating that, even in the absence of adaptive variation, migration into small and inbred populations can lead to increases in fitness and population size consistent with those observed in empirical systems (e.g., Hogg et al. 2006; Johnson et al. 2010; Adams et al. 2011; Åkesson et al. 2016), our results suggest that heterosis alone may be able to explain much of the beneficial effects of genetic rescue. However, a more thorough investigation of the relative roles of heterosis and adaptive evolution as mechanisms of genetic rescue could be conducted by incorporating adaptive mutations into our simulation framework. Finally, our finding that increases in fitness following migration do not always lead to increases in population size due to the effects of environmental stochasticity (Figure S1-12) suggests that definitions of genetic rescue based on demographic effects alone may be restrictively narrow, as other authors have suggested (Hedrick et al. 2011). In particular, this result has relevance to the debate of whether the Isle Royale wolf population truly experienced genetic rescue, given that the population size did not increase substantially following migration, perhaps due to poor environmental conditions (Adams et al. 2011; Hedrick et al. 2011)

Our simulation framework has several notable limitations. First, due to the high computational load of our simulations (see Supplementary Methods), we were unable to examine ancestral populations with carrying capacities larger than 15,000, limiting the observed impact of ancestral demography. Second, we did not examine heterozygote advantage as a potential mechanism for

inbreeding depression, which could impact the negative relationship between extinction times and source population heterozygosity that we observed (Figure 1.5E). However, empirical support for heterozygote advantage as a mechanism for inbreeding depression is scarce (Charlesworth and Willis 2009; Hedrick and Garcia-Dorado 2016), suggesting that it may not substantially impact our results. In addition, we did not include adaptive mutations in our model, which may also be relevant to the ability of small populations to persist under environmental change, as well as for exploring the impacts of outbreeding depression due to differential local adaptation. Although recent work has suggested that concerns about outbreeding depression may have been overstated (Whiteley et al. 2015; Frankham et al. 2017), assessing its influence in determining source population selection nevertheless represents an important area for future research. Finally, we emphasize that the demographic scenarios explored here may not be applicable to all small and isolated populations. Specifically, our assumption of an instantaneous contraction from a large ancestral population to a small endangered population may not capture the demographic trajectory of many populations that have experienced more gradual declines. In these cases, a gradual decline may have facilitated purging of strongly deleterious mutations (Figure S1-5), decreasing the necessity for genetic rescue (e.g., Xue et al. 2015; Robinson et al. 2018). Overall, we recommend that any conservation actions motivated by our results carefully consider the demography of the population of interest, ideally using simulations.

In conclusion, our results highlight the detrimental effects of strongly deleterious variation in small populations, and suggest that many conservation strategies for endangered species may be improved by minimizing strongly deleterious variation rather than maximizing heterozygosity. Heterozygosity at putatively neutral markers (e.g., microsatellites and RAD loci) has long served

as an essential tool for assessing population health and risk of extinction due to inbreeding depression (Teixeira and Huber 2020); here, we highlight ways in which this approach may be misleading. These results are especially relevant to the ongoing reintroduction of wolves to Isle Royale, which has been guided by the goal of maximizing the genetic diversity of the new population. Although our simulations are motivated by this example, by examining a wide range of demographic scenarios, our results have implications beyond the Isle Royale wolf population. Future research should explore implementation of these strategies by expanding the use of genomic tools and assessments of deleterious variation in the context of the conserving small and isolated populations (Fitzpatrick and Funk 2019). Given the great expense of most translocation programs, incorporating genomic approaches represents a sound investment with the potential to substantially postpone the need for future intervention.

Figures

Figure 1.1

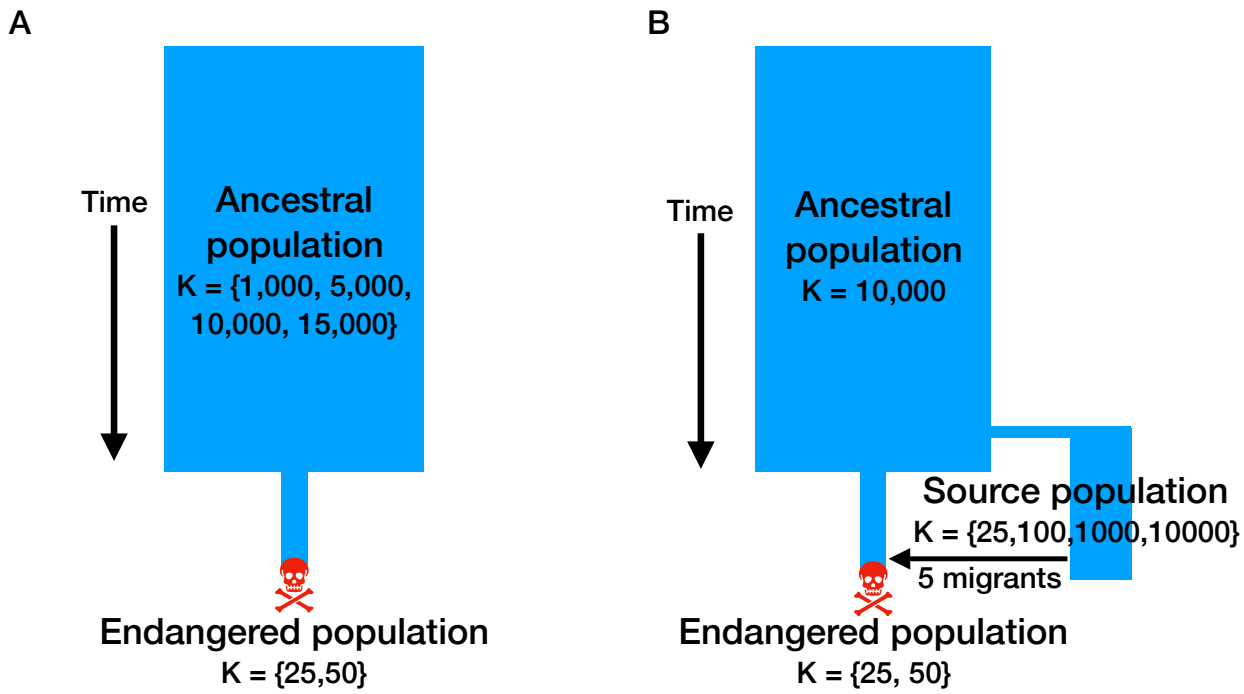

Figure 1.1: Schematic of the demographic scenarios used for simulations. (A) Schematic for 'population contraction' simulations. (B) Schematic for 'genetic rescue' simulations. Note that migration occurs in the genetic rescue scenario when the endangered population decreases in size to five or fewer individuals when $K_{endangered}$ =25 and 15 or fewer individuals when $K_{endangered}$ =50.

Figure 1.2

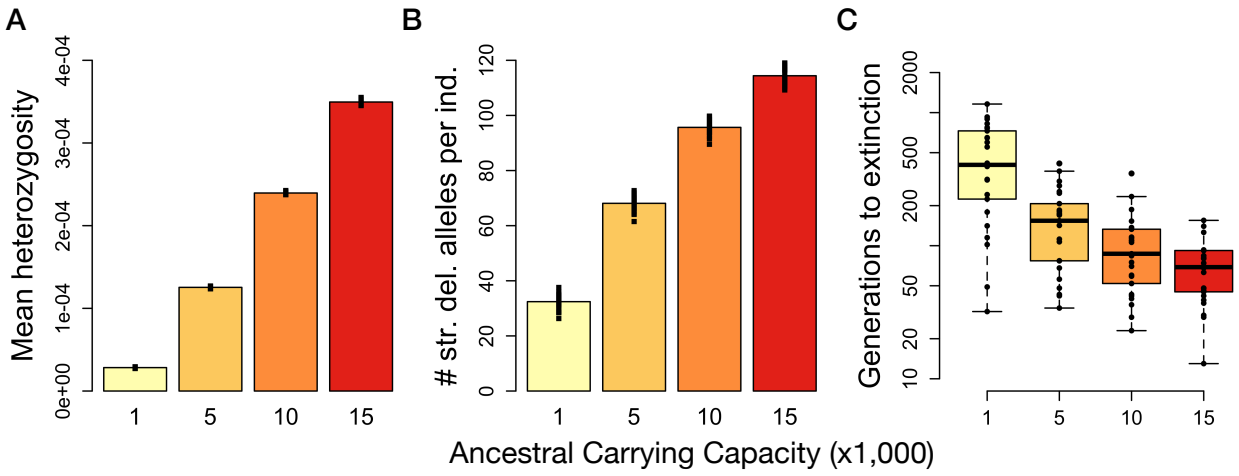

Figure 1.2: Results for population contraction simulations under the *hmix* model of dominance. (A) Mean heterozygosity of ancestral populations prior to contraction. (B) Average number of strongly deleterious alleles ($s < -0.01$) per individual in the ancestral populations prior to contraction. (C) Time to extinction following contraction from ancestral populations of varying size to an endangered population with K=25. Extinction times for $K_{endangered} = 50$ shown in Figure S1-8. Note that the y-axis is on a log scale. For each parameter setting, 25 simulation replicates were run.

Figure 1.3

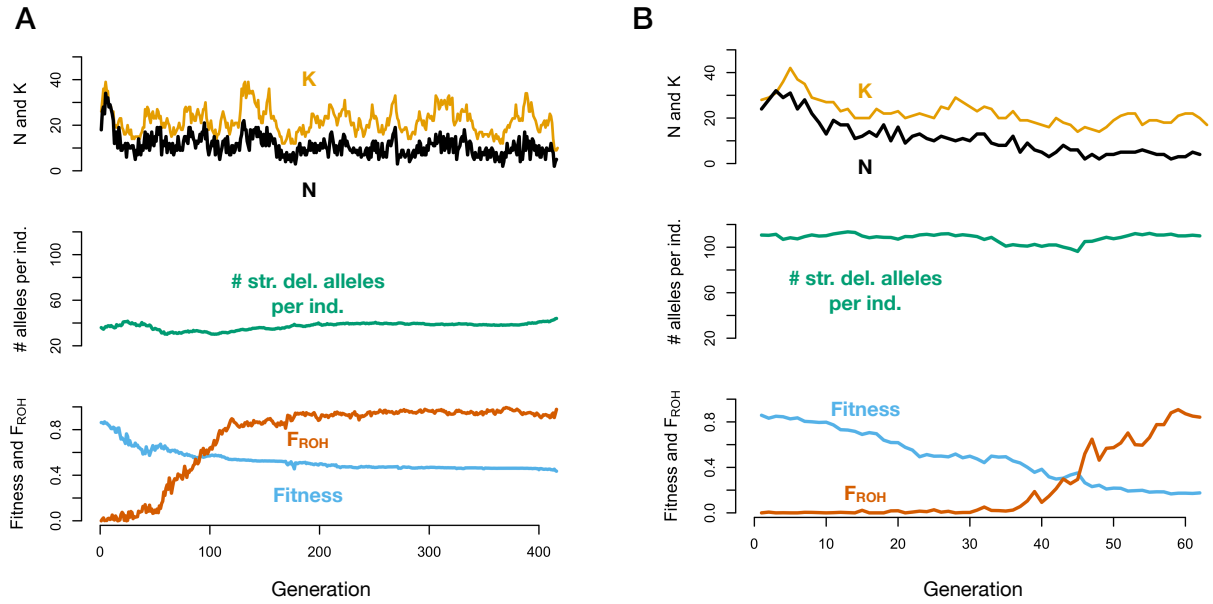

Figure 1.3: Representative examples of population contraction simulations with ancestral populations of varying size. (A) Example with $K_{ancestral} = 1{,}000$. (B) Example with $K_{ancestral} = 15{,}000$. The top of each panel shows population size (N) in black and carrying capacity (K) in gold, the middle shows the average number of strongly deleterious alleles ($s < -0.01$) per individual, and the bottom shows mean absolute fitness in blue and mean inbreeding coefficient (F_{ROH}) in orange. For both replicates, $K_{endangered} = 25$ and an *hmix* model of dominance was assumed. Note the differing x-axis scales for panels A and B.

Figure 1.4

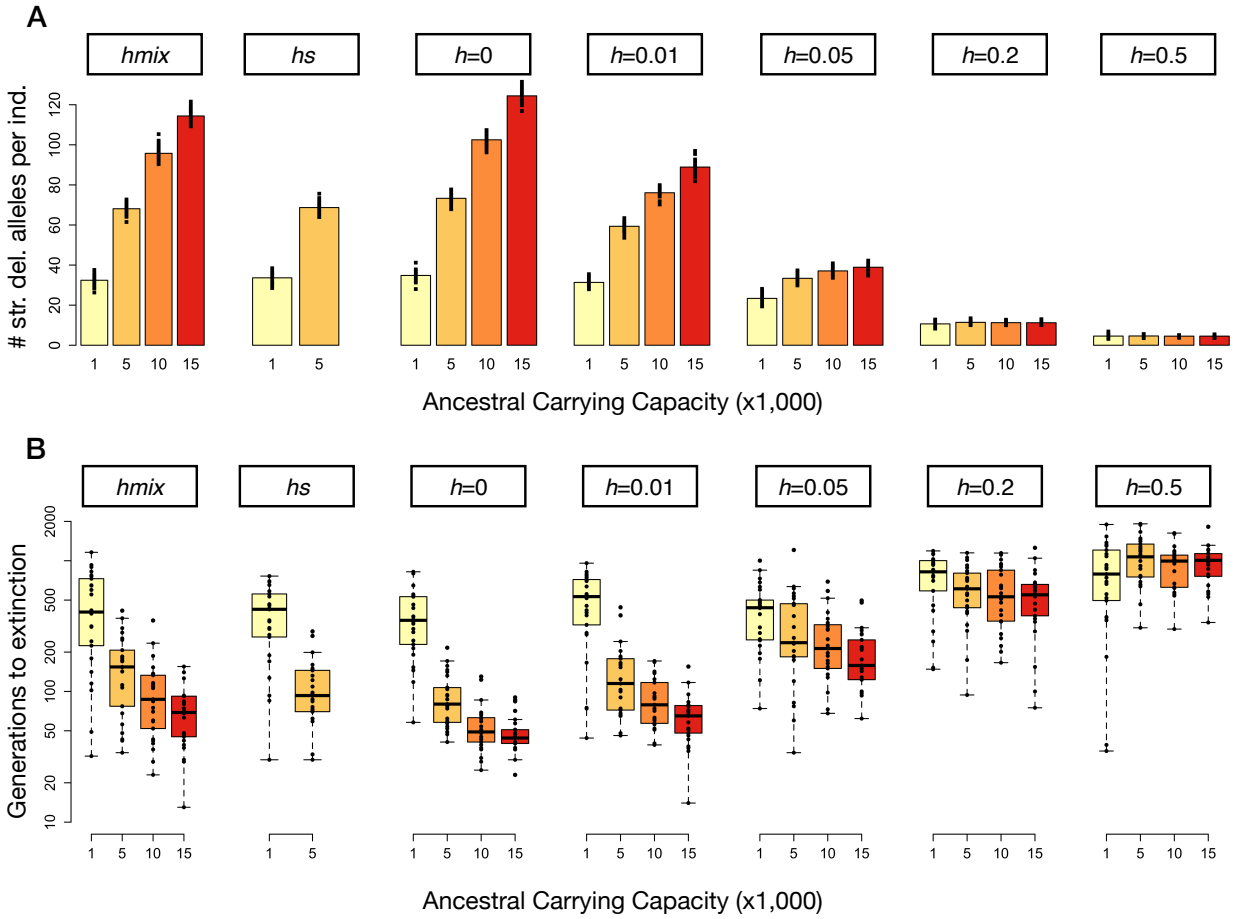

Figure 1.4: Impact of dominance coefficients on the accumulation of strongly deleterious mutations and extinction times following a contraction. (A) Mean number of strongly deleterious alleles per individual (s < -0.01) prior to contraction in ancestral populations of varying size and under varying models of dominance. (B) Time to extinction following contraction to $K_{endangered}$ = 25 plotted on a log scale. Note that we were unable to obtain results for $K_{ancestral}$ = 10,000 and 15,000 under the *hs* relationship due to computational limitations. For each parameter setting, 25 simulation replicates were run.

Figure 1.5

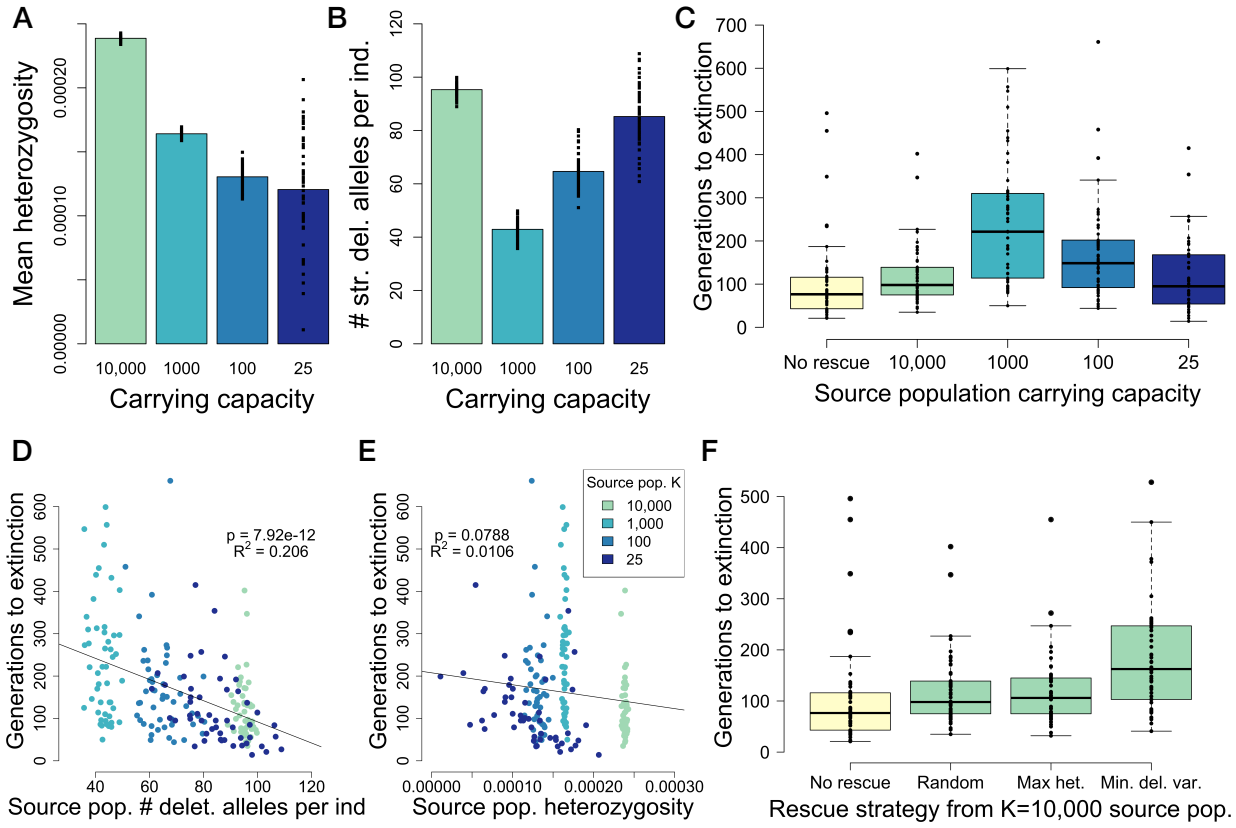

Figure 1.5: Source population deleterious variation determines the effectiveness of genetic rescue. (A) Average heterozygosity of source populations used for genetic rescue during the generation of rescue. (B) Mean number of strongly deleterious alleles (s < -0.01) per individual in the source populations used for genetic rescue. See Figure S1-10 for source population fitness and levels of inbreeding. (C) Time to extinction following genetic rescue from source populations of varying size. (D) Time to extinction following genetic rescue is negatively correlated with the number of recessive strongly deleterious alleles (s < -0.01) per individual used for rescue. (E) Time to extinction following genetic rescue is not correlated with the heterozygosity of the source population. See Figure S1-14 for regression results when considering only the K=25 source population. (F) Time to extinction under different strategies of genetic rescue from the K=10,000 source population. For each parameter setting, 50 simulation replicates were run.

Figure 1.6

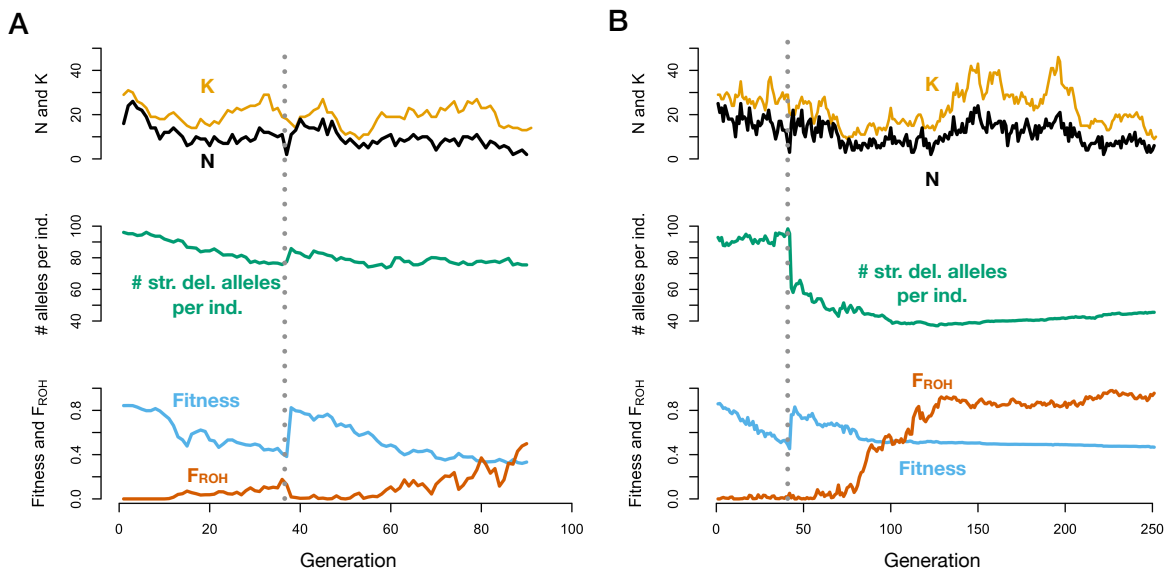

Figure 1.6: Representative examples of genetic rescue simulations with source populations of varying size. (A) Example when a large source population (K=10,000) is used for genetic rescue. (B) Example when a moderate-sized (K=1,000) is used. The top of each panel shows population size (N) in black and carrying capacity (K) in gold, the middle shows the average number of strongly deleterious alleles ($s < -0.01$) per individual, and the bottom shows mean absolute fitness in blue and mean inbreeding coefficient (F_{ROH}) in green. The dashed grey line indicates the generation in which migration occurred. For both replicates, $K_{endangered} = 25$ and an *hmix* model of dominance was assumed. Note the differing x-axis scales for panels A and B.

References

Adams JR, Vucetich LM, Hedrick PW, Peterson RO, Vucetich JA. 2011. Genomic sweep and potential genetic rescue during limiting environmental conditions in an isolated wolf population. *Proc. R. Soc. B Biol. Sci.* [Internet] 278:3336–3344. Available from: http://rspb.royalsocietypublishing.org/cgi/doi/10.1098/rspb.2011.0261

Agrawal AF, Whitlock MC. 2011. Inferences about the distribution of dominance drawn from yeast gene knockout data. *Genetics* 187:553–566.

Åkesson M, Liberg O, Sand H, Wabakken P, Bensch S, Flagstad Ø. 2016. Genetic rescue in a severely inbred wolf population. *Mol. Ecol.* 25:4745–4756.

Allendorf FW, Leary RF. 1986. Heterozygosity and fitness in natural populations of animals. In: Conservation biology: the science of scarcity and diversity. p. 58–72.

Battaillon T, Kirkpatrick M. 2000. Inbreeding depression due to mildly deleterious mutations in finite populations: size does matter. *Genet. Res. (Camb).* 75:75–81.

Beichman AC, Huerta-Sanchez E, Lohmueller KE. 2018. Using Genomic Data to Infer Historic Population Dynamics. *Annu. Rev. Ecol. Evol. Syst.* 49:433–456.

Bell DA, Robinson ZL, Funk WC, Fitzpatrick SW, Allendorf FW, Tallmon DA, Whiteley AR. 2019. The Exciting Potential and Remaining Uncertainties of Genetic Rescue. *Trends Ecol. Evol.* [Internet]:1–11. Available from: https://linkinghub.elsevier.com/retrieve/pii/S0169534719301739

Caballero A, Bravo I, Wang J. 2017. Inbreeding load and purging: Implications for the short-term survival and the conservation management of small populations. *Heredity (Edinb).* [Internet] 118:177–185. Available from: http://dx.doi.org/10.1038/hdy.2016.80

Caughley G. 1994. Directions in Conservation Biology. *J. Anim. Ecol.* 63:215–244.

Charlesworth D, Willis JH. 2009. The genetics of inbreeding depression. *Nat. Rev. Genet.* 10:783–796.

Eilbeck K, Quinlan A, Yandell M. 2017. Settling the score: Variant prioritization and Mendelian disease. *Nat. Rev. Genet.* [Internet] 18:599–612. Available from: http://dx.doi.org/10.1038/nrg.2017.52

Fitzpatrick SW, Bradburd GS, Kremer CT, Salerno PE, Angeloni LM, Funk WC. 2020. Genomic and Fitness Consequences of Genetic Rescue in Wild Populations. *Curr. Biol.* [Internet] 30:1–6. Available from: https://doi.org/10.1016/j.cub.2019.11.062

Fitzpatrick SW, Funk WC. 2019. Genomics for Genetic Rescue. In: Wildlife Conservation Genomics.

Frankham R. 2015. Genetic rescue of small inbred populations: meta-analysis reveals large and consistent benefits of gene flow. *Mol. Ecol.* 24:2610–2618.

Frankham R, Ballou JD, Ralls K, Eldridge M, Dudash MR, Fenster CB, Lacy RC, Sunnucks P. 2017. Genetic Management of Fragmented Animal and Plant Populations. Oxford, UK: Oxford University Press

Grossen C, Guillaume F, Keller LF, Croll D. 2020. Purging of highly deleterious mutations through severe bottlenecks in Alpine ibex. *Nat. Commun.* [Internet] 11:1001. Available from: http://dx.doi.org/10.1038/s41467-020-14803-1

Haller BC, Messer PW. 2019. SLiM 3: Forward Genetic Simulations Beyond the Wright-Fisher Model. *Mol. Biol. Evol.* 36:632–637.

Harris K, Zhang Y, Nielsen R. 2019. Genetic rescue and the maintenance of native ancestry. *Conserv. Genet.* [Internet] 20:59–64. Available from: http://link.springer.com/10.1007/s10592-018-1132-1

Heber Sol, Briskie J V., Apiolaza LA. 2012. A test of the "genetic rescue" technique using bottlenecked donor populations of Drosophila melanogaster. *PLoS One* 7.

Heber S., Varsani A, Kuhn S, Girg A, Kempenaers B, Briskie J. 2012. The genetic rescue of two bottlenecked South Island robin populations using translocations of inbred donors. *Proc. R. Soc. B Biol. Sci.* [Internet] 280. Available from: http://rspb.royalsocietypublishing.org/cgi/doi/10.1098/rspb.2012.2228

Hedrick PW. 2002. Lethals in Finite Populations. *Evolution (N. Y).* 56:654–657.

Hedrick PW, Adams JR, Vucetich JA. 2011. Reevaluating and Broadening the Definition of Genetic Rescue. *Conserv. Biol.* 25:1069–1070.

Hedrick PW, Garcia-Dorado A. 2016. Understanding Inbreeding Depression, Purging, and Genetic Rescue. *Trends Ecol. Evol.* [Internet] 31:940–952. Available from: http://dx.doi.org/10.1016/j.tree.2016.09.005

Hedrick PW, Peterson RO, Vucetich LM, Adams JR, Vucetich JA. 2014. Genetic rescue in Isle Royale wolves: genetic analysis and the collapse of the population. *Conserv. Genet.* 15:1111–1121.

Hedrick PW, Robinson JA, Peterson RO, Vucetich JA. 2019. Genetics and extinction and the example of Isle Royale wolves. *Anim. Conserv.* [Internet] 22:302–309. Available from: http://doi.wiley.com/10.1111/acv.12479

Henn BM, Botigué LR, Peischl S, Dupanloup I, Lipatov M, Maples BK, Martin AR, Musharoff S, Cann H, Snyder MP, et al. 2016. Distance from sub-Saharan Africa predicts mutational load in diverse human genomes. *Proc. Natl. Acad. Sci.* [Internet] 113:E440–E449. Available from: http://www.pnas.org/lookup/doi/10.1073/pnas.1510805112

Hogg JT, Forbes SH, Steele BM, Luikart G. 2006. Genetic rescue of an insular population of

large mammals. *Proc. R. Soc. B* [Internet] 273:1491–1499. Available from: http://rspb.royalsocietypublishing.org/cgi/doi/10.1098/rspb.2006.3477

Huber CD, Durvasula A, Hancock AM. 2018. Gene expression drives the evolution of dominance. *Nat. Commun.* [Internet] 9:1–11. Available from: http://dx.doi.org/10.1038/s41467-018-05281-7

Huber CD, Kim BY, Marsden CD, Lohmueller KE. 2017. Determining the factors driving selective effects of new nonsynonymous mutations. *Proc. Natl. Acad. Sci.* 114:4465–4470.

Johnson WE, Onorato DP, Roelke ME, Land ED, Cunningham M, Belden RC, McBride R, Jansen D, Lotz M, Shindle D, et al. 2010. Genetic restoration of the Florida panther. *Science (80-.).* 329:1641–1645.

Kim BY, Huber CD, Lohmueller KE. 2017. Inference of the Distribution of Selection Coefficients for New Nonsynonymous Mutations Using Large Samples. *Genetics* [Internet] 206:345–361. Available from: http://www.genetics.org/content/genetics/206/1/345.full.pdf

Kimura M, Maruyama T, Crow JF. 1963. The mutation load in small populations. *Genetics*:1303–1312.

Lande R. 1994. Risk of population extinction from fixation of new deleterious mutations. *Evolution (N. Y).* 48:1460–1469.

Laws RJ, Jamieson IG. 2011. Is lack of evidence of inbreeding depression in a threatened New Zealand robin indicative of reduced genetic load? *Anim. Conserv.* 14:47–55.

Lindblad-Toh K, Wade CM, Mikkelsen TS, Karlsson EK, Jaffe DB, Kamal M, Clamp M, Chang JL, Kulbokas EJ, Zody MC, et al. 2005. Genome sequence, comparative analysis and haplotype structure of the domestic dog. *Nature* 438:803–819.

Lynch M, Conery IJ, Burger R. 1995. Mutation accumulation and the extinction of small

populations. *Am. Nat.* 146:489–518.

Lynch M, Gabriel W. 1990. Mutation load and the survival of small populations. *Evolution (N. Y).* 44:1725–1737.

McCune AR, Fuller RC, Aquilina AA, Dawley RM, Fadool JM, Houle D, Travis J, Kondrashov AS. 2002. A low genomic number of recessive lethals in natural populations of bluefin killifish and zebrafish. *Science (80-.).* 296:2398–2401.

McLaren BE, Peterson RO. 1994. Wolves, Moose, and Tree Rings on Isle Royale. *Science (80-.).* 266:1555–1558.

Mech LD. 1966. The Wolves of Isle Royale.

Nei M. 1968. The frequency distribution of lethal chromosomes in finite populations. *Proc. Natl. Acad. Sci.* 60:517–524.

O'Grady JJ, Brook BW, Reed DH, Ballou JD, Tonkyn DW, Frankham R. 2006. Realistic levels of inbreeding depression strongly affect extinction risk in wild populations. *Biol. Conserv.* 133:42–51.

Peterson RO, Page RE, Dodge KM. 1984. Wolves, Moose, and the Allometry of Population Cycles. *Science (80-.).* 224:1350–1352.

Pickup M, Field DL, Rowell DM, Young AG. 2012. Source population characteristics affect heterosis following genetic rescue of fragmented plant populations. *Proc. R. Soc. B* 280:1–9.

Ralls K, Sunnucks P, Lacy RC, Frankham R. 2020. Genetic rescue: A critique of the evidence supports maximizing genetic diversity rather than minimizing the introduction of putatively harmful genetic variation. *Biol. Conserv.* [Internet] 251:108784. Available from: https://doi.org/10.1016/j.biocon.2020.108784

Reed DH, Frankham R. 2003. Correlation between Fitness and Genetic Diversity. *Conserv. Biol.* 17:230–237.

Robinson JA, Brown C, Kim BY, Lohmueller KE, Wayne RK. 2018. Purging of Strongly Deleterious Mutations Explains Long-Term Persistence and Absence of Inbreeding Depression in Island Foxes. *Curr. Biol.* [Internet] 28:3487-3494.e4. Available from: https://doi.org/10.1016/j.cub.2018.08.066

Robinson JA, Ortega-Del Vecchyo D, Fan Z, Kim BY, Vonholdt BM, Marsden CD, Lohmueller KE, Wayne RK. 2016. Genomic Flatlining in the Endangered Island Fox. *Curr. Biol.* [Internet] 26:1183–1189. Available from: http://dx.doi.org/10.1016/j.cub.2016.02.062

Robinson JA, Räikkönen J, Vucetich LM, Vucetich JA, Peterson RO, Lohmueller KE, Wayne RK. 2019. Genomic signatures of extensive inbreeding in Isle Royale wolves, a population on the threshold of extinction. *Sci. Adv.* 5:1–13.

Simmons MJ, Crow JF. 1977. Mutations affecting fitness in Drosophila populations. *Ann. Rev. Genet.* 11:49–78.

Spielman D, Brook BW, Frankham R. 2004. Most species are not driven to extinction before genetic factors impact them. *Proc. Natl. Acad. Sci.* 101:15261–15264.

Szpiech ZA, Mak ACY, White MJ, Hu D, Eng C, Burchard EG, Hernandez RD. 2019. Ancestry-Dependent Enrichment of Deleterious Homozygotes in Runs of Homozygosity. *Am. J. Hum. Genet.* [Internet] 105:747–762. Available from: https://doi.org/10.1016/j.ajhg.2019.08.011

Teixeira JC, Huber CD. 2020. Dismantling a dogma: the inflated significance of neutral genetic diversity in conservation genetics. *arXiv*:1–31.

Van Der Valk T, Manuel M De, Marquez-Bonet T, Guschanski K. 2019. Estimates of genetic

load suggest extensive genetic purging in mammalian populations. *bioRxiv*.

Wayne R, Lehman N, Girman D, Gogan P, Gilbert D, Hansen K, Peterson R, Seal U, Eisenhawer A, Mech L, et al. 1991. Conservation Genetics of the Endangered Isle Royale Gray Wolf. *Conserv. Biol.* 5:41–51.

Whiteley AR, Fitzpatrick SW, Funk WC, Tallmon DA. 2015. Genetic rescue to the rescue. *Trends Ecol. Evol.* [Internet] 30:42–49. Available from: http://dx.doi.org/10.1016/j.tree.2014.10.009

Xue Y, Prado-Martinez J, Sudmant PH, Narasimhan V, Ayub Q, Szpak M, Frandsen P, Chen Y, Yngvadottir B, Cooper DN, et al. 2015. Mountain gorilla genomes reveal the impact of long-term population decline and inbreeding. *Science (80-.).* 348:242–245.

Chapter 2: The critically endangered vaquita is not doomed to extinction by inbreeding depression

Originally published in *Science*

Supplementary materials available online from *Science:*

https://www.science.org/doi/full/10.1126/science.abm1742

Abstract

In cases of severe wildlife population decline, a key question is whether recovery efforts will be impeded by genetic factors such as inbreeding depression. Decades of excess mortality from gillnet fishing have driven Mexico's vaquita porpoise (*Phocoena sinus*) to ~10 remaining individuals. We analyzed whole genome sequences from 20 vaquitas and integrated genomic and demographic information into stochastic, individual-based simulations to quantify the species' recovery potential. Our analysis suggests the vaquita's historical rarity has resulted in a low burden of segregating deleterious variation, reducing the risk of inbreeding depression. Similarly, genome-informed simulations suggest the vaquita can recover if bycatch mortality is immediately halted. This study provides hope for vaquitas and other naturally rare endangered species and highlights the utility of genomics in predicting extinction risk.

Main Text

A central question for populations that have undergone severe declines is whether recovery is possible, or if it may be hindered by deleterious genetic factors (Wiedenfeld et al. 2021). Perhaps the most immediate genetic threat in populations of very small size (<25 individuals) is the deterioration of fitness due to inbreeding depression (Keller and Waller 2002; Charlesworth and Willis 2009). Thus, predicting the threat of inbreeding depression under various genetic and demographic conditions is essential for the conservation of endangered species.

The critically endangered vaquita porpoise (*Phocoena sinus*), found only in the northernmost Gulf of California, Mexico, has declined from ~600 individuals in 1997 to around 10 individuals at present (Jaramillo-Legorreta et al. 2019). This precipitous decline has been driven by incidental mortality in fishing gillnets (bycatch) ((see Supplemental Methods; Jaramillo-Legorreta et al. 2019); Figure 2.1A). Efforts to reduce the intensity of illegal gillnet fishing and implement stronger protections for vaquitas have not been successful, and vaquitas are now considered the most endangered marine mammal (Jaramillo-Legorreta et al. 2019). A recent viability analysis found that the vaquita population could theoretically rebound if bycatch mortality is eliminated (Cisneros-Mata et al. 2021). However, the degree to which genetic factors may prevent a robust recovery is unknown, leading some to argue that the species is doomed to extinction from genetic threats (see discussion in (Taylor and Rojas-Bracho 1999; Sonne et al. 2021; Wiedenfeld et al. 2021)).

Population viability analysis (PVA) has long been an important tool for modelling extinction risk (Brook et al. 2000). However, it is often challenging to parameterize PVA models for highly

endangered species where information on the potential impact of inbreeding depression is limited. Genomic data offer a potential solution, as they can be used to estimate the fundamental genetic and demographic parameters underlying inbreeding depression. Although the potential applications of genomics in conservation have been widely discussed (Allendorf et al. 2010; Lewin et al. 2018), genomics remain under-utilized in forecasts of population viability and extinction risk.

To investigate the impact of the vaquita's recent decline and to quantify the species' recovery potential, we sequenced genomic DNA of 19 archival tissue samples to high depth (total n = 20 including genome from (Morin et al. 2021), mean coverage = 60X; Table S2-1). Samples were obtained across three time periods: 1985-1993, 2004, and 2016-2017, spanning ~3 vaquita generations (assuming a generation time of 11.9 years; (Taylor et al. 2007)) and an estimated ~99% decline in population size (Figure 2.1A, (See Supplemental Methods)). All 20 vaquita genomes contain uniformly low heterozygosity (mean = 9.04×10^{-5}, standard deviation (S.D.) = 2.44×10^{-6} heterozygotes/site; Figure 2.1B and S2-1), consistent with a previous estimate from a single individual (Morin et al. 2021). Additionally, genome-wide diversity appears stable over the sampling period (Figure 2.1B, C), as expected given the short duration of the decline.

We also investigated whether vaquita genomes show signs of recent inbreeding. We found that the mean cumulative fraction of vaquita genomes in long (≥1 Mb) runs of homozygosity (ROH) is 5.42% (S.D. = 1.7%), implying a low average inbreeding coefficient of $F_{ROH} = 0.05$ (Figure 2.1D and Figure S2-2). Furthermore, ROH in our sample are relatively short (mean length 1.59-3.18 Mb), suggesting that they trace to a common ancestor from roughly 15-31 generations ago

(178-369 years; (See Supplemental Methods)). This result indicates that these ROH are a consequence of the vaquita's historically limited population size rather than recent inbreeding. Finally, we found limited evidence for close relatives in our dataset, aside from two known mother-fetus pairs (Figure S2-3).

To better characterize the vaquita's long-term demographic history, we used the distribution of allele frequencies to perform model-based demographic inference. Overall, we found good fit for a two-epoch model in which the vaquita effective population size (N_e) declined from 4,485 to 2,807 individuals ~2,162 generations ago (~25.7 KYA; (See Supplemental Methods); Figure 2.1E, figs. S4 and S5, tables S2 to S4). Thus, vaquitas have persisted at relatively small population sizes for at least tens of thousands of years, resulting in uniformly low genome-wide diversity that is among the lowest documented in any species to date (Morin et al. 2021). Here, we use 'long-term small population size' to mean N_e on the order of a few thousand individuals over thousands of generations, as opposed to 'small population size' meaning $N_e \leq 100$, as in some other contexts (e.g., (Kimura et al. 1963; Lynch et al. 1995))).

A predicted consequence of long-term small population size is the reduced efficacy of purifying selection against weakly deleterious alleles with selection coefficients $<<1/(2*N_e)$ (Kimura et al. 1963; Lynch et al. 1995). Such alleles can drift to high frequencies and become fixed, potentially contributing to reduced fitness. To investigate this, we compared the burden of putatively deleterious protein-coding variants in vaquitas with 11 other cetacean species (Table S2-2-5, Figure S2-6). Specifically, we focused on nonsynonymous mutations at sites under strong evolutionary constraint (Ng and Henikoff 2001), and loss-of-function (LOF) mutations that are

predicted to disrupt gene function. We used the ratio of deleterious to synonymous variants as a proxy for the efficacy of purifying selection (See Supplemental Methods) and used genome-wide heterozygosity as a proxy for N_e (Figure 2.2A, B and Figure S2-7). The ratio of deleterious variants is significantly negatively correlated with N_e (phylogenetic generalized least squares (PGLS) regression, $p_{del.} = 1.32x10^{-2}$, $p_{LOF} = 7.88x10^{-3}$), consistent with expectation. Among all species in our study, vaquitas have the highest proportional burden of deleterious alleles. Compared to the species with the next lowest diversity (orca, *Orcinus orca*), ratios for deleterious and LOF mutations in vaquitas are 1.14x and 1.23x higher, respectively. Furthermore, we demonstrate using simulations that this elevated ratio is minimally impacted by the vaquita's recent population decline, and is instead attributable to its historical population size (Figure S2-9; (See Supplemental Methods)). Similar trends exist for homozygous deleterious mutations, which includes variants that may be fixed in the species (Figure S2-8). Thus, elevated ratios of deleterious to neutral variation among polymorphisms (heterozygotes) and substitutions (homozygotes) in vaquitas are consistent with an accumulation of weakly deleterious alleles under long-term small population size. The remaining vaquita individuals appear healthy and are actively reproducing (Taylor et al. 2019; Gulland et al. 2020), suggesting the species' fitness has not been severely compromised by its longstanding elevated burden of weakly deleterious alleles.

A larger concern for vaquita recovery is future fitness declines due to inbreeding depression, given the inevitability of inbreeding in any recovery scenario. However, the risk of inbreeding depression (or "inbreeding load") is predicted to be reduced in species with long-term small population size because 1) increased homozygosity exposes recessive strongly deleterious alleles

to selection more frequently, and 2) drift decreases the absolute number of segregating recessive deleterious variants (Glémin 2003; Kyriazis et al. 2021). To assess the potential for future inbreeding depression in vaquitas relative to other cetaceans, we quantified the total number of heterozygous deleterious alleles per genome, which reflect alleles that could contribute to inbreeding depression when made homozygous through inbreeding. We found that the total number of heterozygous putatively deleterious alleles per genome is positively correlated with genome-wide diversity (PGLS $p_{del.} = 5.57x10^{-6}$, $p_{LOF} = 1.91x10^{-5}$) (Figure 2.2C, D). Among all cetaceans in our study, vaquitas harbor the fewest deleterious heterozygotes per genome. Compared to the orca, vaquitas have 0.33x and 0.36x the number of deleterious and LOF heterozygotes, respectively. Similar trends are evident in all mutation classes, including conserved noncoding regions (Figure S2-10). Thus, although vaquitas have an elevated proportion of deleterious relative to neutral variants (Figure 2.2A, B, S2-8), they nevertheless have a low absolute number of segregating deleterious variants (Figure 2.2C, D), implying a low inbreeding load.

To model potential recovery scenarios for the vaquita, we combined our genomic results with information about vaquita life history to parameterize stochastic, individual-based simulations using SLiM3 ((See Supplemental Methods; Haller and Messer 2019); Figure 2.3A, S2-11). These simulations were designed to model vaquita protein-coding regions, incorporating both neutral mutations and recessive deleterious mutations, the latter of which are thought to underlie inbreeding depression (McCune et al. 2002; Charlesworth and Willis 2009). We used our genomic dataset to estimate a vaquita mutation rate (Figure S2-12) as well as a distribution of selection coefficients for new mutations (Figure S2-13), and assumed an inverse relationship

between dominance and selection coefficients (See Supplemental Methods). Importantly, our model allows for deleterious mutations to drift to fixation and impact fitness (figs. S14 to S16; (See Supplemental Methods)). We used our demographic model (Figure 2.1E) to simulate the historical vaquita population (figs. S17 and S18), then initiated a bottleneck by introducing stochastic bycatch mortality at a rate calibrated to the empirical rate of recent decline as of 2018 (Figure 2.1A and S2-19; (See Supplemental Methods)). Finally, we allowed for recovery by reducing the bycatch mortality rate after the population reached a 'threshold population size' of 10 or fewer individuals, based on the current estimated population size.

We first used this model to examine the impact of varying levels of bycatch mortality on extinction risk over the next 50 years. We estimate a high probability of recovery if bycatch mortality ceases entirely, with only 6% of simulation replicates going extinct (Figs. 3B, 4A). In addition, simulated populations that persist exhibit substantial growth, with a mean population size in 2070 of 298.7 individuals (S.D. = 218.2; Figure 2.4A). However, if bycatch mortality rates are decreased by just 90%, extinction rates increase to 27% (Figs. 3B and 4B), with more limited recovery in population sizes (mean of 49.2 individuals in 2070, S.D. = 34.4; Figure 2.4B). Finally, if bycatch mortality rates are decreased by just 80%, extinction occurs in 62% of simulation replicates. Thus, recovery potential critically depends on reducing bycatch mortality rates, with even moderate levels of bycatch resulting in a high likelihood of extinction.

Next, we examined the importance of the threshold population size, given uncertainty in the 2018 estimate of 10 individuals (Jaramillo-Legorreta et al. 2019). As expected, extinction rates decrease when assuming a threshold population size of 20 and increase when assuming a

threshold population size of 5 (Figure 2.3B). These results emphasize that the number of remaining vaquita individuals is also a critical factor underlying extinction risk.

To quantify the inbreeding load in our model, we estimated the 'number of diploid lethal equivalents' (or *2B*), which characterizes the rate at which fitness is lost with increasing levels of inbreeding (Morton et al. 1956; Keller and Waller 2002). Typically, inbreeding load is quantified by comparing estimates of individual fitness and inbreeding in natural populations (Ralls et al. 1988; Keller and Waller 2002); however, such data do not exist for most species, including the vaquita. Under our simulation parameters, we estimate an inbreeding load of $2B = 0.95$ in vaquitas (Table S2-6), significantly lower than the median empirical estimate for mammals of 6.2 (Ralls et al. 1988), likely due to the vaquita's relatively small historical N_e. Nevertheless, simulations that exclude deleterious mutations result in a significantly lower extinction rate (Figure 2.3B), confirming that inbreeding depression impacts recovery potential in our model.

To further explore how the inbreeding load in our model depends on historical demography, we ran simulations with the historical N_e increased x20. We found an increased extinction rate of 52%, compared to 27% with our empirical population size parameters, with minimal recovery for replicates that persisted (mean of 16.2 individuals in 2070, S.D. = 14.5, Figure 2.4C). Additionally, with this larger historical N_e, we observe a greatly increased inbreeding load of $2B = 3.32$ (Figure S2-20 and Table S2-6). These findings further demonstrate the importance of the vaquita's natural rarity as a factor underlying their low inbreeding load and increased potential for recovery.

Given the uncertainty in many of our model parameters, we conducted sensitivity analyses varying the calving interval, mutation rate, distribution of dominance and selection coefficients, and target size for deleterious mutations (See Supplemental Methods). Although these factors influence extinction probabilities, recovery remains the likely outcome (>50% probability) in nearly all cases when assuming a threshold population size of 10 and a 90% reduction of bycatch mortality (Figure S2-21 and Table S2-6). Two notable exceptions to this are for models with a higher mutation rate, where we observed a 55% extinction rate compared to 27% in our 'base' model, and for models with decreased calving interval, where we also observed a 55% extinction rate (Figure S2-21 and Table S2-6). Thus, although uncertainty exists in our projections, the overall conclusion that recovery is possible if bycatch is greatly reduced remains robust to our model assumptions. Finally, we note that our simulations do not consider factors such as reduced adaptive potential or increased susceptibility to disease caused by low genetic variability, which may impact future persistence. Vaquitas have survived with low diversity for tens of thousands of years and have endured environmental changes in the past (Morin et al. 2021), suggesting that these factors alone do not doom the species to extinction. Conceivably, low diversity in the vaquita may limit the species' capacity to adapt to increasing global change over the long term, but this risk is challenging to quantify and should not preclude recovery efforts in the short term.

In conclusion, our results suggest there is a high potential for vaquita recovery in the absence of gillnet mortality, refuting the view that the species is doomed to extinction by genetic factors. Our approach leverages genomic data and methodology to forecast population viability and extinction risk, enabling a more nuanced assessment of the threat of genetic factors to persistence. The key aspect of the vaquita that our analysis reveals is that its historical population

size was large enough to prevent the fixation of all but weakly deleterious alleles, and small enough to reduce the inbreeding load from recessive strongly deleterious mutations. Numerous other examples of species rebounding from bottlenecks of similar magnitude to that of the vaquita have been documented (reviewed in (Wiedenfeld et al. 2021)). For example, many parallels exist between the vaquita and Channel Island foxes, which similarly have exceptionally low genetic diversity, yet were able to rebound from severe recent bottlenecks without apparent signs of inbreeding depression (Robinson et al. 2018). Together, these examples challenge the assumption that populations that have experienced catastrophic declines are genetically doomed and provide hope for the recovery of endangered species that are naturally rare. Finally, our analysis demonstrates the potential for genomics-informed population viability modelling, which may have widespread applications given the increasing feasibility of genomic sequencing for non-model species amid a worsening extinction crisis (Ceballos et al. 2020).

Figures

Figure 2.1

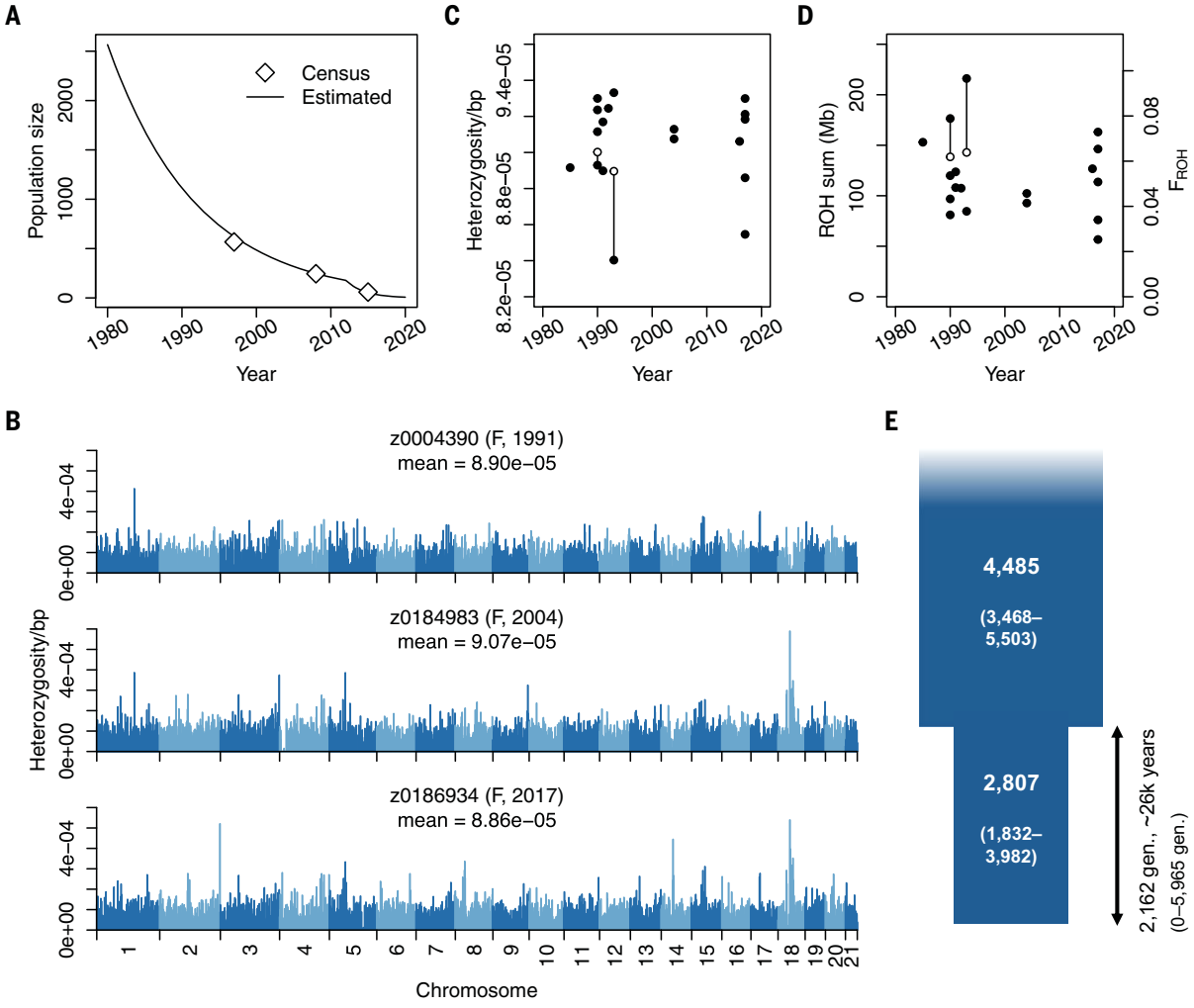

Figure 2.1. Vaquita genome-wide diversity and demographic history. (**A**) Model of vaquita census population size based on previous surveys (See Supplemental Methods) shows a dramatic recent decline. (**B**) Bar plots of per-site heterozygosity in 1-Mb genomic windows in three individuals (one from each sampling period; see Figure S2-1 for all) show little variability within or between individuals. (**C, D**) Genome-wide heterozygosity and ROH burden are consistent between sampling periods. Lines connect mother-fetus pairs; open symbols indicate offspring.

(**E**) Two-epoch demographic model inferred with ∂a∂i. Parameter 95% confidence intervals indicated in parentheses.

Figure 2.2

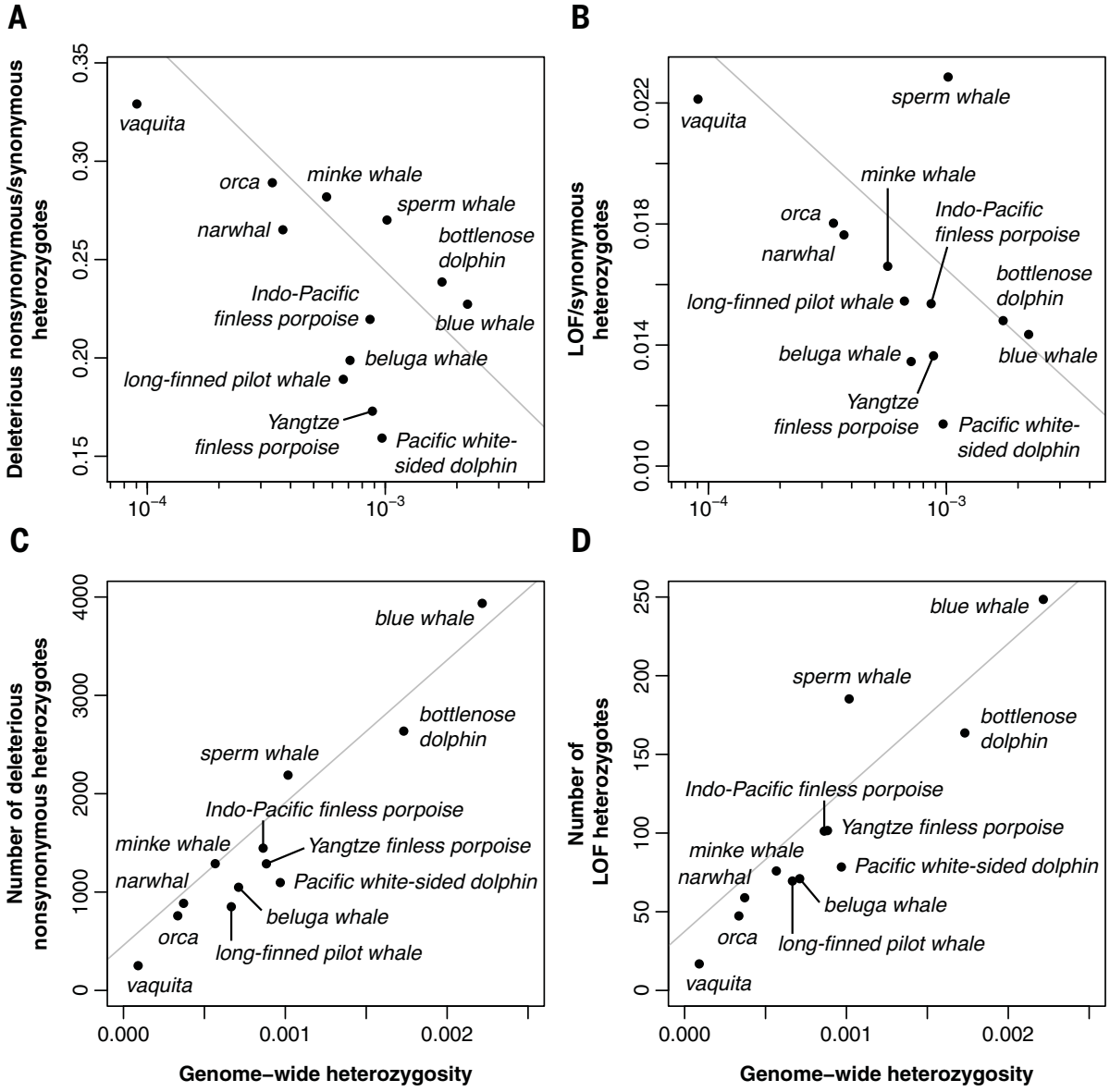

Figure 2.2. Deleterious variation in vaquitas and other cetaceans. Ratios of deleterious nonsynonymous (A) and LOF (B) heterozygotes to synonymous heterozygotes are significantly negatively correlated with genome-wide heterozygosity (per bp, log-scaled). Total numbers of deleterious nonsynonymous (C) and LOF (D) heterozygotes per genome are significantly positively correlated with genome-wide heterozygosity (per bp). Grey lines show phylogeny-corrected regressions.

Figure 2.3

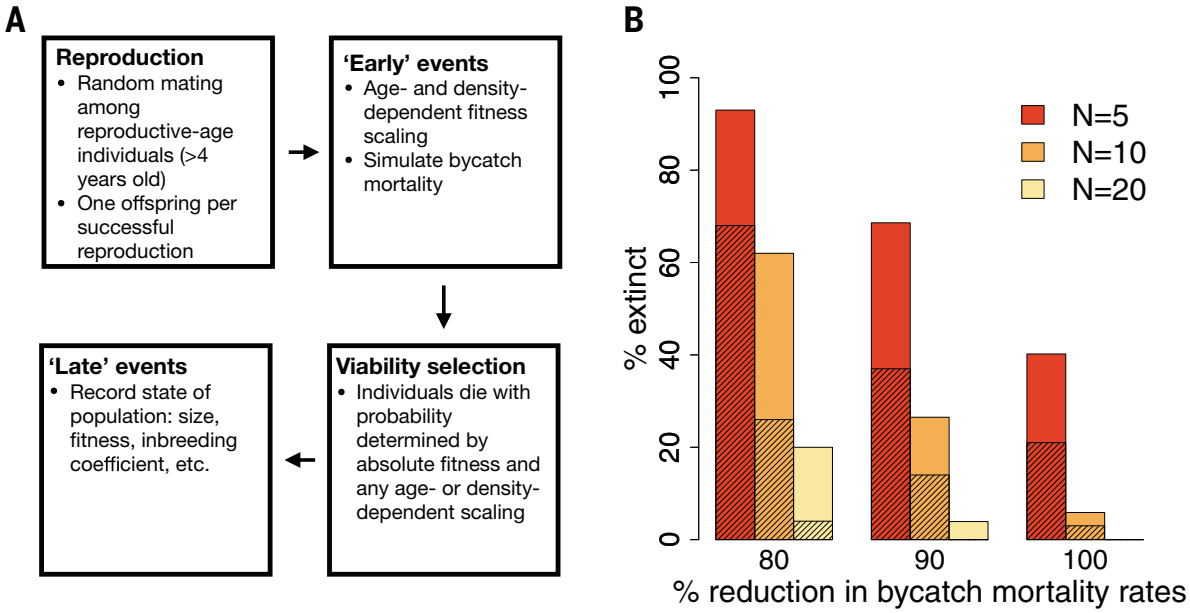

Figure 2.3. Model schematic and extinction rates under various simulation parameters. (A) Diagram of events that occur during one year in our SLiM simulation model. (B) Percent of replicates going extinct over the next 50 years under varying recovery parameters. Shading indicates extinction rates when only neutral mutations are simulated, and "N" represents the threshold population size.

Figure 2.4

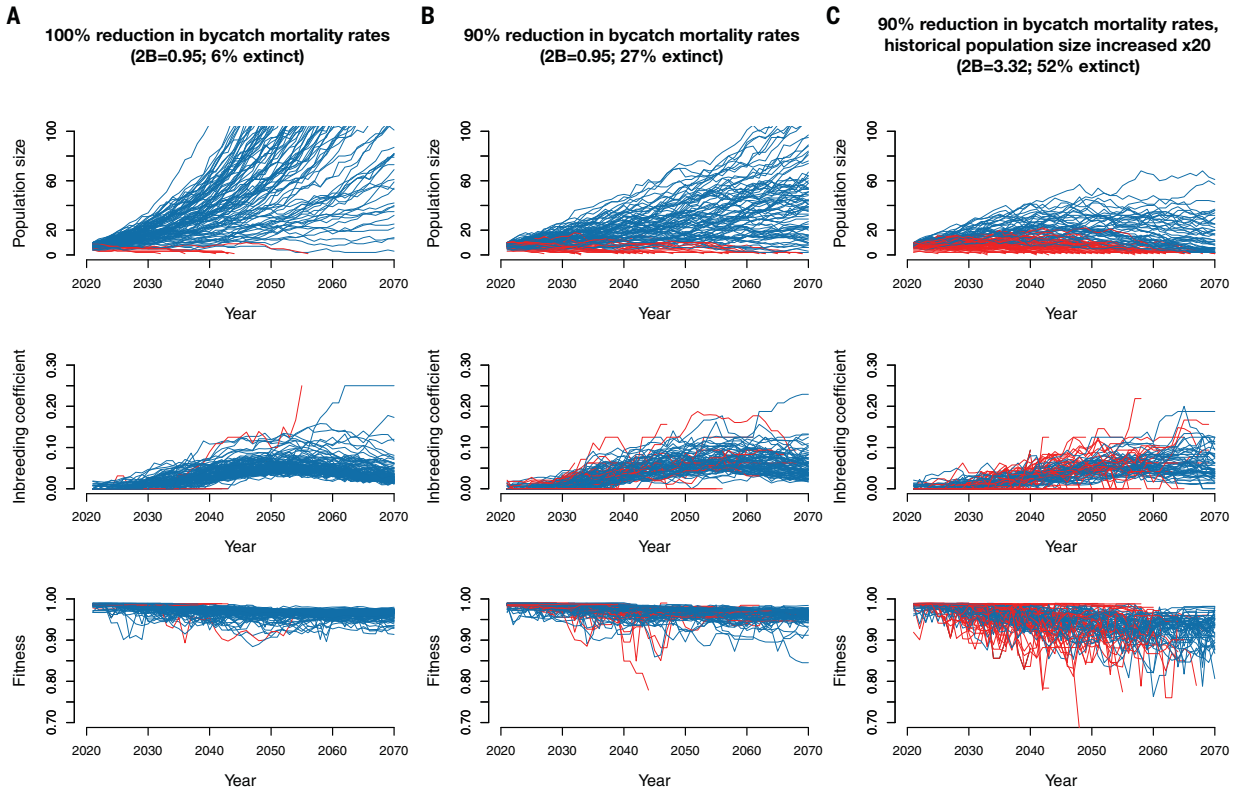

Figure 2.4. Simulation trajectories under various recovery scenarios. (A) Simulation trajectories under empirically-inferred historical demographic parameters assuming a reduction in bycatch mortality of 100%. (B) Simulation trajectories with bycatch mortality rate decreased by only 90%. (C) Simulation trajectories with historical population size increased x20 and assuming a decrease in bycatch mortality of 90%. For all simulations, we assumed a population size threshold of 10 individuals. Replicates that went extinct are colored red and replicates that persisted are colored blue.

References

Allendorf FW, Hohenlohe PA, Luikart G. 2010. Genomics and the future of conservation genetics. *Nat. Rev. Genet.* [Internet] 11:697–709. Available from: http://dx.doi.org/10.1038/nrg2844

Brook BW, O'Grady JJ, Chapman AP, Burgman MA, Resit Akçakaya H, Frankham R. 2000. Predictive accuracy of population viability analysis in conservation biology. *Nature* 404:385–387.

Ceballos G, Ehrlich PR, Raven PH. 2020. Vertebrates on the brink as indicators of biological annihilation and the sixth mass extinction. *Proc. Natl. Acad. Sci. U. S. A.* 117:13596–13602.

Charlesworth D, Willis JH. 2009. The genetics of inbreeding depression. *Nat. Rev. Genet.* 10:783–796.

Cisneros-Mata MA, Delgado JA, Rodríguez-Félix D. 2021. Viability of the vaquita, Phocoena sinus (Cetacea: Phocoenidae) population, threatened by poaching of Totoaba macdonaldi (Perciformes: Sciaenidae). *Rev. Biol. Trop.* 69:588–600.

Glémin S. 2003. How Are Deleterious Mutations Purged? Drift versus Nonrandom Mating. *Evolution (N. Y).* 57:2678–2687.

Gulland F, Danil K, Bolton J, Ylitalo G, Okrucky RS, Rebolledo F, Alexander-Beloch C, Brownell RL, Mesnick S, Lefebvre K, et al. 2020. Vaquitas (Phocoena sinus) continue to die from bycatch not pollutants. *Vet. Rec.* 187:1–4.

Haller BC, Messer PW. 2019. SLiM 3: Forward Genetic Simulations Beyond the Wright-Fisher Model. *Mol. Biol. Evol.* 36:632–637.

Jaramillo-Legorreta AM, Cardenas-Hinojosa G, Nieto-Garcia E, Rojas-Bracho L, Thomas L, Hoef JMV, Moore J, Taylor B, Barlow J, Tregenza N. 2019. Decline towards extinction of

Mexico's vaquita porpoise (Phocoena sinus). *R. Soc. Open Sci.* 6.

Keller L, Waller DM. 2002. Inbreeding effects in wild populations. *Trends Ecol. Evol.* 17:19–23.

Kimura M, Maruyama T, Crow JF. 1963. The mutation load in small populations. *Genetics*:1303–1312.

Kyriazis CC, Wayne RK, Lohmueller KE. 2021. Strongly deleterious mutations are a primary determinant of extinction risk due to inbreeding depression. *Evol. Lett.* 5:33–47.

Lewin HA, Robinson GE, Kress WJ, Baker WJ, Coddington J, Crandall KA, Durbin R, Edwards S V., Forest F, Gilbert MTP, et al. 2018. Earth BioGenome Project: Sequencing life for the future of life. *Proc. Natl. Acad. Sci. U. S. A.* 115:4325–4333.

Lynch M, Conery IJ, Burger R. 1995. Mutation accumulation and the extinction of small populations. *Am. Nat.* 146:489–518.

McCune AR, Fuller RC, Aquilina AA, Dawley RM, Fadool JM, Houle D, Travis J, Kondrashov AS. 2002. A low genomic number of recessive lethals in natural populations of bluefin killifish and zebrafish. *Science (80-.).* 296:2398–2401.

Morin PA, Archer FI, Avila CD, Balacco JR, Bukhman Y V., Chow W, Fedrigo O, Formenti G, Fronczek JA, Fungtammasan A, et al. 2021. Reference genome and demographic history of the most endangered marine mammal, the vaquita. *Mol. Ecol. Resour.* 21:1008–1020.

Morton NE, Crow JF, Muller HJ. 1956. An Estimate of the Mutational Damage in Man From Data on Consanguineous Marriages. *Proc. Natl. Acad. Sci.* [Internet] 42:855–863. Available from: http://www.ncbi.nlm.nih.gov/entrez/query.fcgi?db=pubmed&cmd=Retrieve&dopt=AbstractPlus&list_uids=16589958

Ng PC, Henikoff S. 2001. Predicting Deleterious Amino Acid Substitutions Predicting

Deleterious Amino Acid Substitutions. *Genome Res.* [Internet] 11:863–874. Available from: www.genome.org/cgi/doi/10.1101/ gr.176601

Ralls K, Ballou JD, Templeton A, Ralls K, Ballou JD. 1988. Estimates of Lethal Equivalents and the Cost of Inbreeding in Mammals. *Soc. Conserv. Biol.* 2:185–193.

Robinson JA, Brown C, Kim BY, Lohmueller KE, Wayne RK. 2018. Purging of Strongly Deleterious Mutations Explains Long-Term Persistence and Absence of Inbreeding Depression in Island Foxes. *Curr. Biol.* [Internet] 28:3487-3494.e4. Available from: https://doi.org/10.1016/j.cub.2018.08.066

Sonne C, Diaz-Jaimes P, Adams DH. 2021. Mexico's final death blow to the vaquita. *Science (80-.).* 373:863–864.

Taylor BL, Chivers SJ, Larese J, Perrin WF. 2007. Generation length and percent mature estimates for IUCN assessments of cetaceans.

Taylor BL, Rojas-Bracho L. 1999. Examining the Risk of Inbreeding Depression in a Naturally Rare Cetacean , the Vaquita (Phocoena Sinus)'. *Mar. Mammal Sci.* 15:1004–1028.

Taylor BL, Wells RS, Olson PA, Brownell RL, Gulland FMD, Read AJ, Valverde-Esparza FJ, Ortiz-García OH, Ruiz-Sabio D, Jaramillo-Legorreta AM, et al. 2019. Likely annual calving in the vaquita, Phocoena sinus: A new hope? *Mar. Mammal Sci.* 35:1603–1612.

Wiedenfeld DA, Alberts AC, Angulo A, Bennett EL, Byers O, Contreras-MacBeath T, Drummond G, da Fonseca GAB, Gascon C, Harrison I, et al. 2021. Conservation resource allocation, small population resiliency, and the fallacy of conservation triage. *Conserv. Biol.* 35:1388–1395.

Chapter 3: Genomic underpinnings of population persistence in Isle Royale moose

In revision at *Molecular Biology and Evolution*

Supplementary materials available online as this dissertation's Supplementary Materials: Chapter3_Supplementary_Information.pdf

Abstract

Island ecosystems provide models to assess the impacts of isolation on population persistence. However, most studies of persistence have focused on a single species, without comparisons to other organisms they interact with in the ecosystem. The simple predator-prey system of moose and gray wolves on Isle Royale provides allows a direct contrast of genetic variation in a prey species with their natural predator. Wolves on Isle Royale exhibited signs of severe inbreeding depression, which nearly drove the population to extinction in 2019. In the relative absence of wolves, the moose population has thrived and exhibits no obvious signs of inbreeding depression despite being isolated for ~120 years. Here, we examine the genomic underpinnings of population persistence in the Isle Royale moose population. We document high levels of inbreeding in the population, roughly as high as the wolf population at the time of its decline. However, inbreeding in the moose population manifests in the form of intermediate-length runs of homozygosity indicative of gradual inbreeding, contrasting with the severe recent inbreeding observed in the wolf population. Using simulations, we demonstrate that this more gradual inbreeding in the moose population has resulted in an estimated 50% purging of the inbreeding load. However, we also document notable increases in genetic load, which could eventually threaten population viability over the long term. Overall, our results demonstrate a complex relationship between inbreeding, genetic diversity, and population viability that

highlights the importance of maintaining isolated populations at moderate size to avert extinction from genetic factors.

Introduction

Anthropogenic habitat fragmentation has dramatically increased the number of isolated and inbred populations (Haddad et al. 2015). To conserve these populations, a crucial question is whether they will be able to persist in isolation, or if they will be driven to extinction by deleterious genetic factors, such as inbreeding depression (Hedrick and Garcia-Dorado 2016). Numerous examples exist of inbreeding depression driving population decline in isolated populations (reviewed in (Keller and Waller 2002)). However, in some populations, harmful recessive mutations may potentially be 'purged' by purifying selection and such purging may avert inbreeding depression (Glémin 2003; Xue et al. 2015; Hedrick and Garcia-Dorado 2016; Robinson et al. 2018; Grossen et al. 2020; Pérez-Pereira et al. 2021). Purging may be most effective in populations where inbreeding is gradual due to a moderate population size (Day et al. 2003; Glémin 2003; Pekkala et al. 2012; Robinson et al. 2018; Kyriazis et al. 2021; Pérez-Pereira et al. 2021). However, the extent to which purging is a relevant factor for the conservation of threatened populations, and more broadly, the degree to which populations can persist with low genome-wide diversity, is controversial (Ralls et al. 2020; Kardos et al. 2021; Khan et al. 2021; Kyriazis et al. 2021; Teixeira and Huber 2021; Kleinman-Ruiz et al. 2022; Pérez-Pereira et al. 2022; Willi et al. 2022).

One of the best-studied examples of inbreeding depression driving population decline is the gray wolf population on Isle Royale, an island in Lake Superior roughly 544 km^2 in area. After ~70 years of isolation at a population size of ~25 individuals, the Isle Royale wolf population declined nearly to extinction, with just two individuals remaining in the population in 2018 (Hoy, Peterson, et al. 2020). Recent research has demonstrated that this population collapse was a

consequence of severe inbreeding depression in the form of widespread congenital deformities (Hedrick et al. 2019; Robinson et al. 2019). The decline of the Isle Royale wolf population allowed its main prey, moose, to thrive. The most recent moose census count was ~2000 individuals, though the population generally numbers ~1000 individuals (Hoy, Peterson, et al. 2020). Moreover, despite the moose population having low genetic diversity and being isolated on the island for ~120 years (Murie 1934; Mech 1966; Wilson et al. 2003; Sattler et al. 2017), it exhibits no obvious signs of inbreeding depression and has population growth rates similar to mainland populations (Hoy, MacNulty, et al. 2020). Thus, the contrasting fates of the Isle Royale wolf and moose populations provides a compelling case study for understanding the genetic underpinnings of population persistence in isolation and effects on predator-prey dynamics.

Outside of the Isle Royale population, North American moose are also known to have low genetic diversity relative to Eurasian moose, which is thought to be a consequence of a relatively recent founder event following the Last Glacial Maximum (Hundertmark et al. 2002; Hundertmark et al. 2003; Decesare et al. 2020). Evidence for this recent founder also comes from a relative lack of population structure across North America as well as the near absence of moose in the North American fossil record prior to 15,000 years ago (Hundertmark et al. 2002; Hundertmark et al. 2003; Decesare et al. 2020; Dussex 2020). Depending on how recent and severe this founding bottleneck was, the effects of purging associated with the bottleneck may still be apparent in the North American moose population. Thus, the ability of moose to persist in isolation on Isle Royale may be enhanced by purging from historical bottlenecks.

Here, we use a dataset of high coverage whole genome sequences from 20 North American moose and one Eurasian moose to characterize the impacts of bottlenecks, population isolation, and purging in North American moose, focusing on the Isle Royale population. We confirm previous findings of low genetic diversity in North American moose, especially Isle Royale moose, where levels of inbreeding are comparable to that of the Isle Royale gray wolf population at the time of its decline. Furthermore, we demonstrate that this low diversity is a consequence of severe founder events in both the North American and Isle Royale populations. Finally, we conduct extensive simulations exploring the impact of bottlenecks and population isolation on genetic load and purging in North American moose. These results suggest substantial purging associated with founding bottlenecks for the North American and Isle Royale populations. However, this purging also has been accompanied by a notable increase in genetic load. Overall, our analysis provides insight into how populations can persist despite severe bottlenecks and high inbreeding and emphasizes the importance of maintaining moderate population size to ensure viability in isolated populations. Moreover, our results highlight the differential impacts of inbreeding depression in isolated predator and prey populations, with implications for maintaining healthy ecosystems in the increasingly-fragmented landscape of the Anthropocene.

Results

Sampling and population structure

To examine patterns of moose genetic diversity in North America, we generated a high-coverage whole genome sequencing dataset for nine moose sampled from Minnesota and seven moose sampled from Isle Royale between 2005 and 2014. We added existing moose genomes to our dataset from Sweden, Alaska, Idaho, Wyoming, and Vermont. These genomes were aligned,

genotyped, and annotated relative to the cattle reference genome (ARS-UCD1.2). Although a moose reference genome was recently published (Dussex 2020), we used the more distantly-related cattle reference in order to leverage its fully assembled chromosomes and high-quality annotations (see SI for further discussion). Average sequencing coverage after mapping was 21x (range 11-27; Table S1).

We first used these data to characterize population structure among North American moose, primarily aiming to assess evidence for isolation of the Isle Royale population. Principal component analysis (PCA) revealed a tight clustering of Isle Royale samples relative to other North American samples, which were distinctly clustered on the first PC (Figure 3.1B). However, when down-sampled to one individual per North American population, the Isle Royale and Minnesota samples grouped more closely together, with overall patterns roughly reflecting North American geography (Figure 3.1B, inset). Nevertheless, we observe notable differentiation between Isle Royale and Minnesota samples, with a mean $F_{ST} = 0.083$. These patterns were also reflected in a tree based on identity-by-state, which found a tight clustering of Isle Royale samples nested within other North American samples (Figure 3.1C). Furthermore, using fastSTRUCTURE analysis we found no evidence for admixture between Isle Royale and mainland

samples (Figure 3.1D and S3.1-2). Finally, we also estimated kinship for all North American samples, and found that the mainland samples are not closely related to one another (Figure 3.S3). However, two pairs of samples from Isle Royale exhibited kinship coefficients consistent with first-order relationships (mean kinship = 0.234; Figure S3-3). In summary, these findings

suggest that the Isle Royale population has been entirely isolated from nearby mainland moose populations as suggested by previous work (Wilson et al. 2003; Sattler et al. 2017), and provide a general characterization of moose population structure in North America.

Genetic diversity and inbreeding

Next, we examined levels of genetic diversity and inbreeding across sampled individuals. Overall, we find that moose have relatively low diversity compared to other mammals (Figure 3.2), though these estimates may be slightly downward biased due to using a distant reference genome (see SI for discussion). However, these biases do not impact estimates of relative diversity across moose populations, where several notable patterns are apparent. First, we observe substantially lower diversity in North American samples relative to a sample from Sweden, with a decrease of at least ~34% (Figure 3.2). This decrease in diversity is likely associated with a founder event for North American moose that is thought to have occurred during the last ~15,000 years (Hundertmark et al. 2002; Hundertmark et al. 2003; Decesare et al. 2020). We observe further reductions in diversity in the Isle Royale population, with an estimated reduction of ~30% compared to samples from Minnesota (Figure 3.2). Surprisingly, we find even lower diversity in mainland samples from Idaho, Wyoming, and Vermont, possibly due to these samples being near the southern range edge, where population densities are generally low and declining ((Timmermann and Rodgers 2017); Figure 3.2).

Mirroring these patterns of genetic diversity, the impact of inbreeding was prevalent across North American samples in the form of abundant runs of homozygosity (ROH), chromosomal segments that are inherited identical by descent from a recent common ancestor (Kirin et al.

2010). Specifically, we observed high levels of inbreeding in samples from Isle Royale, Vermont, Idaho, and Wyoming, with ~35% of their autosomal genomes being covered by ROH >100 kb on average (Figure 3.2) and ~26% covered by ROH >1 Mb (Figure S3-5). As this fraction represents an estimate of the inbreeding coefficient (F_{ROH}), this result suggests that these populations are on average more inbred than an offspring from a full-sib mating (F=0.25). Notably, these levels of inbreeding are comparable to the Isle Royale gray wolf population, where ~20-50% of their autosomal genomes contained ROH >100 kb (Robinson et al. 2019). By contrast, much lower levels of inbreeding were present in samples from Minnesota, Alaska, and Sweden, with ~12% of these genomes covered by ROH >100 kb (Figure 3.2), and ~3% covered in ROH >1 Mb (Figure S3-5).

Demographic inference

To understand the demographic processes accounting for these patterns of genetic diversity and inbreeding, we fitted demographic models to the site frequency spectrum (SFS) using ∂a∂i (Gutenkunst et al. 2009). Briefly, this approach uses observed allele frequency information to estimate demographic parameters for a model with an arbitrary number of population size changes (epochs). Our first aim was to estimate the severity of the North American founding bottleneck, given the apparent impact of this bottleneck on observed levels of genetic diversity between Eurasian and North American moose (Figure 3.2; (Hundertmark et al. 2002)). We generated a folded SFS for our Minnesota sample, and inferred various population size change models including one, two, three, and four epoch models. Overall, the best-fitting model was a four-epoch model that included two ancestral epochs followed by a severe bottleneck to an effective population size (N_e) of 49 for 29 generations and then expansion to N_e=193,472 for the

last 1,179 generations (Figure 3.3). Bottlenecks that are mild with long duration can lead to similar patterns in the SFS as short and severe bottlenecks (Beichman et al. 2022). Consequently, we found a similar fit for a model with a slightly more prolonged and less severe bottleneck of N_e=218 for 142 generations followed by expansion to N_e=105,531 for the last 1,223 generations (Table S3-2). Overall, both of these models are consistent in detecting a strong bottleneck of N_e = ~50-225 for ~30-150 generations followed by dramatic population growth taking place ~1,200 years ago. The timing of expansion at ~1,200 generations suggests a recent spread of moose across North America starting ~9,600 years ago, assuming a generation time of 8 years (Gaillard 2007).

Our next aim for demographic inference was to obtain an estimate of the effective population size of the Isle Royale moose population after its founding ~120 years ago using the SFS from our Isle Royale sample. Given the shared evolutionary history of the Minnesota and Isle Royale populations prior to their divergence, we fixed the demographic parameters of our four-epoch model inferred from the Minnesota samples (Figure 3.3), then added a fifth epoch to this model representing the founding of Isle Royale. Furthermore, we fixed the timing of this fifth epoch to 15 generations ago, thus assuming that the population was founded in the early 1900s (120 years ago, assuming a generation time of 8 years; (Gaillard 2007)), as suggested by available evidence (Murie 1934; Mech 1966). We used this approach to retain power for estimating the Isle Royale effective population size when fitting a complex five-epoch model to an SFS from a small sample size. When fixing these parameters, we obtained an estimate of N_e=187 on Isle Royale, highlighting a dramatic disparity in N_e between the North American and Isle Royale populations spanning three orders of magnitude. Additionally, given that the Isle Royale moose population

on average numbers ~1000 individuals (Hoy, Peterson, et al. 2020), these results suggest an N_e:N ratio of ~0.19, consistent with those observed in other species (Frankham 1995). Notably, we observe the same N_e:N ratio of ~0.19 when comparing our estimated North American N_e=193,472 (Figure 3.3) to the current census estimate of one million (Timmermann and Rodgers 2017).

Quantifying putatively deleterious variation

To understand how the vastly reduced effective population size on Isle Royale may have impacted patterns of deleterious variation compared to mainland populations, we examined variants in protein-coding regions that were predicted to be putatively damaging or benign on the basis of evolutionary constraint (Vaser et al. 2016). We observe a reduction in heterozygosity for both damaging and benign variants on Isle Royale, mirrored by an increase in homozygosity for the derived (i.e., mutant relative to the reference) allele (Figure 3.4), as expected given the higher levels of inbreeding in the Isle Royale population. Specifically, we find that homozygous derived genotype counts are 9.7% higher for damaging variants and 6.8% higher for benign variants in Isle Royale moose compared to mainland moose. However, we do not observe an excess of derived alleles on Isle Royale (Figure 3.4), as might be expected for a population that has accumulated an excess of weakly deleterious mutations due to relaxed purifying selection (Lohmueller et al. 2008; Do et al. 2015). Collectively, these results suggest that the genetic load attributable to an accumulation of weakly deleterious mutations is negligible in Isle Royale moose.

Simulations of deleterious variation and genetic load

Empirical measures of deleterious variation are often challenging to interpret given that the functional impact and dominance of mutations are uncertain (Cooper and Shendure 2011; Pedersen et al. 2017). Consequently, we also conducted forward-in-time genetic simulations to assess the impact of bottlenecks on deleterious genetic variation in North American moose using SLiM3 (Haller and Messer 2019). These simulations consisted of a 20 Mb chromosomal segment, which included a combination of introns, exons, and intergenic regions. Neutral and deleterious mutations occurred at a rate of 7e-9 per base pair (Dussex 2020), with deleterious mutations only occurring within exons. Selection coefficients for deleterious mutations were drawn from a distribution estimated from human genetic variation data (Kim et al. 2017), and dominance coefficients were assumed to be inversely related to selection coefficients, such that the most deleterious mutations were also the most recessive (see Materials and Methods).

Our first aim was to examine the impact of the North American colonization bottleneck on genetic diversity, genetic load, and purging. Here, we define "genetic load" as the realized reduction in fitness due to segregating and fixed deleterious mutations (Kirkpatrick and Jarne 2000), and quantify purging as a reduction in the simulated "inbreeding load", a measure of the quantity of recessive deleterious variation concealed in heterozygosis (Hedrick and Garcia-Dorado 2016). To examine the dynamics of inbreeding, genetic diversity, and load in North American moose, we simulated under our best-fit demographic model (Figure 3.3), which includes a founding bottleneck of N_e=49 for 29 generations followed by expansion to N_e=193,472 for 1,179 generations. Over the duration of this bottleneck, we observe a decrease in genetic diversity of 21%, along with a decrease in the inbreeding load of 24%, an increase in

genetic load of 282% and an increase in F_{ROH} to 0.22 (Figure 3.5). However, these increases in genetic load and F_{ROH} are largely absent after 1,179 generations of recovery, though levels of inbreeding notably remain above zero, in agreement with our empirical data (Figure 3.2B). By contrast, genetic diversity and inbreeding load do not greatly increase after recovery, with the inbreeding load continuing to decline after the bottleneck and remaining 34% below its pre-bottleneck value even after 1,179 generations of recovery (Figure 3.5). Thus, this result suggests that the North American moose population may still be experiencing the lingering purging effects of this founding bottleneck, despite occurring ~9,600 years ago. Importantly, we observe qualitatively similar patterns when simulating under a model with a slightly longer and less severe bottleneck (Figure S3-7), suggesting that these simulation results are robust to uncertainty in our estimated demographic parameters.

Next, we examined the impact of isolation and small population size on Isle Royale on patterns of genetic variation and genetic load. We again simulated under our North America demographic model, though added a final epoch with the estimated Isle Royale demographic parameters of N_e=187 for 15 generations. When simulating under this demography, however, we do not recapitulate the differences in genetic diversity and inbreeding observed in our empirical data between Isle Royale and mainland samples (Figure 3.5). Specifically, heterozygosity decreased by only 3.6% compared to a ~30% difference between Minnesota and Isle Royale samples in our empirical data, and levels of inbreeding increase only to F_{ROH}=0.08 compared to F_{ROH}=0.35 from our empirical data (Table S3-3).

We hypothesized that this discrepancy may be due to the absence of a severe founder event at the origination of the Isle Royale population in our model, given that the population is believed to be founded by a small number of individuals (Murie 1934; Mech 1966). To test this hypothesis, we ran simulations where we included a bottleneck during the first three generations following the founding of Isle Royale. We tested three bottleneck severities with effective population sizes during the first three generations of N_e={6,24,96}, N_e={4,16,64}, and N_e={2,8,32}, each followed by expansion to N_e=187 for the final 12 generations. These bottleneck parameters were selected because available evidence suggests that population density was low soon after founding, particularly from 1900-1920, though it is unclear exactly how low or how many founders there were (Murie 1934; Mech 1966). When varying these bottleneck parameters, we find that only the most severe bottleneck of N_e={2,8,32} recapitulated the observed differences in genetic diversity and inbreeding, yielding a decrease in heterozygosity of 32% and increase in inbreeding to F_{ROH}=0.35, in agreement with our empirical results (Figs. 5 and S7-S8; Table S3-3). Under this model, we also observe a relative increase in genetic load on Isle Royale of 206% as well as a 53% reduction in the inbreeding load (Figure 3.5; Table S3-3). Thus, these results suggest that the Isle Royale moose population may have been founded by just two individuals, and that this severe founder event has been an essential factor in shaping patterns of genetic diversity, inbreeding, genetic load, and purging on the island. Finally, we do not observe any differences in allele counts between simulated island and mainland populations for mutations with selection coefficient (s) > -0.01 (Figure S3-9), in agreement with our empirical result suggesting negligible impacts on load due to weakly deleterious mutations (Figure 3.4). However, we do observe a sharp reduction in the number of strongly deleterious (s < -0.1) alleles per individual in the simulated Isle Royale population, suggesting that purging has

largely been driven by a reduction in the number of strongly deleterious recessive alleles (Figure S3-9).

Although our results suggest a substantial decrease in genetic diversity and increase in inbreeding in Isle Royale moose, field observations of the population have not detected obvious signs of inbreeding depression or reduced population growth rates (Hoy, MacNulty, et al. 2020). We hypothesized that this may be in part due to the purging that occurred during the North America founding event, which could enhance the ability of North American moose to persist at small population size. To test this hypothesis, we ran simulations under the above parameters including a severe Isle Royale founding bottleneck, but excluding the North America founding bottleneck. Here, we observe a much greater increase in genetic load on Isle Royale of 350%, compared to 206% when including the North America founding event (Table S3-3). Thus, these results suggest that the lingering effects of purging due to the North American founder event may have aided the ability of moose to persist at small population size on Isle Royale. In other words, the negative genetic consequences of small population size on Isle Royale may have been greater if the North American moose population had not experienced a strong bottleneck during colonization.

Next, we explored the potential impact of a low rate of historical migration on genetic variation in the Isle Royale population. Specifically, we explored the effect of a low rate of migration on genetic diversity, genetic load, levels of inbreeding, and inbreeding load. We ran simulations with migration fractions of 0.5% and 5%, roughly corresponding to 1 and 10 effective migrants per generation, respectively, chosen to model two relatively low but plausible rates of migration.

Under the low migration scenario of 0.5%, results are nearly identical to the no migration scenario (Figure S3-10; Table S3-3), implying that a very low level of historical migration (~1 migrant per generation) would not have had much impact on the genetic state of the population. These results imply that we cannot fully rule out the possibility of a low rate of migration to Isle Royale, as suggested by direct observations of moose swimming between Isle Royale and the mainland (Vucetich 2021). By contrast, when the migration fraction is increased to 5%, heterozygosity is higher and inbreeding lower relative to empirical values (Figure S3-10; Table S3-3). In sum, these results further confirm that historical migration to Isle Royale was either absent or very low. Moreover, these results also suggest that any future attempts to restore genetic diversity and reduce genetic load in the Isle Royale moose population would require a relatively high rate of migration (>10 effective migrants per generation).

Finally, we explored the sensitivity of our results to selection and dominance parameters. Specifically, we simulated under parameters proposed by Kardos et al. 2021, which assume that inbreeding depression is primarily due to recessive lethals and that deleterious mutations with $s > -0.1$ have largely additive effects on fitness. When simulating the North America founder event with these parameters, we observe a much smaller 22% increase in genetic load and a more substantial 60% decrease in the inbreeding load (Figure S3-11). Additionally, the inbreeding load recovers much more rapidly following the bottleneck, due to the faster increase towards equilibrium of recessive lethal mutations (Figure S3-11). When simulating a severe founder event for Isle Royale, we observe a much greater initial increase in genetic load; however, genetic load quickly decreases as recessive lethals are purged from the population, with a net increase of 66% (Figure S3-12). Additionally, we observe substantial purging on Isle Royale,

with a 75% reduction in the inbreeding load (Figure S3-12). Thus, simulations under these parameters predict a much smaller increase in genetic load and much larger impacts of purging. This greater impact of purging is likely a consequence of the increased emphasis on recessive lethals in this model, which are most easily purged (Hedrick 1994; Pérez-Pereira et al. 2021).

Discussion

Highly inbred populations are often thought to be doomed to extinction. However, some can persist, and understanding the factors enabling persistence can aid in conservation efforts. Our results document high inbreeding in the Isle Royale moose population (F_{ROH}=0.35 on average; Figure 3.2), roughly as high as the gray wolf population at the time of its decline. Yet, despite these high levels of inbreeding, the Isle Royale moose population does not exhibit obvious signs of inbreeding depression, and maintains population growth rates that do not noticeably differ from mainland moose (Hoy, MacNulty, et al. 2020). A key factor that likely underlies these different outcomes is the pace of inbreeding in these two populations: whereas the wolf population became quickly inbred while isolated at a population size of ~25 for ~70 years, inbreeding in the moose population was more gradual due to its more moderate population size of ~1000 for a longer duration of ~120 years. These differing demographic histories are reflected in the distribution of ROH lengths in the wolf and moose populations. In the wolf population, ROH were predominantly long (>10 Mb), reflecting recent and severe inbreeding (Robinson et al. 2019), whereas the moose population exhibits an abundance of intermediate-length ROH (1-10 Mb; Figure 3.2). Several recent studies have highlighted the severe fitness consequences of long ROH, which tend to be enriched for highly deleterious recessive alleles, whereas more intermediate-length ROH may be largely purged of such variation (Szpiech et al. 2013; Robinson

et al. 2019; Szpiech et al. 2019; Martin A. Stoffel et al. 2021). Although our results imply an elevated genetic load in the Isle Royale moose population (Figure 3.5), this load has apparently not impacted population growth rates substantially, perhaps due to reduced interspecific competition on Isle Royale and soft selection (Agrawal and Whitlock 2012). Overall, our results emphasize the importance of maintaining moderate size ($N_e > 100$) in isolated populations to enable purging and avert extinction in the short to intermediate term, in agreement with other studies (Day et al. 2003; Glémin 2003; Pekkala et al. 2012; Robinson et al. 2018; Kyriazis et al. 2021; Pérez-Pereira et al. 2021). Over the longer term, maintaining even larger population sizes ($N_e > 1000$) is preferable whenever possible to avoid the impacts of increasing drift load and loss of adaptive potential (Kardos et al. 2021; Willi et al. 2022).

Our results suggest that roughly half of the inbreeding load in Isle Royale moose may have been purged in the ~15 generations or ~120 years since founding (Figure 3.5). The relatively rapid pace of this purging is notable, given that most existing examples of purging in wild populations occurred after thousands of years of isolation (Xue et al. 2015; Robinson et al. 2018; Yang et al. 2018; M. A. Stoffel et al. 2021). In Isle Royale moose, purging appears to have been accelerated by a severe founding bottleneck of perhaps just two individuals (Figure 3.5). The impacts of severe bottlenecks on purging are well known (Kirkpatrick and Jarne 2000), and have also been recently documented in an analysis of Alpine ibex genomes (Grossen et al. 2020). For both Isle Royale moose and Alpine ibex, a severe bottleneck followed by relatively prompt recovery appears to have driven rapid purging on a timescale of ~100 years. Thus, rapid purging on the timescale of anthropogenic fragmentation may only be possible in the presence of severe bottlenecks, perhaps precluding intentional purging as a viable conservation strategy.

Nevertheless, many populations of at-risk species may have experienced historical purging due to severe bottlenecks or long-term moderate population size and identifying these populations could prove useful for future management actions.

Our findings also have important implications for understanding the evolutionary history and conservation status of mainland North American moose populations. Across all North American moose samples, we observe a reduction in genome-wide diversity of at least 34% relative to a sample from Sweden (Figure 3.2), consistent with previous work (Hundertmark et al. 2002; Dussex 2020). Our demographic modeling indicates this reduction in diversity is due to a severe bottleneck in the ancestral North American moose population occurring ~9,600 years ago (Figure 3.3). This timing closely aligns with glacial recession at the onset of the Holocene 11,000 years ago as well as the North American fossil record (Decesare et al. 2020). Furthermore, our simulation results suggest a substantial 34% purging of the inbreeding load associated with this founding bottleneck, the effects of which may persist until present day (Figure 3.5). This phenomenon could further explain the success of the isolated Isle Royale moose population, implying that the founding individuals may have been 'pre-purged' of inbreeding depression. Moreover, the possibility of 'pre-purging' in North American moose could also help explain the success of other introduced moose populations in North American, such as the Newfoundland population, which was founded by just six individuals and now numbers >100,000 individuals (Broders et al. 1999). Nevertheless, many fragmented North American moose populations near the southern range edge have experienced recent declines (Timmermann and Rodgers 2017). Though these declines have generally been linked to synergistic impacts of climate change and increasing disease and pathogen load (Murray et al. 2006; Timmermann and Rodgers 2017), the

potential role of genetic factors has been largely overlooked. For example, we observed low genetic diversity in samples from Idaho and Wyoming (Figure 3.2), perhaps due to the recent founding of these populations in the mid 19th century and low population density (Wolfe et al. 2010). Notably, moose in this region exhibit low adult pregnancy rates (Ruprecht et al. 2016), which could potentially be a consequence of inbreeding depression. Moreover, it is possible that low genetic diversity in these populations has increased their susceptibility to parasites (Gibson and Nguyen 2021). Overall, the causes of moose population declines near the southern range edge appear to be complex, and additional genomic sampling of these populations will be necessary to more fully investigate the potential role of genetic factors.

In conclusion, our results depict a complex relationship between genetic diversity, inbreeding, and population viability in isolated and fragmented populations. The contrasting fates of the Isle Royale wolf and moose populations serve as a dramatic example of the importance of maintaining isolated populations at moderate size to facilitate purging and avert extinction over the short to intermediate term. Moreover, this case study of predator and prey hints at a more far-reaching phenomenon, in which isolated predator populations may be doomed to extinction by inbreeding depression due to their naturally lower density, whereas the higher abundance of prey populations may enable them to purge the most severe impacts of inbreeding depression. In light of the well-documented connections among gray wolf, moose and plant abundance on Isle Royale (McLaren and Peterson 1994), we suggest the possibility of an eco-evolutionary link between purging and the dynamics of the Isle Royale ecosystem. In general, purging may have system-wide effects in other isolated and fragmented ecosystems, where predator populations are declining in part due to inbreeding depression, and prey populations are thriving in their absence,

often to the detriment of the broader ecosystem (Estes et al. 2011; Ripple et al. 2014). Thus, our results highlight a unique connection between deleterious genetic variation and ecosystem health, with implications for best management practices of small and fragmented populations.

Materials and Methods

Sampling and sequencing

Tissue samples were obtained opportunistically from moose carcasses on Isle Royale and Minnesota samples were collected during regular management activities by the Minnesota Department of Natural Resources (MN DNR). Isle Royale tissue samples were frozen and archived at Michigan Technological University and Minnesota tissue samples were provided by the MN DNR. DNA was extracted from samples using Qiagen kits and quantified using a Qubit fluorometer. Whole-genome sequencing was performed on an Illumina NovaSeq at the Vincent J. Coates Genomics Sequencing Laboratory at University of California, Berkeley and MedGenome. Existing genomes from (Kalbfleisch et al. 2018) and (Dussex 2020) were downloaded from the National Center for Biotechnology Information (NCBI) Sequence Read Archive (see Table S3-1).

Read processing and alignment

We processed raw reads using a pipeline adapted from the Genome Analysis Toolkit (GATK) (Van der Auwera et al. 2013) Best Practices Guide. We aligned paired-end 150bp raw sequence reads to the cattle genome (ARS-UCD1.2) using BWA-MEM (Li 2013), followed by removal of low-quality reads and PCR duplicates. Given that we do not have a database of know variants, we did not carry out Base Quality Score Recalibration, but instead carried out hard filtering of genotypes (see below). Although the cattle genome is highly divergent from moose, we opted to use it due to its much higher quality and contiguity compared to existing moose genomes (scaffold N50 of 103 Mb for ARS-UCD1.2 vs 1.7 Mb for NRM_Aalces_1_0) as well as its high-quality annotations and existing resources on the Ensembl Variant Effect Predictor database

(McLaren et al. 2016). To explore the potential impact of this on our downstream analyses, we also mapped a subset of nine genomes to the more closely related hog deer reference genome (ASM379854v1), which has high contiguity with a scaffold N50 of 20.7 Mb. Importantly, we found that the choice of reference genome here does not appear to qualitatively impact our genetic diversity and runs of homozygosity results. Thus, we use the cattle reference genome for all downstream analyses (see SI text for further discussion).

Genotype calling and filtering

We performed joint genotype calling at all sites (including invariant sites) using GATK HaplotypeCaller. Genotypes were filtered to include only high-quality biallelic SNPs and monomorphic sites, removing sites with Phred score below 30 and depth exceeding the 99th percentile of total depth across samples. In addition, we removed sites that failed slightly modified GATK hard filtering recommendations (QD < 4.0 || FS > 12.0 || MQ < 40.0 || MQRankSum < −12.5 || ReadPosRankSum < −8.0 || SOR > 3.0), as well as those with >25% of genotypes missing or >35% of genotypes heterozygous. We masked repetitive regions using a mask file downloaded from ftp://ftp.ncbi.nlm.nih.gov/genomes/Bos_taurus/. Finally, we applied a per-individual excess depth filter, removing genotypes exceeding the 99th percentile of depth for each individual, as well as a minimum depth filter of six reads.

Population structure and relatedness

We used SNPrelate v1.14 (Zheng et al. 2012) to run principal component analysis (PCA), construct a tree based on identity-by-state (IBS), and estimate kinship among sampled genomes. For all analyses, we pruned SNPs for linkage (ld.threshold=0.2) and filtered out sites with minor

allele frequency below 0.05, resulting in 50,361 SNPs for analysis. PCA was run both for all sampled individuals as well as for North American individuals down-sampled to one individual per population. We used the KING method of moments approach (Manichaikul et al. 2010) to estimate kinship among North American moose samples. Finally, we estimated IBS among all samples, then performed hierarchical clustering on the resulting matrix to construct a dendrogram.

As another means of characterizing population structure, we used fastSTRUCTURE v1.0 (Raj et al. 2014) to test for admixture among sampled individuals. We converted our vcf to PLINK bed format with a minor allele frequency of 0.05 and maintained the order of alleles from the original vcf file. We ran fastSTRUCTURE on all sampled individuals as well as only Minnesota and Isle Royale individuals, each down-sampled to five unrelated individuals. For both analyses, we ran fastSTRUCTURE using values of *k* from 1-4. Finally, we used vcftools (Danecek et al. 2011) to estimate Weir and Cockerham's (Weir and Cockerham 1984) F_{ST} between all Minnesota and Isle Royale samples using default settings.

Genetic diversity and runs of homozygosity

We calculated heterozygosity for each individual in non-overlapping 1 Mb windows across the autosomal genome. We removed windows with fewer than 80% of sites called, as well as windows below the 5th percentile of the total number of calls, as these windows have high variance in heterozygosity. We estimated mean genome-wide heterozygosity by averaging heterozygosity across windows for each individual.

Runs of homozygosity were called using BCFtools/RoH (Narasimhan et al. 2016). We used the -G30 flag and allowed BCFtools to estimate allele frequencies. Due to the Swedish sample coming from a highly divergent population with differing allele frequencies, we excluded it from this analysis. We used a custom R script (R Core Team 2021) to partition the resulting ROH calls into length categories 0.1-1 Mb, 1-10 Mb, and 10-100 Mb. We calculated F_{ROH} by summing the total length of all ROH calls >100 kb (or >1 Mb) and dividing by 2489.4 Mb, the autosomal genome length for the cattle reference genome. When conducting this analysis for the subset of samples mapped to the hog deer reference genome, we only used scaffolds >1 Mb in length, which together sum to 2479 Mb (~93% of the total reference length).

Identifying putatively deleterious variation

Variant sites were annotated using the Ensembl Variant Effect Predictor (VEP) v.97 (McLaren et al. 2016). We used SIFT (Vaser et al. 2016) to determine whether a nonsynonymous mutation is likely to be damaging or benign based on phylogenetic constraint. We classified protein-coding variants as "damaging" if they were determined to be "deleterious" nonsynonymous variants (SIFT score of <0.05) or variants that disrupted splice sites, start codons, or stop codons. Variants were classified as "benign" if they were determined to be "tolerated" nonsynonymous variants (SIFT score of ≥0.05) or synonymous mutations. Using these annotations, we tallied the number of derived alleles of each category relative to the cattle reference genome, as well as the number of heterozygous and homozygous derived genotypes, comparing these tallies for genomes sampled from Isle Royale and Minnesota. Variants that were that were fixed derived across the entire sample were ignored.

Demographic inference

We estimated historical demographic parameters for North American moose based on the neutral site frequency spectrum (SFS) using ∂a∂i (Gutenkunst et al. 2009). In brief, we first focused on estimating parameters for the mainland North American population based on the neutral SFS for our nine Minnesota genomes, then used these results to guide inference of the effective population size on Isle Royale based on a neutral SFS from five genomes of unrelated Isle Royale individuals.

To generate a neutral SFS, we began by identifying regions that were >10kb from coding regions and did not overlap with repetitive regions (downloaded from ftp://ftp.ncbi.nlm.nih.gov/genomes/Bos_taurus/). We also excluded un-annotated highly conserved regions that are under strong evolutionary constraint, identified by aligning the remaining regions against the zebra fish genome using BLASTv2.7.1 (Camacho et al. 2009) and removing any region which had a hit above a 1e-10 threshold.

We then generated a folded neutral SFS for these regions using a modified version of EasySFS (https://github.com/isaacovercast/easySFS), which implements ∂a∂i's hypergeometric projection to account for missing genotypes. We found that the number of SNPs was maximized by using a projection value of seven diploids for the Minnesota sample and four diploids for the Isle Royale sample. In addition, we counted the number of monomorphic sites passing the projection threshold in neutral regions and added these to the 0 bin of the SFS.

We then used these SFSs to conduct demographic inference using the diffusion approximation approach implemented in ∂a∂i (Gutenkunst et al. 2009). Using the Minnesota SFS, we fit 1-epoch, 2-epoch, 3-epoch, and 4-epoch models. These models included the following parameters: N_{anc} (the ancestral effective population size), $N_{1\text{-}3}$ (the effective size of the subsequent 1-3 epochs), and $T_{1\text{-}3}$ (the duration of the subsequent 1-3 epochs; Table S3-2). In other words, a 3-epoch model includes the parameters $N_{anc,}$ $N_{1,}$ $N_{2,}$ $T_{1,}$ and T_2. Overall, we found the best fit for a 4-epoch model including expansion in the second epoch followed by a strong bottleneck and a final epoch of expansion, though with poor convergence of estimated parameters. Based on initial results, we constrained parameter space for the 4-epoch model by setting a limit on N_1 to be in the range [10, 30]*N_{anc}, N_2 to be in the range [1e-2, 5]*N_{anc}, and N_3 to be in the range [10, 40]*N_{anc}.

We next sought to obtain an estimate of the effective population size on Isle Royale using a folded neutral SFS from five unrelated individuals, projected to four diploids. Given this limited sample size and the shared evolutionary history of Isle Royale and Minnesota moose, we fixed the parameters estimated from our 4-epoch model inferred above based on the Minnesota SFS. We then added a fifth epoch to the model, fixing the duration of this epoch to 15 generations, based on an estimated date of colonization of 1900 and 8 year generation time (Gaillard 2007). Thus, the only estimated parameter in this approach is N_5, the effective population size on Isle Royale.

We carried out inference by permuting the starting parameter values and conducting 50 runs for each model. We calculated the log-likelihood using ∂a∂i's optimized parameter values

comparing the expected and observed SFSs. For each model, we selected the maximum likelihood estimate from the 50 runs and used AIC to compare across models. We then used a mutation rate of 7e-9 mutations/site/generation and the total sequence length (L) to calculate the diploid ancestral effective population size as $N_{anc}= \Theta/(4*\mu*L)$. We scaled other inferred population size parameters by N_{anc} and time parameters by $2*N_{anc}$, in order to obtain values in units of diploids and numbers of generations.

Simulations of deleterious genetic variation

We performed forward-in-time genetic simulations using SLiM v3.6 (Haller and Messer 2019). We simulated a 20 Mb chromosomal segment with randomly generated introns, exons, and intergenic regions following the approach from (Mooney et al. 2018). Thus, our aim with these simulations is not to quantify genome-wide effects of deleterious mutations, but rather to examine relative changes in deleterious mutations within a 20 Mb chromosomal segment. Deleterious (nonsynonymous) mutations occurred in exonic regions at a ratio of 2.31:1 to neutral (synonymous) mutations (Huber et al. 2017), and only neutral mutations occurred in intronic and intergenic regions. Following (Dussex 2020), we assumed a mutation rate of 7e-9 mutations per site per generation. Selection coefficients (*s*) for deleterious mutations were drawn from a distribution estimated using human genetic variation data by (Kim et al. 2017), consisting of a gamma distribution with mean *s* of -0.01314833 and shape = 0.186. Additionally, we augmented this distribution such that 0.5% of deleterious mutations were recessive lethal, given that this distribution may underestimate the fraction of lethal mutations (Kardos et al. 2021). The dominance coefficients (*h*) of our simulations were set to model an inverse relationship between *h* and *s*, given that highly deleterious mutations also tend to be highly recessive (Agrawal and

Whitlock 2011; Huber et al. 2018). Specifically, we assumed h=0.0 for very strongly deleterious mutations (s < -0.1), h=0.01 for strongly deleterious mutations (-0.1 ≤ s <-0.01), h=0.1 for moderately deleterious mutations (-0.01 ≤ s <-0.001), and h=0.4 for weakly deleterious mutations (s > -0.001). To test the sensitivity of our analysis to our assumed selection and dominance parameters, we also ran simulations under the selection and dominance parameters proposed by Kardos et al. 2021. Specifically, this model assumes that deleterious mutations come from a gamma distribution with mean s of -0.05 and shape = 0.5, augmented with an additional 5% of deleterious mutations being lethal. Dominance coefficients follow the relationship h = 0.5*exp(-13*s); however, we simplified this to five dominance partitions for computational efficiency: h=0.48 for s ≥-0.01, h=0.31 for -0.1 ≤ s < -0.01, h=0.07 for -0.4 ≤ s < -0.1, h=0.001 for -1.0 ≤ s < -0.4, and h=0.0 for s=-1.0. For all simulations, we retained fixed mutations, such that their impact on fitness was allowed to accumulate.

We set the population sizes of our simulations according to our best-fit 4-epoch demographic model based on the SFS from our Minnesota moose genomes (Figure 3.3; Table S3-2). Specifically, this model estimated an ancestral effective population size of N_{anc}=6,548 diploids, followed by expansion to N_1=79,647 for T_1=22,628 generations, then contraction to N_2=49 for T_2=29 generations, and finally expansion to N_3=193,472 for T_3=1,179 generations. We also ran simulations under a second 4-epoch model that had similar log-likelihood and somewhat differing parameters of N_{anc}=7,017, N_1=145,662, T_1=20,883, N_2=218, T_2=142, N_3=105,531 and T_3=1,223. In both cases, we allowed the ancestral population to get to mutation-selection-drift equilibrium by running a burn-in at N_{anc} for 70,000 generations.

Following the fourth epoch of both models, we added a fifth and final epoch representing the founding of the Isle Royale population, consisting of N_e=187 for 15 generations. However, when simulating under this demography, we observed that the simulated levels of inbreeding and genetic diversity for the Isle Royale population did not recapitulate those observed in our empirical data (Figure 3.5). Specifically, we observed only a 3.6% reduction in heterozygosity (compared to ~30% in our empirical data) and an increase in F_{ROH} to just 0.08 (compared to 0.35 in our empirical data). We hypothesized that this was due to the lack of a founder event at the origination of the Isle Royale population in our model. To explore the impact of a founder event, we modified the effective population sizes during the first three generations of the Isle Royale population, using three plausible bottleneck parameters of N_e={6,24,96}, N_e={4,16,64}, and N_e={2,8,32}. We focused on the three initial generations after founding, reflecting the period from ~1900-1924 when census estimates are crude and/or unavailable (Murie 1934; Mech 1966). Specifically, little is known about the number of founding individuals, though it is likely this number was small, particularly if the population was naturally founded. Additionally, available records indicate a population size of ~300 by 1920 and perhaps several thousand by 1930, suggesting that population growth was rapid following founding (Murie 1934; Mech 1966). Following this three-generation bottleneck, we simulated the final 12 generations at our estimated N_e=187, representing an average effective population size for the period ~1924-2020 when census estimates ranged from ~500-2000 (average of ~1000; (Hoy, Peterson, et al. 2020)).

During simulations, we recorded mean heterozygosity, mean F_{ROH} for ROH >100 kb and >1 Mb, mean genetic load (calculated multiplicatively across sites), mean inbreeding load (measured as the number of diploid lethal equivalents), and the mean number of strongly deleterious (s < -

0.01), moderately deleterious ($-0.01 \leq s < -0.001$), and weakly deleterious ($s > -0.001$) alleles per individual. These quantities were estimated from a sample of 40 diploids every 1,000 generations during the burn-in, every 100 generations during the second epoch, every 5 generations during the North America founding bottleneck, every 20 generations during the fourth epoch, and every generation during the Isle Royale bottleneck. For all simulated scenarios, we ran 25 replicates.

Figures

Figure 3.1

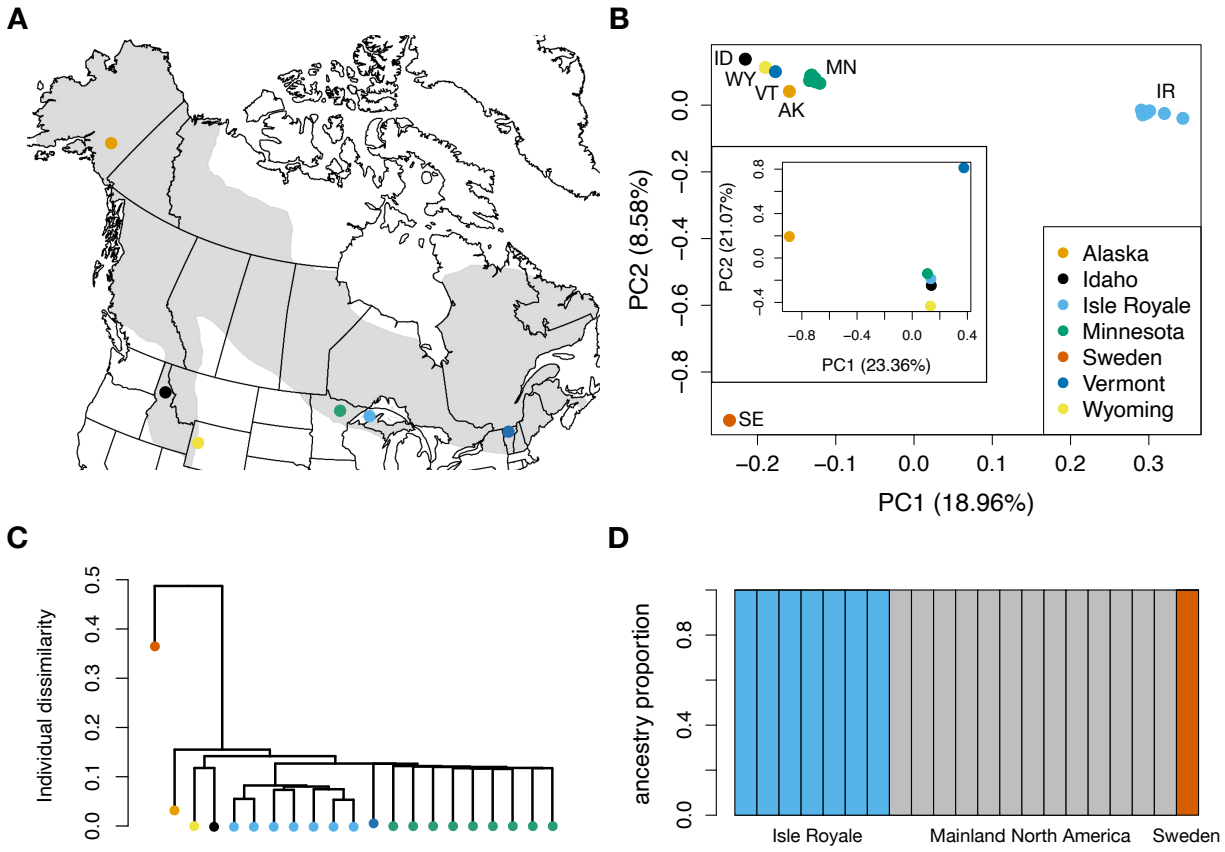

Figure 3.1. Moose sampling and population structure. (A) Map of North America including localities for individuals sampled for genomic data in our study. Note that Sweden is excluded. (B) PCA of 50,361 LD-pruned SNPs for all sequenced samples. Inset are results when down-sampling to one individual per population and excluding the Swedish sample. (C) Tree based on identity-by-state constructed using 50,361 LD-pruned SNPs. (D) fastSTRUCTURE results for K=3. See Figure S3-1 for results with varying K values and Figure S3-2 for results when down-sampling to four unrelated individuals each from Isle Royale and Minnesota.

Figure 3.2

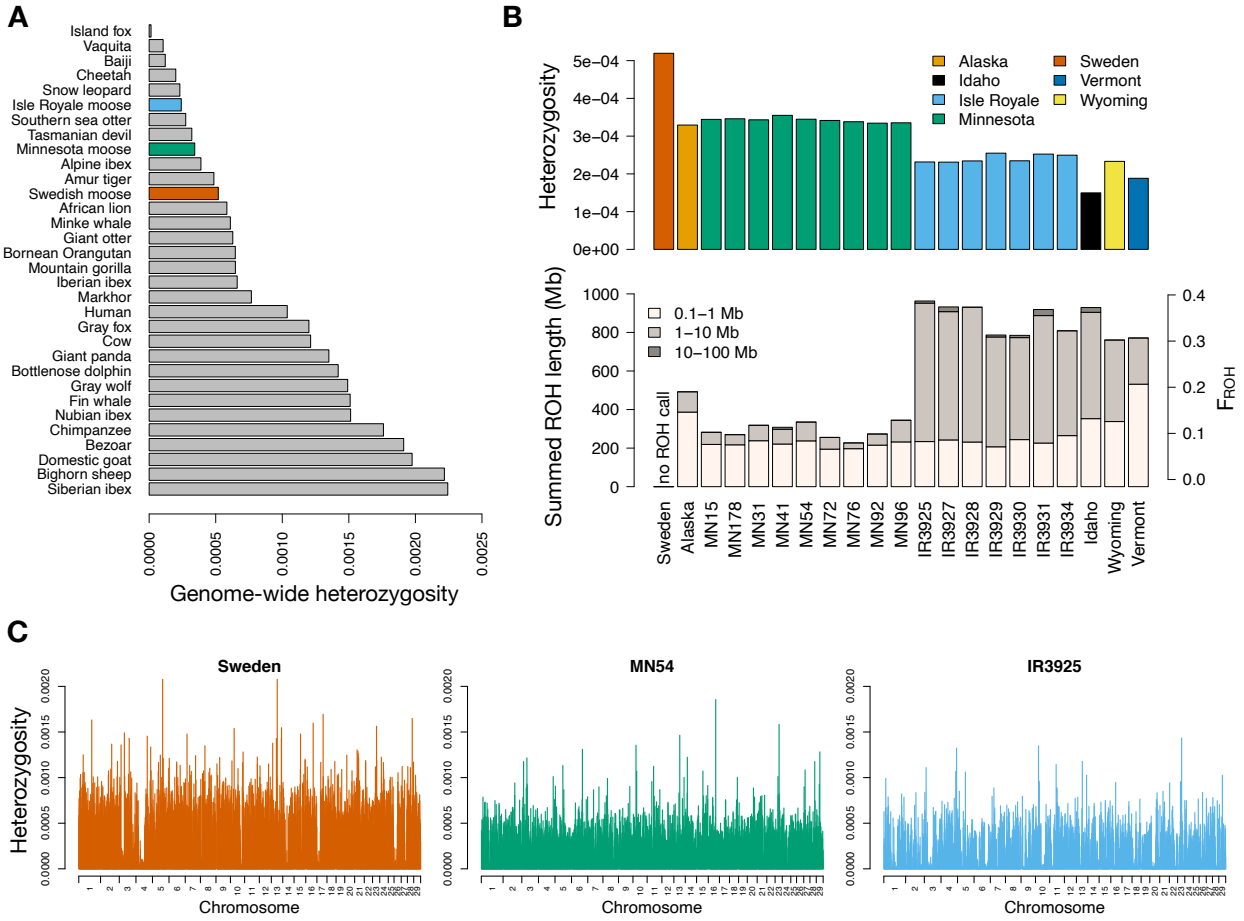

Figure 3.2. Moose genetic diversity and inbreeding. (A) Comparison of mean genome-wide diversity in three moose populations to published values for other mammals. (B). Plots of mean genome-wide diversity and summed ROH levels for North American moose genomes, with the corresponding F_{ROH} values on the right-hand axis. Note that we were not able to obtain ROH calls for the Sweden sample due to its differing population origin. (C) Per-site heterozygosity plotted in non-overlapping 1 Mb windows for representative individuals from Sweden, Minnesota, and Isle Royale. See Figure S3-4 for plots of all individuals.

Figure 3.3

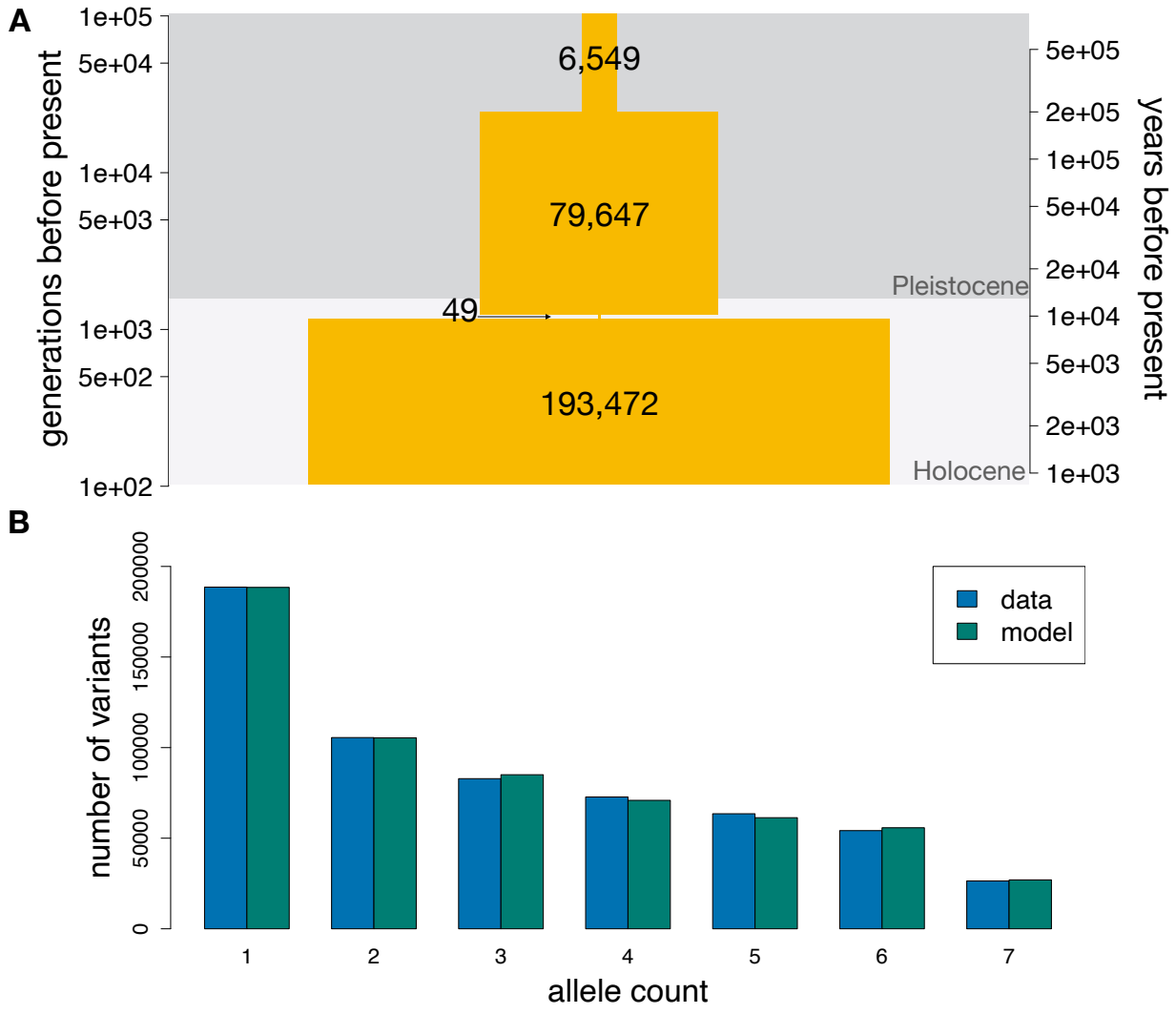

Figure 3.3. Demographic inference results. (A) Schematic of best-fit four epoch model based on the site frequency spectrum (SFS) for the Minnesota sample. Right-hand axis assumes a generation time of 8 years. Numbers denote maximum likelihood estimates of the effective population sizes at the various time points. Note the rapid and severe bottleneck occuring near the onset of the Holocene. See Table S3-2 for parameters of the second-best fitting run, which differs somewhat in bottleneck duration and magnitude and pre/post-bottleneck population sizes.

(B) Comparison of the empirical projected folded SFS from the Minnesota sample with the SFS predicted by the model in shown in (A).

Figure 3.4

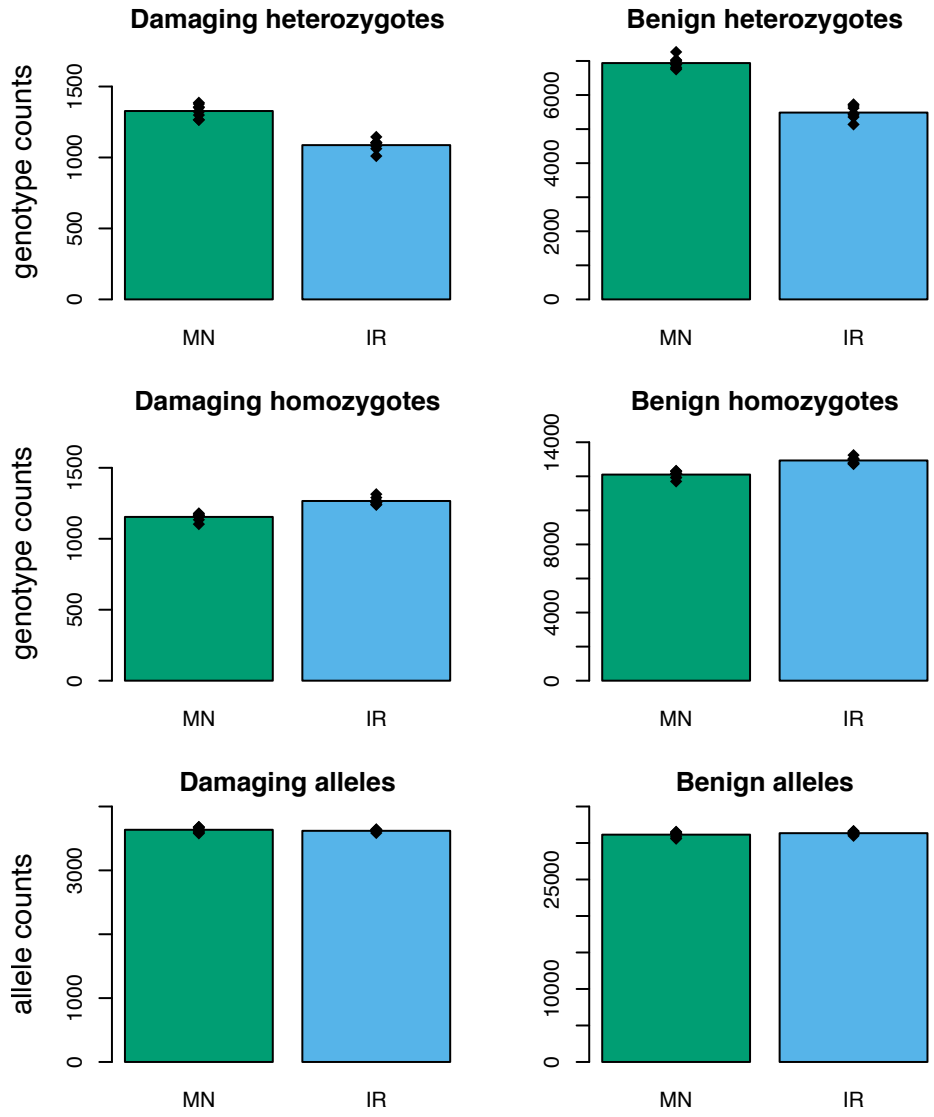

Figure 3.4. Empirical measures of deleterious variation in Isle Royale and Minnesota moose. Top row depicts counts of putatively damaging and benign heterozygotes, demonstrating that heterozygosity is reduced for both mutation types on Isle Royale. Middle row depicts counts of homozygotes for the derived allele at damaging and benign variants, similarly demonstrating increased homozygosity for both mutation types on Isle Royale. Bottom row depicts damaging

and benign derived allele counts, demonstrating no differences between Isle Royale and Minnesota.

Figure 3.5

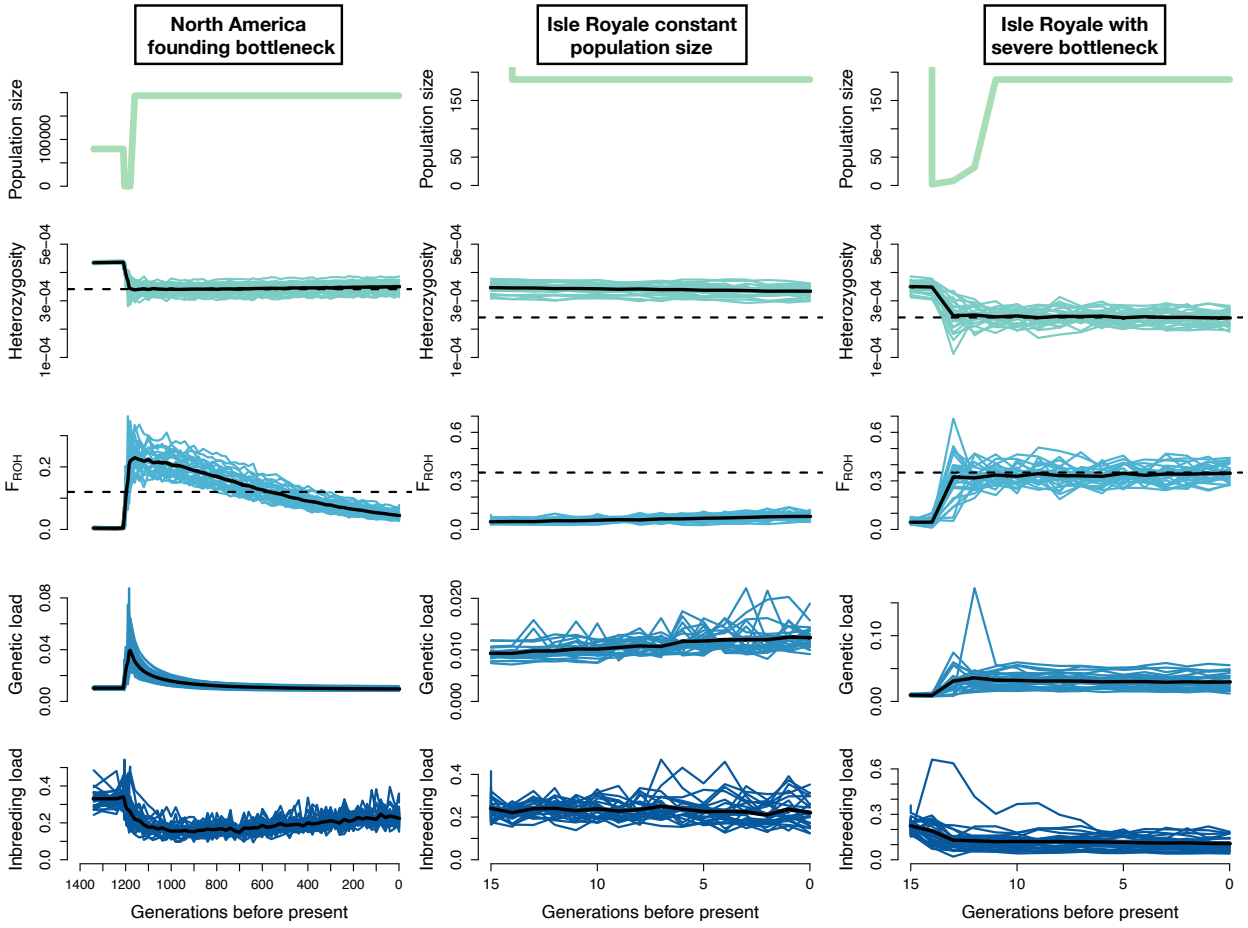

Figure 3.5. Simulation results under three demographic scenarios. Left column depicts simulation dynamics during the North America founding bottleneck; middle column depicts results when simulating the Isle Royale population at constant population size; right column depicts results when simulating the Isle Royale population including a severe founder event (N_e={2,8,32} for the first three generations). Each column includes plots of the simulated effective population size, mean heterozygosity, mean levels of inbreeding ($F_{ROH>100kb}$), mean genetic load, and mean inbreeding load from 25 simulation replicates. The black line represents the average from all replicates. The dashed lines represent the empirical estimates for heterozygosity and F_{ROH} from the Minnesota and Isle Royale populations, respectively. Note that

the simulation trajectories do not reach these empirical estimates when assuming constant population size (middle column) but do when a founder event is included (right column). See Figure S3-7 for results under additional bottleneck parameters.

References

Agrawal AF, Whitlock MC. 2011. Inferences about the distribution of dominance drawn from yeast gene knockout data. *Genetics* 187:553–566.

Agrawal AF, Whitlock MC. 2012. Mutation Load: The Fitness of Individuals in Populations Where Deleterious Alleles Are Abundant. *Annu. Rev. Ecol. Evol. Syst.* [Internet] 43:115–135. Available from: http://www.annualreviews.org/doi/10.1146/annurev-ecolsys-110411-160257

Van der Auwera GA, Carneiro MO, Hartl C, Poplin R, del Angel G, Levy-Moonshine A, Jordan T, Shakir K, Roazen D, Thibault J, et al. 2013. From fastQ data to high-confidence variant calls: The genome analysis toolkit best practices pipeline.

Beichman AC, Kalhori P, Kyriazis CC, DeVries AA, Nigenda-Morales S, Heckel G, Schramm Y, Moreno-Estrada A, Kennett DJ, Hylkema M, et al. 2022. Genomic analyses reveal range-wide devastation of sea otter populations. *Mol. Ecol.*:1–18.

Broders HG, Mahoney SP, Montevecchi WA, Davidson WS. 1999. Population genetic structure and the effect of founder events on the genetic variability of moose , Alces alces , in Canada. *Mol. Ecol.* 8:1309–1315.

Camacho C, Coulouris G, Avagyan V, Ma N, Papadopoulos J, Bealer K, Madden TL. 2009. BLAST+: architecture and applications. [BMC Bioinformatics. 2009] - PubMed - NCBI. *BMC Bioinformatics* [Internet] 10:421. Available from: http://www.ncbi.nlm.nih.gov/pubmed/20003500?dopt=Citation%5Cnhttp://pubmedcentralcanada.ca/picrender.cgi?accid=PMC2803857&blobtype=pdf

Cooper GM, Shendure J. 2011. Needles in stacks of needles: Finding disease-causal variants in a wealth of genomic data. *Nat. Rev. Genet.* [Internet] 12:628–640. Available from:

http://dx.doi.org/10.1038/nrg3046

Danecek P, Auton A, Abecasis G, Albers CA, Banks E, DePristo MA, Handsaker RE, Lunter G, Marth GT, Sherry ST, et al. 2011. The variant call format and VCFtools. *Bioinformatics* 27:2156–2158.

Day SB, Bryant EH, Meffert LM. 2003. The influence of variable rates of inbreeding on fitness, environmental responsiveness, and evolutionary potential. *Evolution (N. Y)*. 57:1314–1324.

Decesare NJ, Weckworth B V., Pilgrim KL, Walker ABD, Bergman EJ, Colson KE, Corrigan R, Harris RB, Hebblewhite M, Jesmer BR, et al. 2020. Phylogeography of moose in western North America. *J. Mammal*. 101:10–23.

Do R, Balick D, Li H, Adzhubei I, Sunyaev S, Reich D. 2015. No evidence that selection has been less effective at removing deleterious mutations in Europeans than in Africans. *Nat. Genet*. 47:126–131.

Dussex N. 2020. Moose genomes reveal past glacial demography and the origin of modern lineages. *BMC Genomics* 21:1–13.

Estes JA, Terborgh J, Brashares JS, Power ME, Berger J, Bond WJ, Carpenter SR, Essington TE, Holt RD, Jackson JBC, et al. 2011. Trophic downgrading of planet earth. *Science (80-.)*. 333:301–306.

Frankham R. 1995. Effective population size/adult population size ratios in wildlife: A review. *Genet. Res. Cambridge* 66:95–107.

Gaillard J-M. 2007. Are Moose Only a Large Deer?: Some Life History Considerations. *Alces* 43:1–12.

Gibson AK, Nguyen AE. 2021. Does genetic diversity protect host populations from parasites? A meta-analysis across natural and agricultural systems. *Evol. Lett*. 5:16–32.

Glémin S. 2003. How Are Deleterious Mutations Purged? Drift versus Nonrandom Mating. *Evolution (N. Y)*. 57:2678–2687.

Grossen C, Guillaume F, Keller LF, Croll D. 2020. Purging of highly deleterious mutations through severe bottlenecks in Alpine ibex. *Nat. Commun*. [Internet] 11:1001. Available from: http://dx.doi.org/10.1038/s41467-020-14803-1

Gutenkunst RN, Hernandez RD, Williamson SH, Bustamante CD. 2009. Inferring the joint demographic history of multiple populations from multidimensional SNP frequency data. *PLoS Genet*. 5:1–11.

Haddad NM, Brudvig LA, Clobert J, Davies KF, Gonzalez A, Holt RD, Lovejoy TE, Sexton JO, Austin MP, Collins CD, et al. 2015. Habitat fragmentation and its lasting impact on Earth's ecosystems. *Sci. Adv*. 1:1–10.

Haller BC, Messer PW. 2019. SLiM 3: Forward Genetic Simulations Beyond the Wright-Fisher Model. *Mol. Biol. Evol*. 36:632–637.

Hedrick PW. 1994. Purging inbreeding depression and the probability of extinction: full-sib mating. *Heredity (Edinb)*. 73:363–372.

Hedrick PW, Garcia-Dorado A. 2016. Understanding Inbreeding Depression, Purging, and Genetic Rescue. *Trends Ecol. Evol*. [Internet] 31:940–952. Available from: http://dx.doi.org/10.1016/j.tree.2016.09.005

Hedrick PW, Robinson JA, Peterson RO, Vucetich JA. 2019. Genetics and extinction and the example of Isle Royale wolves. *Anim. Conserv*. [Internet] 22:302–309. Available from: http://doi.wiley.com/10.1111/acv.12479

Hoy SR, MacNulty DR, Smith DW, Stahler DR, Lambin X, Peterson RO, Ruprecht JS, Vucetich JA. 2020. Fluctuations in age structure and their variable influence on population growth.

Funct. Ecol. 34:203–216.

Hoy SR, Peterson RO, Vucetich JA. 2020. Ecological Studies of Wolves on Isle Royale: Annual Report 2019-2020.

Huber CD, Durvasula A, Hancock AM. 2018. Gene expression drives the evolution of dominance. *Nat. Commun.* [Internet] 9:1–11. Available from: http://dx.doi.org/10.1038/s41467-018-05281-7

Huber CD, Kim BY, Marsden CD, Lohmueller KE. 2017. Determining the factors driving selective effects of new nonsynonymous mutations. *Proc. Natl. Acad. Sci.* 114:4465–4470.

Hundertmark KJ, Bowyer RT, Shields GF, Schwartz CC. 2003. Mitochondrial Phylogeography of Moose (Alces alces) in North America. *J. Mammal.* 84:718–728.

Hundertmark KJ, Shields GF, Udina IG, Bowyer RT, Danilkin AA, Schwartz CC. 2002. Mitochondrial Phylogeography of Moose (Alces alces): Late Pleistocene Divergence and Population Expansion. 22:375–387.

Kalbfleisch TS, Murdoch BM, Smith TPL, Murdoch JD, Heaton MP, McKay SD. 2018. A SNP resource for studying North American moose. *F1000Research* 7:1–17.

Kardos M, Armstrong EE, Fitzpatrick SW, Hauser S, Hedrick PW, Miller JM, Tallmon DA, Chris Funk W. 2021. The crucial role of genome-wide genetic variation in conservation. *Proc. Natl. Acad. Sci. U. S. A.* 118:1–10.

Keller L, Waller DM. 2002. Inbreeding effects in wild populations. *Trends Ecol. Evol.* 17:19–23.

Khan A, Patel K, Shukla H, Viswanathan A, van der Valk T, Borthakur U, Nigam P, Zachariah A, Jhala Y V., Kardos M, et al. 2021. Genomic evidence for inbreeding depression and purging of deleterious genetic variation in Indian tigers. *Proc. Natl. Acad. Sci. U. S. A.* 118.

Kim BY, Huber CD, Lohmueller KE. 2017. Inference of the Distribution of Selection

Coefficients for New Nonsynonymous Mutations Using Large Samples. *Genetics* [Internet] 206:345–361. Available from: http://www.genetics.org/content/genetics/206/1/345.full.pdf

Kirin M, McQuillan R, Franklin CS, Campbell H, Mckeigue PM, Wilson JF. 2010. Genomic runs of homozygosity record population history and consanguinity. *PLoS One* 5:1–7.

Kirkpatrick M, Jarne P. 2000. The Effects of a Bottleneck on Inbreeding Depression and the Genetic Load. *Am. Nat.* [Internet] 155:154–167. Available from: http://www.journals.uchicago.edu/doi/10.1086/303312

Kleinman-Ruiz D, Lucena-Perez M, Villanueva B, Fernandez J, Saveljev AP, Ratkiewicz M, Schmidt K, Galtier N, Garcia-Dorado A, Godoy JA. 2022. Purging of deleterious burden in the endangered Iberian lynx. *Proc. Natl. Acad. Sci.* 119.

Kyriazis CC, Wayne RK, Lohmueller KE. 2021. Strongly deleterious mutations are a primary determinant of extinction risk due to inbreeding depression. *Evol. Lett.* 5:33–47.

Li H. 2013. Aligning sequence reads, clone sequences and assembly contigs with BWA-MEM. *arXiv:1303.3997v2* [Internet] 00:1–3. Available from: http://arxiv.org/abs/1303.3997

Lohmueller KE, Indap AR, Schmidt S, Boyko AR, Hernandez RD, Hubisz MJ, Sninsky JJ, White TJ, Sunyaev SR, Nielsen R, et al. 2008. Proportionally more deleterious genetic variation in European than in African populations. *Nature* 451:994–997.

Manichaikul A, Mychaleckyj JC, Rich SS, Daly K, Sale M, Chen WM. 2010. Robust relationship inference in genome-wide association studies. *Bioinformatics* 26:2867–2873.

McLaren BE, Peterson RO. 1994. Wolves, Moose, and Tree Rings on Isle Royale. *Science (80-.).* 266:1555–1558.

McLaren W, Gil L, Hunt SE, Riat HS, Ritchie GRS, Thormann A, Flicek P, Cunningham F. 2016. The Ensembl Variant Effect Predictor. *Genome Biol.* [Internet] 17:1–14. Available

from: http://dx.doi.org/10.1186/s13059-016-0974-4

Mech LD. 1966. The Wolves of Isle Royale.

Mooney JA, Huber CD, Service S, Sul JH, Marsden CD, Zhang Z, Sabatti C, Ruiz-Linares A, Bedoya G, Endophenotypes C 5 RC for GI of B, et al. 2018. Understanding the Hidden Complexity of Latin American Population Isolates. *Am. J. Hum. Genet.*:1–53.

Murie A. 1934. Moose of Isle Royale. *Univ. Michigan Museum Zool. Misc. Publ. No. 25*.

Murray DL, Cox EW, Ballard WB, Whitlaw HA, Lenarz MS, Custer TW, Barnett T, Fuller TK. 2006. Pathogens, Nutritional Deficiency, and Climate Influences on a Declining Moose Population. *Wildl. Monogr.* 166:1–30.

Narasimhan V, Danecek P, Scally A, Xue Y, Tyler-Smith C, Durbin R. 2016. BCFtools/RoH: A hidden Markov model approach for detecting autozygosity from next-generation sequencing data. *Bioinformatics* 32:1749–1751.

Pedersen CET, Lohmueller KE, Grarup N, Bjerregaard P, Hansen T, Siegismund HR, Moltke I, Albrechtsen A. 2017. The effect of an extreme and prolonged population bottleneck on patterns of deleterious variation: Insights from the Greenlandic Inuit. *Genetics* 205:787–801.

Pekkala N, Knott KE, Kotiaho JS, Puurtinen M. 2012. Inbreeding rate modifies the dynamics of genetic load in small populations. *Ecol. Evol.* 2:1791–1804.

Pérez-Pereira N, Caballero A, García-Dorado A. 2022. Reviewing the consequences of genetic purging on the success of rescue programs. *Conserv. Genet.* [Internet] 23:1–17. Available from: https://doi.org/10.1007/s10592-021-01405-7

Pérez-Pereira N, Pouso R, Rus A, Vilas A, López-Cortegano E, García-Dorado A, Quesada H, Caballero A. 2021. Long-term exhaustion of the inbreeding load in Drosophila

melanogaster. *Heredity (Edinb)*. [Internet]:1–11. Available from: http://dx.doi.org/10.1038/s41437-021-00464-3

R Core Team. 2021. R: A language and environment for statistical computing. Available from: https://www.r-project.org/

Raj A, Stephens M, Pritchard JK. 2014. FastSTRUCTURE: Variational inference of population structure in large SNP data sets. *Genetics* 197:573–589.

Ralls K, Sunnucks P, Lacy RC, Frankham R. 2020. Genetic rescue: A critique of the evidence supports maximizing genetic diversity rather than minimizing the introduction of putatively harmful genetic variation. *Biol. Conserv*. [Internet] 251:108784. Available from: https://doi.org/10.1016/j.biocon.2020.108784

Ripple WJ, Estes JA, Beschta RL, Wilmers CC, Ritchie EG, Hebblewhite M, Berger J, Elmhagen B, Letnic M, Nelson MP, et al. 2014. Status and ecological effects of the world's largest carnivores. *Science (80-.)*. 343.

Robinson JA, Brown C, Kim BY, Lohmueller KE, Wayne RK. 2018. Purging of Strongly Deleterious Mutations Explains Long-Term Persistence and Absence of Inbreeding Depression in Island Foxes. *Curr. Biol*. [Internet] 28:3487-3494.e4. Available from: https://doi.org/10.1016/j.cub.2018.08.066

Robinson JA, Räikkönen J, Vucetich LM, Vucetich JA, Peterson RO, Lohmueller KE, Wayne RK. 2019. Genomic signatures of extensive inbreeding in Isle Royale wolves, a population on the threshold of extinction. *Sci. Adv*. 5:1–13.

Ruprecht JS, Hersey KR, Hafen K, Monteith KL, Decesare NJ, Kauffman MJ, Macnulty DR. 2016. Reproduction in moose at their southern range limit. *J. Mammal*. 97:1355–1365.

Sattler RL, Willoughby JR, Swanson BJ. 2017. Decline of heterozygosity in a large but isolated

population: a 45-year examination of moose genetic diversity on Isle Royale. *PeerJ* 5:1–18.

Stoffel Martin A., Johnston SE, Pilkington JG, Pemberton JM. 2021. Mutation load decreases with haplotype age in wild Soay sheep. *Evol. Lett.* 5:187–195.

Stoffel M. A., Johnston SE, Pilkington JG, Pemberton JM. 2021. Genetic architecture and lifetime dynamics of inbreeding depression in a wild mammal. *Nat. Commun.* [Internet] 12:1–10. Available from: http://dx.doi.org/10.1038/s41467-021-23222-9

Szpiech ZA, Mak ACY, White MJ, Hu D, Eng C, Burchard EG, Hernandez RD. 2019. Ancestry-Dependent Enrichment of Deleterious Homozygotes in Runs of Homozygosity. *Am. J. Hum. Genet.* [Internet] 105:747–762. Available from: https://doi.org/10.1016/j.ajhg.2019.08.011

Szpiech ZA, Xu J, Pemberton TJ, Peng W, Zöllner S, Rosenberg NA, Li JZ. 2013. Long runs of homozygosity are enriched for deleterious variation. *Am. J. Hum. Genet.* 93:90–102.

Teixeira JC, Huber CD. 2021. The inflated significance of neutral genetic diversity in conservation genetics. *Proc. Natl. Acad. Sci.* 118:1–10.

Timmermann HR, Rodgers AR. 2017. The Status and Management of Moose in North America - Circa 2015. *Alces A J. Devoted to Biol. Manag. Moose* 53:1–22.

Vaser R, Adusumalli S, Leng SN, Sikic M, Ng PC. 2016. SIFT missense predictions for genomes. *Nat. Protoc.* [Internet] 11:1–9. Available from: http://dx.doi.org/10.1038/nprot.2015-123

Vucetich JA. 2021. Restoring the Balance: What Wolves Tell Us about Our Relationship with Nature. Johns Hopkins Press

Weir BS, Cockerham CC. 1984. Estimating F-statistics for the analysis of population structure. *Evolution (N. Y).*:1358–1370.

Willi Y, Kristensen TN, Sgro CM, Weeks AR, Ørsted M, Hoffmann AA. 2022. Conservation genetics as a management tool: The five best-supported paradigms to assist the management of threatened species. *Proc. Natl. Acad. Sci. U. S. A.* 119:1–10.

Wilson PJ, Grewal S, Rodgers A, Rempel R, Saquet J, Hristienko H, Burrows F, Peterson R, White BN. 2003. Genetic variation and population structure of moose (Alces alces) at neutral and functional DNA loci. *Can. J. Zool.* 683:670–683.

Wolfe ML, Hersey KR, Stoner DC. 2010. A History of Moose Management in Utah. *Alces A J. Devoted to Biol. Manag. Moose* 46:37-52–52.

Xue Y, Prado-Martinez J, Sudmant PH, Narasimhan V, Ayub Q, Szpak M, Frandsen P, Chen Y, Yngvadottir B, Cooper DN, et al. 2015. Mountain gorilla genomes reveal the impact of long-term population decline and inbreeding. *Science (80-.).* 348:242–245.

Yang Y, Ma T, Wang Z, Lu Z, Li Y, Fu C, Chen X, Zhao M, Olson MS, Liu J. 2018. Genomic effects of population collapse in a critically endangered ironwood tree Ostrya rehderiana. *Nat. Commun.* [Internet] 9:5449. Available from: http://www.nature.com/articles/s41467-018-07913-4

Zheng X, Levine D, Shen J, Gogarten S, Laurie C, Weir B. 2012. A High-performance Computing Toolset for Relatedness and Principal Component Analysis of SNP Data. *Bioinformatics* 28:3326–3328.

Chapter 4: Using computational simulations to quantify genetic load and predict extinction risk

In preparation for submission to *PNAS*

A Supplemental Appendix is available online as this dissertation's Supplementary Materials: Chapter4_Supplementary_Information.pdf

Abstract

Small and isolated populations face numerous threats to extinction, among which is the deterioration of fitness due to an accumulation of deleterious genetic variation. Genomic tools are increasingly used to quantify the impacts of deleterious variation in these populations, however, these approaches remain limited by an inability to accurately predict the selective and dominance effects of individual mutations. Computational simulations of deleterious genetic variation offer an alternative and complementary tool that can help overcome these limitations, though such approaches have yet to be widely employed. In this Perspective, we aim to encourage conservation genomics researchers to adopt greater use of computational simulations to aid in quantifying and predicting the threat that deleterious genetic factors pose to extinction. We first provide an overview of the components of a simulation of deleterious genetic variation, describing key parameters involved in such models. Next, we clarify several misconceptions about an essential simulation parameter, the distribution of fitness effects (DFE) of new mutations, and review recent debates over what the most appropriate DFE parameters are. We conclude by comparing modern simulation tools to those that have long been employed in population viability analysis, discussing the pros and cons of a "genomics-informed" simulation approach. Our aim is that this Perspective will facilitate broader use of computational

simulations in conservation genomics, enabling a deeper understanding of the threat that deleterious genetic variation poses to biodiversity.

Introduction

Anthropogenic pressures are resulting in a growing number of small and isolated populations facing an elevated risk of extinction due in part to deleterious genetic factors. Deleterious genetic variation can contribute to extinction in small populations via two related mechanisms: fixation of weakly deleterious alleles due to relaxed purifying selection (Lynch et al. 1995a,b) and inbreeding depression due to the exposure of recessive deleterious variation (Keller and Waller 2002; Hedrick and Garcia-Dorado 2016). The burden of deleterious variation carried by a population is typically referred to as its "genetic load", often defined as the reduction in fitness due to segregating and fixed deleterious mutations (Muller 1950; Agrawal and Whitlock 2012; Hedrick and Garcia-Dorado 2016). Genomic tools are now commonly used to quantify deleterious variation and genetic load in wild populations (Kardos et al. 2016; Díez-del-Molino et al. 2018; Bertorelle et al. 2022), though the best approaches for leveraging such datasets to help conserve small populations remains an active area of research. In particular, empirical measures of putatively deleterious variation have seen increased use in conservation genomics studies (Bertorelle et al. 2022); however, these measures remain relatively crude and often challenging to interpret (Cooper and Shendure 2011; She and Jarosz 2018; Huber et al. 2020; Sandell and Sharp 2022).

In light of the limitations of empirical measures of deleterious variation and genetic load, the aim of this review is to encourage more conservation genomics researchers to employ computational genetic simulations. To that end, we first provide an overview of simulations of deleterious genetic variation, illustrating how such approaches can be used to estimate genetic load. Next, we review recent debates on deleterious mutation parameters, focusing on the distribution of

fitness effects of new mutations (or DFE), aiming to determine which parameters are best supported by empirical evidence. Finally, we compare modern simulation approaches for modelling inbreeding depression to existing methods that have long been employed in population viability analysis, discussing the pros and cons of "genomics-informed" models of inbreeding depression. Our hope is that this review will provide useful information for researchers aiming to incorporate simulation-based approaches into genomics-based studies of genetic load, enabling more comprehensive assessments of the genomic risks to extinction in small and isolated populations.

Defining genetic load

Understanding the implications of genetic load for organismal fitness and population viability has been a topic of long-standing interest in population and conservation genetics (Haldane 1937; Muller 1950; Morton et al. 1956; Agrawal and Whitlock 2012; Henn et al. 2015; Hedrick and Garcia-Dorado 2016). Several definitions of genetic load have been put forth in the literature recently, often with the aim of partitioning genetic load into "realized" and "potential" load (e.g., (Mathur and DeWoody 2021; Bertorelle et al. 2022)). Here, we adhere to the definition of genetic load as the realized reduction in mean fitness in a population due to segregating and fixed deleterious mutations (note that the "mutation load" refers only mutations segregating under mutation-selection balance; (Muller 1950; Agrawal and Whitlock 2012)). The genetic load of a population at a single locus is given by:

$$L = 2hsq(1-q) + sq^2$$

Here, s is the selection coefficient of a mutation, h is the dominance coefficient, and q is the mutation frequency. Here, the effect of deleterious mutations found as heterozygotes is captured

by the $2hsq(1-q)$ term and the effect of homozygous deleterious mutations is captured by the sq^2 term. Genetic load at a single locus can be related to mean population fitness ($\overline{w}$) as: $\overline{w} = 1-L$. To obtain the mean genome-wide genetic load of a population, L is typically multiplied across sites, thus assuming no epistasis and no linkage disequilibrium (Agrawal and Whitlock 2012). Thus, the units of genetic load are in terms of multiplicative absolute fitness scaled from 0 to 1.

Another important quantity for predicting the impacts of inbreeding and small population size is the inbreeding load, which quantifies the potential reduction in fitness after inbreeding exposes segregating recessive deleterious mutations (Morton et al. 1956; Hedrick and Garcia-Dorado 2016). Unlike the genetic load, the inbreeding load is measured in terms of lethal equivalents, which represent a summed quantity of s for recessive deleterious mutations that are masked as heterozygotes. For a population at equilibrium, the inbreeding load (B) at a single locus is given by (Morton et al. 1956):

$$B = sq - sq^2 - 2hsq(1-q) = sq - L$$

Thus, this equation demonstrates that the inbreeding load is determined by the frequency and fitness effect of a mutation (sq), minus the expressed effects of the mutation in homozygotes (sq^2) as well as any heterozygous effects of the mutation due to partial recessivity ($2q(1-q)sh$). To calculate the total inbreeding load across a diploid genome (2B), this quantity can be summed across sites with deleterious mutations and multiplied by two to account for diploidy.

These fundamental principles demonstrate that an essential component of estimating the genetic load and inbreeding load (hereafter, referred to together as "load") using genetic variation data is knowing s and h for individual mutations. However, although some progress has been made in

predicting whether a mutation is likely to be neutral or deleterious (e.g., (Cooper et al. 2005; Kumar et al. 2009; Choi et al. 2012; Cingolani et al. 2012; Kircher et al. 2014)), accurately predicting *h* and *s* for individual mutations in genomic sequencing data remains a major challenge, even in humans and model organisms (Cooper and Shendure 2011; She and Jarosz 2018; Huber et al. 2020; Sandell and Sharp 2022). For example, a recent simulation study demonstrated that Genomic Evolutionary Rate Profiling (GERP; (Cooper et al. 2005)), a popular method for predicting the deleterious effect of mutations based on evolutionary conservation, cannot reliably distinguish weakly deleterious mutations from strongly deleterious mutations (Huber et al. 2020), though it is commonly used for this purpose (e.g., (Henn et al. 2016; Marsden et al. 2016; Van Der Valk et al. 2019; Dussex et al. 2021)). Similarly, experimental studies in yeast have found that methods such as SIFT (Kumar et al. 2009) and PROVEAN (Choi et al. 2012) are poor predictors of the functional impact of a mutation (She and Jarosz 2018; Sandell and Sharp 2022) that provide only crude proxies of *s*. Moreover, these methods do not provide any information on dominance, an essential component of quantifying load. These limitations are unlikely to be fully overcome, particularly for non-model organisms, implying that methods for quantifying load based on sequence data will remain only crude approximations for the foreseeable future.

Overview of simulation-based approaches

Computational simulations using evolutionary models provide an alternate way of quantifying load that alleviates many of the limitations discussed above. Simulations are widely used in population genetics (e.g., (Marjoram and Donnelly 1994; Akey et al. 2004; Ramachandran et al. 2005; Fu et al. 2014; Harris and Nielsen 2016; Henn et al. 2016; Uricchio et al. 2016; Adrion et

al. 2020a)), yet remain underused in conservation genomics. Historically, this may be due to a relative lack of simulation tools capable of modelling ecologically-realistic scenarios and an often steep learning curve for using simulation software that may be poorly documented (Hoban et al. 2012). However, many of these challenges have been addressed by the forward-in-time genetic simulation program SLiM (Haller and Messer 2016, 2019), which offers a flexible array of models incorporating realistic ecological dynamics as well as comprehensive documentation and accompanying user-friendly graphic user interface. Other similar programs include Nemo (Guillaume and Rougemont 2006; Cotto et al. 2020) and SimBit (Matthey-Doret 2021), both of which have been applied in a conservation genetics context (Grossen et al. 2020; Grummer et al. 2022).

Simulations are broadly useful in evolutionary genetics because they can serve the critical function of revealing which evolutionary scenarios are consistent with observed patterns of genetic variation. All sequence-based evolutionary genetics studies suffer from the limitation that they are observing a single outcome of a stochastic evolutionary process, where underlying mechanisms are largely unobservable. Simulations allow researchers to model this evolutionary process and determine which mechanisms (e.g., genetic drift, gene flow, selection, migration) are needed to explain observed patterns in a dataset. Moreover, this process of using simulations can be extremely valuable for developing intuition on how various evolutionary forces interact to influence patterns of genetic variation, improving the ability of researchers to design evolutionary genetics studies and interpret their results.

For studies aiming to characterize the impacts of small population size on deleterious variation, simulations can be especially useful for quantifying load, which can be directly tabulated from the simulation output (see Supplemental Appendix 1). Simulations can therefore be used to complement empirical measures of load, providing a framework in which to interpret observed patterns and verify that they are expected under a plausible evolutionary model. Moreover, simulations can go beyond empirical measures by projecting load under various future scenarios, illuminating how management actions in the present-day may impact load decades or centuries from now. Finally, modern simulation tools, such as the ecologically-realistic models supported by SLiM3 (Haller and Messer 2019), also offer the potential to conduct an analysis of future extinction risk while incorporating genome-scale genetic variation, analogous to the population viability analysis (PVA) approaches that have long been employed in conservation genetics (e.g., (Lacy 1993, 2019; Beissinger and Westphal 1998; Brook et al. 2000); see below for further discussion).

In summary, simulation-based approaches have much to offer for genomic studies of deleterious variation in wild populations, yet their application remains relatively limited. In Table 4.1, we have summarized existing studies that employ simulations along with genomic analyses to investigate genetic load in organisms ranging from ibex to Chinese crocodile lizards. We suggest that future research should incorporate similar approaches those implemented in these studies to provide a more thorough investigation of load in wild populations.

What are the components of a simulation of deleterious genetic variation?

Modelling deleterious genetic variation in a simulation framework at a minimum requires specifying a population history, mutation rate, recombination rate, genome structure, and distribution of selection and dominance coefficients. The extent to which these parameters need to be tailored to a focal organism will vary depending on questions being asked. For example, many studies may be interested in using simulations primarily to explore qualitative dynamics of deleterious variation under various demographic and genetic scenarios. For example, one may be interested in asking: what are the qualitative effects of a bottleneck on genetic load under two extreme scenarios where deleterious mutations are either fully additive or fully recessive? For these studies, tailoring the simulation parameters to the focal organism may not be crucial, so long as the chosen parameters are reasonable or justified.

For studies aiming to make more quantitative statements about genetic load or project future extinction risk, tailoring simulation parameters to the focal organism may be more critical. For example, demographic history can vary widely between populations and has a large influence on deleterious genetic variation and is therefore a crucial factor in modelling load and extinction risk. Fortunately, historical demographic parameters can be inferred from genomic datasets, though estimating recent demography (i.e., during the last tens or hundreds of generations) remains challenging (reviewed in (Beichman et al. 2018)). The mutation rate is another essential component influencing levels of deleterious variation in a population, though high-quality mutation rate estimates (i.e., based on a large number of sequenced trios) do not exist for the vast majority of species. However, mutation rates can also be estimated from substitution rates between species, an approach that is now widely feasible given the abundance of whole genome

sequencing data (Lynch et al. 2016). Precisely estimating recombination rates may be less important for modelling load, though a growing number of approaches exist for estimating recombination rates from genomic datasets from as little as one diploid individual (e.g., (Barroso et al. 2019; Adrion et al. 2020b)). Tailoring the genome structure (i.e., the length and number of genes and extent of non-coding variation) of a simulation to a specific organism can also be an important component of a simulation, particularly for studies aiming to model extinction risk in more ecologically-realistic models (Kyriazis et al. 2021; Robinson et al. 2022). To aid in this, a growing number of annotated reference genomes are now available, which can provide useful information on genome structure, particularly for protein-coding regions of the genome.

Finally, the joint distributions of selection and dominance coefficients are essential components of modelling deleterious variation and load. These distributions determine the effect that new mutations exert on fitness, as well as the corresponding dominance coefficient of a mutation based on its selection coefficient. Although there is broad agreement that more deleterious mutations tend to be more recessive, the parameters of the distribution of dominance coefficients remain especially poorly known (Simmons and Crow 1977; Caballero and Keightley 1994; Agrawal and Whitlock 2011; Huber et al. 2018). Much more is known about the distribution of selection coefficients for new mutations, often termed "the distribution of fitness effects" or DFE, though most studies remain focused on humans and model organisms such as *Drosophila* ((Eyre-Walker and Keightley 2007; Huber et al. 2017; Kim et al. 2017); Figure 4.1). Given the importance of the DFE for simulations of deleterious variation, as well as recent debate over DFE parameters (Kardos et al. 2021; Pérez-Pereira et al. 2021, 2022), below we provide a more detailed review of this topic.

Determining the appropriate DFE and dominance parameters for a simulation

The DFE is a probability distribution that quantifies the selective effect (s) of new mutations entering the population, i.e., what fraction of new mutations are adaptive, neutral, weakly deleterious, or strongly deleterious. Here, we focus our discussion on the deleterious portion of the DFE, given that adaptive mutations do not influence load. Importantly, the DFE is not an estimate of segregating variation and therefore does not directly quantify load (see Supplemental Appendix 1; Figure S4-1), a misconception that has recently spread in the literature (e.g., (Jones et al. 2020; Kutschera et al. 2020)). Instead, the fate of a mutation after it enters a population, and whether it will segregate and potentially reach fixation, will be influenced by selection as well as the stochastic effects of genetic drift and linkage. Thus, quantifying segregating variation and load using the DFE requires modelling these effects under a given demographic model (see Supplemental Appendix 1 for an example; Figure S4-1).

Historically, the DFE was estimated primarily using experimental mutation accumulation approaches (Mukai 1964; Simmons and Crow 1977; Eyre-Walker and Keightley 2007; Halligan and Keightley 2009). However, these approaches are limited to detecting the small fraction of deleterious mutations that have large enough effects to be observed in a laboratory setting ((Davies et al. 1999; Eyre-Walker and Keightley 2007; Halligan and Keightley 2009); see Supplemental Appendix 2). These limitations motivated the development of sequence-based approaches for estimating the DFE over the past two decades (Eyre-Walker and Keightley 2007). Sequence-based methods estimate the DFE based on differences in the synonymous (assumed to be neutral) and nonsynonymous (assumed to be primarily neutral and deleterious) site frequency

spectrum (SFS), a summary of allele frequencies in a sample ((Eyre-Walker et al. 2006; Eyre-Walker and Keightley 2007; Boyko et al. 2008; Kim et al. 2017; Tataru et al. 2017); see Supplemental Appendix 2). Specifically, these methods typically use the synonymous SFS to control for neutral demographic effects and, conditioning on inferred demographic or nuisance parameters, then estimate the parameters of the distribution of *s* for new nonsynonymous mutations (most frequently, the mean and shape parameters of a gamma distribution). Thus, although these approaches have much greater power for estimating the weakly deleterious portion of the DFE, existing sequence-based DFEs are generally limited to nonsynonymous single nucleotide variants (though see (Torgerson et al. 2009)). Finally, one important limitation of sequence-based approaches is that they typically assume that all mutations have additive effects on fitness, given that information on the distribution of dominance coefficients is very limited (though see (Huber et al. 2018)). Consequently, sequence-based DFE approaches may not be well powered for estimating the relatively small portion of the DFE that is highly recessive and strongly deleterious (Wade et al. 2022).

A growing number of studies have used sequence-based methods to estimate the DFE for nonsynonymous mutations in various taxa including humans, non-human primates, mice, *Arabidopsis*, *Drosophila,* and the highly endangered vaquita porpoise ((Eyre-Walker et al. 2006; Boyko et al. 2008; Ma et al. 2013; Chen et al. 2017; Huber et al. 2017, 2018; Kim et al. 2017; Tataru et al. 2017; Castellano et al. 2019; Robinson et al. 2022); Figure 4.1). In general, these studies estimate a relatively high proportion of weakly deleterious mutations (here defined as $s > -1e-3$), though this fraction varies among major taxonomic groups. For example, studies in mammals generally estimate ~50% of mutations as weakly deleterious, whereas studies in

Arabidopsis, *Drosophila*, and yeast suggest that >80% of new nonsynonymous mutations are weakly deleterious (Figure 4.1). Comparative analyses of the DFE have suggested that such differences may be related to species complexity (Huber et al. 2017) as well as life history traits, such as selfing (Arunkumar et al. 2015; Chen et al. 2017).

Recently, these sequence-based DFE estimates have been criticized on the grounds that they underestimate the fraction of highly deleterious mutations (Kardos et al. 2021; Pérez-Pereira et al. 2021, 2022). Specifically, Kardos et al. 2021 argued that a DFE with mean s = -0.05 and an additional 5% of mutations being recessive lethal was more realistic and Pérez-Pereira et al. 2022 argued that a DFE with mean s = -0.2 was more realistic (Figure 4.2). Along with these DFEs, the Pérez-Pereira et al. 2022 and Kardos et al. 2021 models each assume dominance distributions that are based on mean estimates of h=~0.3 from experimental studies in *Drosophila* ((Simmons and Crow 1977; Caballero and Keightley 1994; Lynch et al. 1995a); Figure 4.2; Supplemental Appendix 3). These models imply that ~67% and ~71% of new mutations are strongly deleterious (here defined as s < -0.01), respectively (Figure 4.2). By contrast, one of the more recent sequence-based DFE estimates for nonsynonymous mutations in humans estimated a mean s = -0.0131 with ~26% of mutations being strongly deleterious (Kim et al. 2017), a result that is generally concordant with other estimates in humans and non-human mammals (Figure 4.1). Moreover, these sequence-based estimates are also in agreement with a broad literature in population genetics and functional genomics suggesting that the majority of nonsynonymous mutations have relatively minimal effects on fitness (Kruglyak et al. 2022).

To determine whether the Pérez-Pereira et al. 2022 and Kardos et al. 2021 models make predictions that are consistent with genetic variation datasets, we ran simulations under a human demographic model (Kim et al. 2017) where we compared the predicted nonsynonymous SFS from each model to the empirical SFS from the 1000G dataset for humans (Auton et al. 2015). We find that both models exhibit poor agreement with the empirical 1000G SFS, predicting nonsynonymous SFSs that are greatly shifted towards rare mutations (Figure 4.3; Table S4-1). For example, the Kardos et al. 2021 and Pérez-Pereira et al. 2022 models predict ~72-76% of nonsynonymous mutations to be singletons (variants with frequency 1/2n), whereas ~57% of variations are singletons in the 1000G dataset (Figure 4.3; Table S4-1). This surplus of rare variation is due to the very strong predicted effects of purifying selection under these models, which results in deleterious mutations being held at low frequency. This result is consistent with the expectation that such models based on experimental studies are biased towards detecting highly deleterious mutations (Davies et al. 1999; Eyre-Walker and Keightley 2007; Halligan and Keightley 2009). By contrast, the Kyriazis et al. 2021 model, which consists of the Kim et al. 2017 DFE and a dominance distribution proposed by Henn et al. 2016, is in much better agreement with empirical data, predicting ~55% of variants as singletons (Figure 4.3; Table S4-1). Thus, these results demonstrate that the Kardos et al. 2021 and Pérez-Pereira et al. 2022 models make predictions that are inconsistent with patterns of genetic variation in human genomic sequencing datasets (see Supplemental Appendix 4 for further discussion).

Another way to test whether proposed DFE and dominance models fit empirical data is to compare the predicted inbreeding load from each model to empirical estimates of inbreeding load (2B). Such empirical estimates can be derived by regressing measurements of fitness against

estimates of individual inbreeding in a population (Morton et al. 1956; Ralls et al. 1988; Keller and Waller 2002; Hedrick and Garcia-Dorado 2016; Nietlisbach et al. 2018). These estimates therefore represent an orthogonal source of information on deleterious mutation parameters. When making comparisons of the predicted inbreeding load from the Kardos et al. 2021, Pérez-Pereira et al. 2022, and Kyriazis et al. 2021 DFE and dominance models under simulations assuming human genomic and demographic parameters (i.e., assuming a genomic deleterious mutation rate of U=0.63; see Supplemental Appendix 3), we find that all models over-predict the estimated inbreeding load in humans of 2B=1.4 (Bittles and Neel 1994), as well as the median estimated inbreeding load in captive mammals of 2B=3.1 (Ralls et al. 1988) and wild vertebrates of 2B=4.5 (Nietlisbach et al. 2018). Specifically, the Kardos et al. 2021 and Pérez-Pereira et al. 2022 models very high inbreeding loads of 2B=20.0 and 2B=28.4, respectively, while the Kyriazis et al. 2021 model also predicts a substantial inbreeding load of 2B=11.3 (Figure 4.4). Additionally, the partitioning of the inbreeding load (i.e., the contribution of the inbreeding load from detrimental mutations, semi-lethal mutations, and lethal mutations) in these models is also not consistent with empirical measures. For example, whereas an empirical estimate suggests 0.6 recessive lethal mutations per human, the Kardos et al. 2021 and Pérez-Pereira et al. 2022 models predict 16.0 and 12.2 recessive lethal mutations per individual, respectively (Figure 4.4; see Supplemental Appendix 4 for further discussion). By contrast, the Kyriazis et al. 2021 predicts no recessive lethal mutations. Thus, none of these models are consistent with empirical inbreeding load estimates, though over-predictions are especially notable for the Kardos et al. 2021 and Pérez-Pereira et al. 2022 models, due to these original analyses assuming unrealistically low effective population sizes (see Supplemental Appendix 5). Importantly, this over-prediction of the inbreeding load becomes much more extreme when assuming the original

genomic deleterious mutation rate (U=1.2) of the Kardos et al. 2021 model, and somewhat less extreme when assuming the original genomic deleterious mutation rate (U=0.4) from the Pérez-Pereira et al. 2022 model (Figure S4-5).

Given the shortcomings of these existing models, we propose a new model based on recent analysis of the DFE in humans under non-additive model (Cavassim & Lohmueller, in prep) as well as an estimation of the recessive lethal portion of the DFE (Wade et al. 2022). In brief, this 'preferred model' assumes a somewhat less recessive dominance distribution compared to the Henn et al. (Henn et al. 2016) distribution assumed by Kyriazis et al. 2021 model and is augmented with a small proportion (0.3%) of recessive lethal mutations (see Supplemental Appendix 3 for details). Indeed, simulation results under this model are in much better agreement with empirical estimates. Specifically, our preferred model predicts an inbreeding load of 2B=6.3, which is relatively evenly partitioned into contributions from detrimentals, semi-lethals, and lethals (Figure 4.4), in agreement with empirical evidence (Simmons and Crow 1977; Gao et al. 2015; Clark and et al 2019; Stoffel et al. 2021a). Although this value exceeds empirical estimates in humans (2B=1.4) and captive mammals (2B=3.1), this result is expected given that these estimates are based on juvenile survival and may therefore be underestimates (Ralls et al. 1988; Bittles and Neel 1994). Overall, this analysis demonstrates that sequence-based DFE estimates can explain empirical patterns of the inbreeding load when making slight adjustments to account for their shortcomings in estimating the proportion of recessive lethal mutations (Wade et al. 2022). Thus, these DFEs remain preferable for modelling deleterious variation in coding regions in that they account for the impacts of both weakly and strongly deleterious variation.

Comparing genomics-informed models of inbreeding load to traditional PVA approaches

Although simulation-based approaches remain under-used in genomic studies of genetic load in wild populations, simulations have long been employed in conservation genetics in the context of population viability analyses (PVAs; (Lacy 1993, 2019; Beissinger and Westphal 1998; Brook et al. 2000)). For example, the simulation software VORTEX has been widely used to model inbreeding depression in wild populations (Lacy 1993, 2000). Such programs allow the user to specify an empirical estimate of the inbreeding load for their focal organism. However, a key limitation of this approach is that empirical estimates of the inbreeding load do not exist for the vast majority of species, and many existing estimates are not reliable (Nietlisbach et al. 2018). Accurately estimating the inbreeding load is not a trivial task: it requires large sample sizes, accurate estimates of the inbreeding coefficient ideally from genomic data, high variance in inbreeding in a population, and a reliable proxy for fitness (Kalinowski and Hedrick 1999; Nietlisbach et al. 2018). Relatively few studies exist that combine all of these elements, leading to wide variance in available estimates (see Supplemental Appendix 6 for further discussion).

Given the relative lack of empirical estimates of the inbreeding load, most existing PVA studies of inbreeding depression instead employ a default inbreeding load of 2B=3.1, a value derived from captive mammals by Ralls et al. 1988. Many studies opt to use a much higher value of 2B=12 from O'Grady et al. 2006, though this estimate has been shown to be unreliable ((Nietlisbach et al. 2018); see Supplemental Appendix 6). This use of a default, one-size-fits-all inbreeding load estimate is a critical limitation for many existing PVA studies, as it ignores the

possibility of the inbreeding load varying across species and being influenced by the genetic and demographic characteristics of a given population. This issue may be most important for species with long-term small population size, for which inbreeding load is likely to be reduced due to purging.

A genomics-informed simulation approach for modelling inbreeding depression offers many potential advantages to help overcome the limitations of using default inbreeding load values. In a genomics-informed approach, inbreeding load is modeled as an emergent property of fundamental genetic and demographic parameters that can be estimated from genomic data, rather than being predetermined. Based on these parameters, such models can predict the inbreeding load for a given species, helping avoid use of a default estimate. The benefits of a genomics-based approach are illustrated by the analysis of extinction risk for the critically endangered vaquita porpoise presented in Robinson et al. 2022, a species for which inbreeding load is expected to be low due to long-term small population size (Figure S4-4), though no empirical estimate of the inbreeding load exists. By parameterizing simulations with genomics-based estimates of demographic parameters, mutation rates, and the DFE, we predicted an inbreeding load of 2B=0.95 and a high potential for recovery in the absence of excess mortality driven by the use of illegal gillnets. Moreover, we demonstrated that this low inbreeding load is largely a consequence of the small historical population size of the vaquita, finding that simulations with a 20x increased historical population size resulted in an increased predicted inbreeding load of 2B=3.32 and a much lower potential for recovery. Thus, the conclusion of high recovery potential for the vaquita would not have been reached when assuming a default inbreeding load for mammals of 2B=3.1.

There are several potential drawbacks to a genomics-informed simulation approach for modelling inbreeding depression, which should be taken into consideration before attempting to employ such an approach in a PVA model. First, forward-in-time simulations of genome-scale genetic variation tend to be highly computationally intensive, particularly when modelling large effective population sizes ($N_e >> 10{,}000$). This high computational load is largely due to the need for long burn-in periods for each simulation replicate during which mutations are allowed to reach their equilibrium frequency, a process that typically takes $10*N_e$ generations. However, these long burn-ins can be shortened by instead using durations long enough for inbreeding load to reach equilibrium, which typically takes $<1*N_e$ generations (Figure S4-6). Second, the reliability of a genomics-based PVA depends in large part on obtaining accurate estimates of relevant genetic and demographic parameters, which may be challenging for many species. In particular, mutation rates can be especially difficult to accurately estimate and have a large influence on the predicted inbreeding load in a model. For example, Robinson et al. 2022 estimated a mutation rate for the vaquita of 5.8e-9 per site per generation using a substitution-based approach, though with a plausible range of 2.2e-9 and 1.08e-8. When conducting sensitivity analyses under these varying mutation rates, we found that the predicted inbreeding load ranged from 2B=0.2 to 2B=2.4 and these varying inbreeding loads led to notable differences in projected extinction rates (Robinson et al. 2022). Thus, genomics-based PVAs should be subject to extensive sensitivity analyses for genetic and demographic parameters and, given the challenges of validating these models, should be interpreted cautiously, as is the case for any PVA model (Beissinger and Westphal 1998).

Finally, although our discussion here focuses on modelling the influence of deleterious variation and genetic load on extinction, numerous other genetic threats to extinction can also be included in a genomics-informed PVA using modern simulation tools. For example, increased susceptibility to disease due to low genetic diversity could contribute to population declines (Gibson 2022), as can the challenge of adapting to changing environmental conditions (Cotto et al. 2017). Future work should aim to better parameterize these processes in wild populations in order to more fully integrate evolutionary processes into PVAs (Pierson et al. 2015).

Remaining questions

How much does the DFE and inbreeding load partitioning differ across taxa?

Much of our analysis in this paper focuses on the human DFE, given that genomic and demographic parameters in humans have been subject to extensive study. However, the extent to which the DFE may differ across species remains poorly known. Although available DFE estimates in mammals are generally similar to humans (Figure 4.1), relatively few species have been examined, and little to no information is available on the DFE in non-mammalian vertebrates. Obtaining a better understanding of the DFE across diverse vertebrate species will provide insight not only into the factors shaping the evolution of the DFE, but also on whether mammalian DFEs, such as the human DFE presented in this paper (Figure 4.2), can reasonably be used in simulations for other vertebrate taxa where DFE estimates are not available. Moreover, additional DFE estimates will also be informative as to the extent to which inbreeding load partitioning may vary across taxa.

How can we reconcile sequence-based DFEs for Arabidopsis and Drosophila with evidence for inbreeding depression in these species?

As discussed above, sequence-based DFE estimates for *Arabidopsis, Drosophila,* and yeast contain a very high proportion (>80%) of weakly deleterious mutations, substantially more than inferred in mammalian DFEs in that (Figure 4.1; (Huber et al. 2017)). The abundance of weakly deleterious mutations in non-mammal model organisms could appear to be at odds with evidence for inbreeding depression in these species (e.g., (Swindell and Bouzat 2006; Sletvold et al. 2013; Pérez-Pereira et al. 2021)). Specifically, a DFE with many weakly deleterious mutations would have few recessive strongly deleterious mutations that can contribute to inbreeding depression. However, available evidence in *Drosophila* suggests that inbreeding depression is primarily due to lethal or semi-lethal mutations (Swindell and Bouzat 2006; Pérez-Pereira et al. 2021), and these mutations are challenging to detect using genetic-variation based methods (Wade et al. 2022). For example, Pérez-Pereira et al. 2021 estimated an inbreeding load of 2B=1.5-2 in *D. melanogaster* and demonstrated that this load could be nearly entirely purged, implying that it is due to a small number of highly deleterious mutations, rather than a large number of weakly deleterious recessive mutations. Additionally, estimates of the number of segregating recessive lethals in *Drosophila* are generally in the range of 1-3 per individual (Simmons and Crow 1977; McCune et al. 2002), also implying that inbreeding depression in *Drosophila* is almost entirely due to recessive lethals. Taken together, these results suggests that the genetic architecture of inbreeding depression may differ between *Drosophila* and mammals, as studies in mammals suggest a much larger contribution from deleterious mutations of more modest effect (Clark and et al 2019; Stoffel et al. 2021a). Nevertheless, further work is needed to establish the differences in architecture of inbreeding depression across species.

What is the distribution of dominance coefficients?

Minimal information exists on the distribution of dominance coefficients, and the few studies that exist are based on a handful of species (Simmons and Crow 1977; Caballero and Keightley 1994; Agrawal and Whitlock 2011; Huber et al. 2018). Moreover, results from these studies sometimes conflict with one another, with available evidence in yeast and *Drosophila* suggesting a much less recessive distribution of dominance coefficients compared to results from *Arabidopsis* (Simmons and Crow 1977; Caballero and Keightley 1994; Agrawal and Whitlock 2011; Huber et al. 2018). Whether this discrepancy is a consequence of true biological differences among these taxa or is instead due to methodological issues remains unclear. Obtaining additional information on the distribution of dominance coefficients represents one of the most essential components for studies modelling inbreeding depression. Specifically, if most deleterious mutations are found to have dominance coefficients that are highly recessive (h<0.05) as suggested by a recent study (Huber et al. 2018), this would suggest a high severity of inbreeding depression due to contributions from both weakly and strongly deleterious mutations. Moreover, a highly recessive dominance distribution would also suggest a very large dependence of inbreeding depression on historical population size (Nei 1968; Hedrick 2002; Kyriazis et al. 2021).

What is the role of heterozygote advantage and non-coding variation in inbreeding depression?

Understanding the genetic basis of inbreeding depression has long been a topic of interest in evolutionary genetics (Charlesworth and Willis 2009). Although many of the simulation models

discussed above focus solely on the contribution of recessive deleterious mutations at nonsynonymous sites in coding regions (e.g., (Kyriazis et al. 2021; Robinson et al. 2022; Xie et al. 2022)), it is likely that other mechanisms and types of mutations also contribute to some extent. For example, heterozygote advantage could play a role in influencing inbreeding depression, though its contribution has been hard to quantify (Charlesworth and Willis 2009). Similarly, deleterious mutations in conserved noncoding regions could also contribute, given that ~4.5% of the non-coding genome has been shown to be highly conserved across mammals, potentially implying a high strength of purifying selection in these regions (Cooper et al. 2005; Siepel et al. 2005; Oosterhout 2019; Huber et al. 2020).

Although these mechanisms and types of mutations likely play some role in influencing inbreeding depression, available evidence suggests that their impact may be relatively minimal. Specifically, studies on heterozygote advantage generally suggest that it occurs only at a small number of loci in the genome (Hedrick 2012), implying a small contribution to inbreeding depression (Charlesworth and Willis 2009). Similarly, although deleterious mutations in conserved noncoding regions appear to be widespread, several studies suggest that these mutations tend to be weakly deleterious (s on the order of 1e-3; (Torgerson et al. 2009; Murphy et al. 2021; Dukler et al. 2022)), such that they likely do not contribute much to inbreeding depression. These considerations imply that recessive deleterious mutations in coding regions likely represent the predominant driver of inbreeding depression. In support of this, we note that the models of inbreeding depression summarized in Figure 4 all ignore contributions of these mechanisms, yet all of these models predict inbreeding loads that are at least as large as those observed empirically. Nevertheless, we emphasize that additional research is needed to explore

the potential contribution of heterozygote advantage and noncoding variation to inbreeding depression and extinction risk. For example, simulation studies that parameterize these factors based on the literature and quantify their effect on inbreeding depression would be a valuable step towards better determining their importance.

How do simulation dynamics in a Wright-Fisher model compare to those in more ecologically-complex models?

The Wright-Fisher (WF) model is a ubiquitous model in population genetics that underlies many of the methodological approaches discussed above. For example, sequence-based DFE methods assume a WF model (Eyre-Walker et al. 2006; Boyko et al. 2008; Kim et al. 2017; Tataru et al. 2017; Ragsdale et al. 2018), as do the simulation results presented in Figures 3 and 4. However, in many cases, it may be desirable to use parameter estimates derived from a Wright-Fisher model in the context of more ecologically complex simulation models, such as the non-Wright-Fisher (nonWF) model in SLiM3 (Haller and Messer 2019). This model allows for populations with overlapping generations, an important departure from the WF model that is also present in other ecologically-realistic simulation programs such as Nemo-age (Cotto et al. 2020).

A key question when using these more complex models with overlapping generations is whether parameters that are inferred assuming a WF model apply in a nonWF setting. For example, DFEs inferred assuming a WF model are scaled in terms of per-generation selection coefficients rather than per-year. As models with overlapping generations assume selection occurs on a yearly timescale (or some other arbitrary unit of time), the selection coefficients from the DFE will need to be rescaled. Although theory suggests that selection coefficients in this case can be rescaled

simply by dividing by the generation time of a species (Charlesworth 1994), the extent to which this rescaling should apply to the full DFE is not clear. For example, highly deleterious mutations that impair development are likely to act during early life stages and not over the span of an entire generation, thus dividing the selection coefficient of such mutations by the generation time may have unintended consequences. In Robinson et al. 2022, our solution to this issue was to rescale selection coefficients for weakly deleterious mutations with $s > -0.01$, but not for strongly deleterious mutations with $s < -0.01$. The validity of this approach, and more broadly the best practices for using parameter estimates derived from WF models under more complex models, remains in need of further investigation.

Tables

Table 4.1

Recent studies combining simulations with empirical genomic data to explore impact of small population size on deleterious variation in non-human species

Paper	Organism	Simulation software	Distribution of fitness effects	Question addressed with simulations
Beichman et al. 2022	Sea otter	SLiM	Kim et al. 2017^	How has the fur trade bottleneck impacted genetic load in the sea otter?
Dussex et al. 2021	Kākāpō	SLiM	mean s = -0.024*	Has purging occurred in the Stewart island kakapo population?
Grossen et al. 2020	Alpine ibex	nemo	mean s = -0.01*	How has deleterious variation been impacted by a recent human-mediated bottleneck?
Kyriazis et al. 2022	North American moose	SLiM	Kim et al. 2017^	How have bottlenecks influenced purging and genetic load in North American moose?
Marsden et al. 2016	Dogs	PReFerSim	Boyko et al. 2008	How has the domestication bottleneck shaped deleterious variation in dogs?
Robinson et al. 2018	Channel island fox	SLiM	Kim et al. 2017	How has recessive deleterious variation been impacted by small population size in island foxes?
Robinson et al. 2019	Gray wolf	SLiM	Kim et al. 2017	How does the large North American wolf population size influence recessive deleterious variation?
Robinson et al. 2022	Vaquita	SLiM	*Estimated by authors*^	Are vaquitas doomed to extinction by inbreeding depression?
Stoffel et al. 2021b	Soay sheep	SLiM	Eyre-Walker et al. 2006#	Are short runs of homozygosity purged of deleterious variation?
Takou et al. 2021	*Arabodopsis lyrata*	PReFerSim	*Estimated by authors*	Do range-edge populations have elevated genetic load?
Xie et al. 2022	Chinese crocodile lizard	SLiM	Kim et al. 2017	Have population declines resulted in purging?

*mean for gamma distribution, not based on explicit analysis
#DFE uses shape parameter from Eyre-Walker et al. 2006 and mean s of -0.01, -0.03, -0.05
^sensitivity analysis conducted with additional DFEs

Figures

Figure 4.1

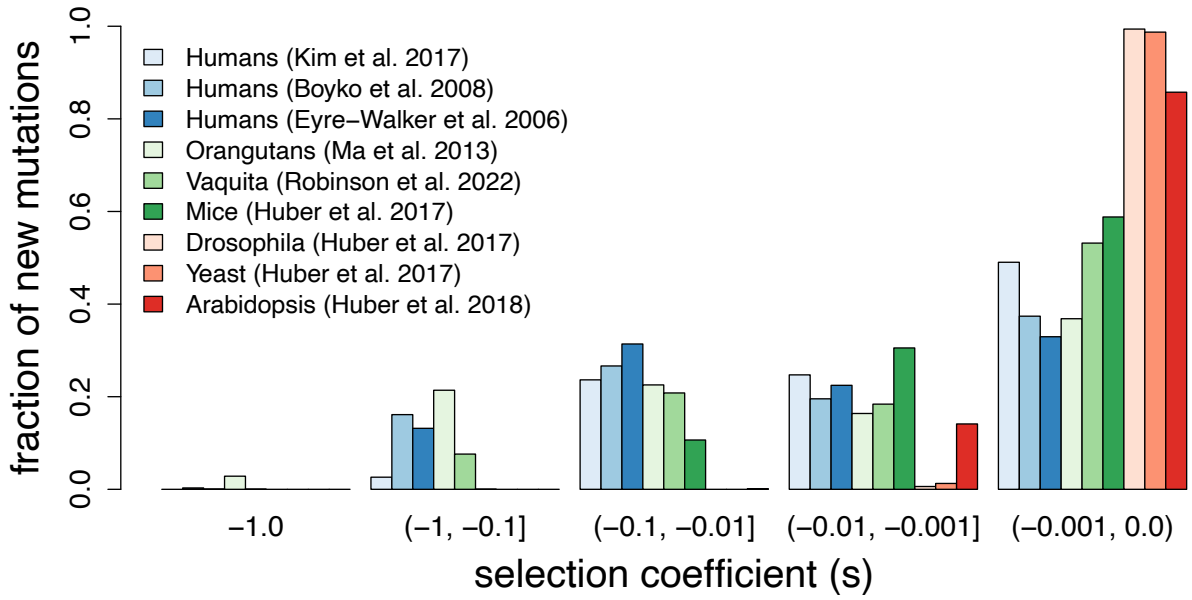

Figure 4.1. Representative estimates of the distribution of fitness effects from sequence-based approaches. Distributions are plotted in discrete bins of weakly deleterious (s >= -0.001), moderately deleterious (-0.001 > s >= -0.01), strongly deleterious (-0.01 > s >= -0.1), semi-lethal (-0.1 > s > -1) and lethal (s = -1.0) mutations. DFEs estimated for humans are colored in shades of blue, DFEs for non-human mammals are in shades of green, and non-mammalian DFEs are in shades of red. Note the higher fraction of weakly deleterious mutations in non-mammalian DFEs.

Figure 4.2

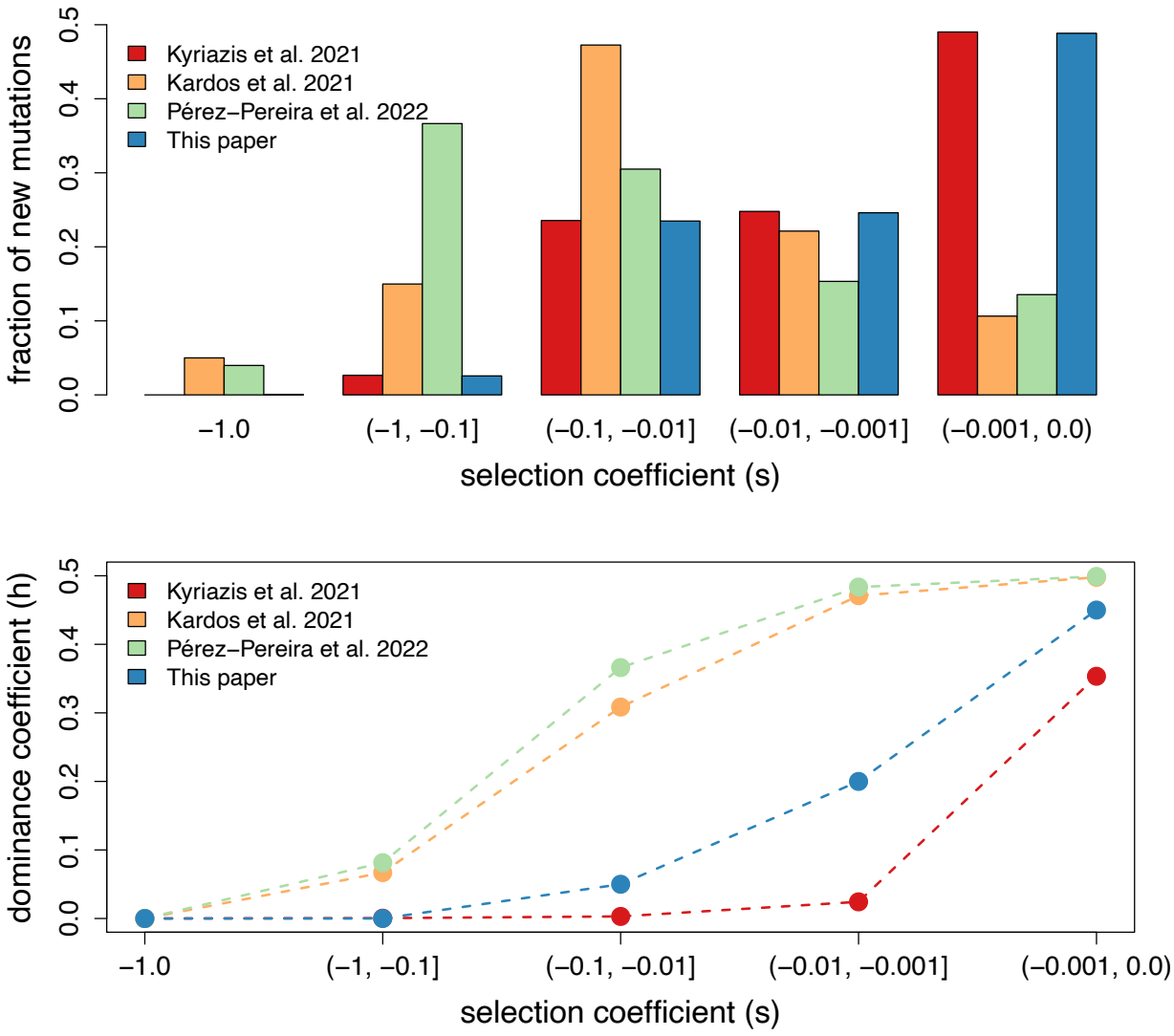

Figure 4.2. Comparison of DFE and dominance models employed by Kyriazis et al. 2021, Kardos et al. 2021, Pérez-Pereira et al. 2022, as well as our 'preferred model; informed on the analysis of Cavassim & Lohmueller, in prep and Wade et al. 2022. Distributions of h and s are plotted in discrete bins of weakly deleterious (s >= -0.001), moderately deleterious (-0.001 > s >= -0.01), strongly deleterious (-0.01 > s >= -0.1), semi-lethal (-0.1 > s > -1) and lethal (s = -1.0) mutations. Note that our preferred model includes 0.3% of mutations being recessive lethal based on results from Wade et al. 2022.

Figure 4.3

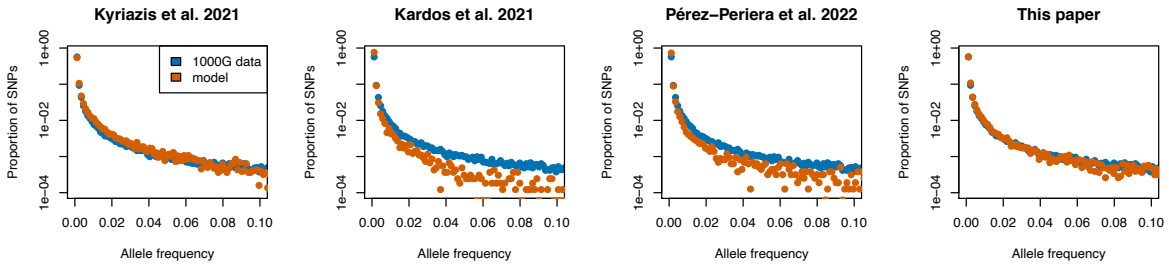

Figure 4.3. Predicted proportional nonsynonymous SFS from various DFE and dominance models compared to SFS from 1000G data plotted on a log scale. Predicted nonsynonymous SFS derived from simulations of ~8.1 Mb of coding sequence under a human demographic model inferred using the synonymous SFS from the same 1000G dataset. Note that the predicted SFS from the Kyriazis et al. 2021 model and the model proposed in this paper fit the 1000G data well, whereas the predicted SFSs from the Pérez-Pereira et al. 2022 and Kardos et al. 2021 models are greatly shifted towards rare alleles due to the overabundance of strongly deleterious variation in these models. Also note that many entries of the Perez-Pereira et al. 2022 and Kardos et al. 2021 SFSs about allele frequency 5% are 0 and are therefore omitted due to log scaling. See Figure S3 for plots of simulated vs empirical synonymous SFSs and Table S4-1 for proportion of singletons and common variants predicted by each model.

Figure 4.4

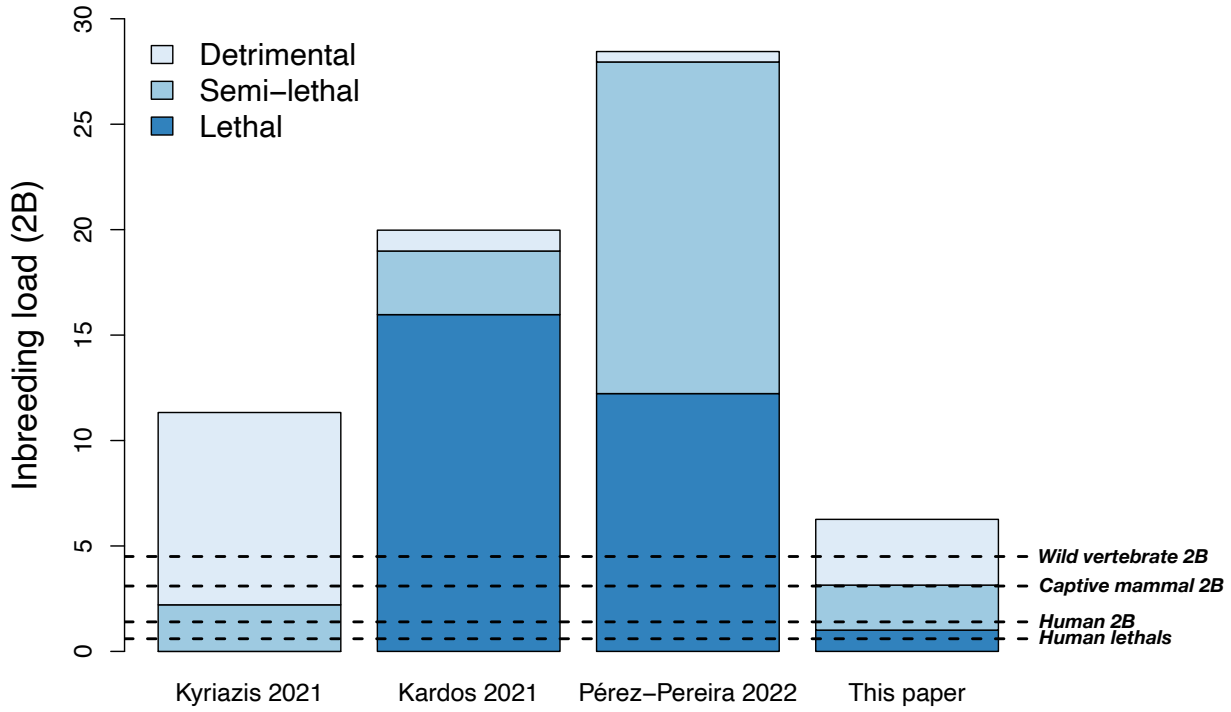

Figure 4.4. Inbreeding load partitioning under various DFE and dominance models using demographic and genomic parameters for humans. Colors depict contribution of inbreeding load from each class of deleterious mutations, with the total height of each bar representing the total predicted inbreeding load (2B). Detrimentals are here defined as mutations with $s > -0.1$, semi-lethals as mutations with $-0.99 < s <= -0.1$, and lethals as mutations with $s < -0.99$. Dashed lines show estimated of number of lethals per diploid human from Gao et al 2015 ("human lethals"), inbreeding load estimate for humans from Bittles & Neel 1994 ("human 2B"), and estimate of average inbreeding load for vertebrates from Nietlisbach et al. 2018 ("vertebrate 2B"). Note that predicted inbreeding load partitioning under the model proposed in this paper agrees well with empirical estimates, whereas predicted inbreeding load partitioning from other models do not.

All displayed models assume a genomic deleterious mutation rate of U=0.63; see Figure S4-5 for results under differing mutation rates.

References

Adrion, J. R., C. B. Cole, N. Dukler, J. G. Galloway, A. L. Gladstein, G. Gower, C. C. Kyriazis, A. P. Ragsdale, G. Tsambos, F. Baumdicker, J. Carlson, R. A. Cartwright, A. Durvasula, I. Gronau, B. Y. Kim, P. McKenzie, P. W. Messer, E. Noskova, D. O.-D. Vecchyo, F. Racimo, T. Struck, S. Gravel, R. N. Gutenkunst, K. E. Lohmueller, P. L. Ralph, D. R. Schrider, A. Siepel, J. Kelleher, and A. D. Kern. 2020a. A community-maintained standard library of population genetic models. Elife 9:e54967.

Adrion, J. R., J. G. Galloway, and A. D. Kern. 2020b. Predicting the landscape of recombination using deep learning. Mol. Biol. Evol. 37:1790–1808.

Agrawal, A. F., and M. C. Whitlock. 2011. Inferences about the distribution of dominance drawn from yeast gene knockout data. Genetics 187:553–566.

Agrawal, A. F., and M. C. Whitlock. 2012. Mutation Load: The Fitness of Individuals in Populations Where Deleterious Alleles Are Abundant. Annu. Rev. Ecol. Evol. Syst. 43:115–135.

Akey, J. M., M. A. Eberle, M. J. Rieder, C. S. Carlson, M. D. Shriver, D. A. Nickerson, and L. Kruglyak. 2004. Population history and natural selection shape patterns of genetic variation in 132 genes. PLoS Biol. 2.

Arunkumar, R., R. W. Ness, S. I. Wright, and S. C. H. Barrett. 2015. The evolution of selfing is accompanied by reduced efficacy of selection and purging of deleterious mutations. Genetics 199:817–829.

Auton, A., G. R. Abecasis, D. M. Altshuler, R. M. Durbin, D. R. Bentley, A. Chakravarti, A. G. Clark, P. Donnelly, E. E. Eichler, P. Flicek, S. B. Gabriel, R. A. Gibbs, E. D. Green, M. E. Hurles, B. M. Knoppers, J. O. Korbel, E. S. Lander, C. Lee, H. Lehrach, E. R. Mardis, G. T.

Marth, G. A. McVean, D. A. Nickerson, J. P. Schmidt, S. T. Sherry, J. Wang, R. K. Wilson, E. Boerwinkle, H. Doddapaneni, Y. Han, V. Korchina, C. Kovar, S. Lee, D. Muzny, J. G. Reid, Y. Zhu, Y. Chang, Q. Feng, X. Fang, X. Guo, M. Jian, H. Jiang, X. Jin, T. Lan, G. Li, J. Li, Y. Li, S. Liu, X. Liu, Y. Lu, X. Ma, M. Tang, B. Wang, G. Wang, H. Wu, R. Wu, X. Xu, Y. Yin, D. Zhang, W. Zhang, J. Zhao, M. Zhao, X. Zheng, N. Gupta, N. Gharani, L. H. Toji, N. P. Gerry, A. M. Resch, J. Barker, L. Clarke, L. Gil, S. E. Hunt, G. Kelman, E. Kulesha, R. Leinonen, W. M. McLaren, R. Radhakrishnan, A. Roa, D. Smirnov, R. E. Smith, I. Streeter, A. Thormann, I. Toneva, B. Vaughan, X. Zheng-Bradley, R. Grocock, S. Humphray, T. James, Z. Kingsbury, R. Sudbrak, M. W. Albrecht, V. S. Amstislavskiy, T. A. Borodina, M. Lienhard, F. Mertes, M. Sultan, B. Timmermann, M. L. Yaspo, L. Fulton, V. Ananiev, Z. Belaia, D. Beloslyudtsev, N. Bouk, C. Chen, D. Church, R. Cohen, C. Cook, J. Garner, T. Hefferon, M. Kimelman, C. Liu, J. Lopez, P. Meric, C. O'Sullivan, Y. Ostapchuk, L. Phan, S. Ponomarov, V. Schneider, E. Shekhtman, K. Sirotkin, D. Slotta, H. Zhang, S. Balasubramaniam, J. Burton, P. Danecek, T. M. Keane, A. Kolb-Kokocinski, S. McCarthy, J. Stalker, M. Quail, C. J. Davies, J. Gollub, T. Webster, B. Wong, Y. Zhan, C. L. Campbell, Y. Kong, A. Marcketta, F. Yu, L. Antunes, M. Bainbridge, A. Sabo, Z. Huang, L. J. M. Coin, L. Fang, Q. Li, Z. Li, H. Lin, B. Liu, R. Luo, H. Shao, Y. Xie, C. Ye, C. Yu, F. Zhang, H. Zheng, H. Zhu, C. Alkan, E. Dal, F. Kahveci, E. P. Garrison, D. Kural, W. P. Lee, W. F. Leong, M. Stromberg, A. N. Ward, J. Wu, M. Zhang, M. J. Daly, M. A. DePristo, R. E. Handsaker, E. Banks, G. Bhatia, G. Del Angel, G. Genovese, H. Li, S. Kashin, S. A. McCarroll, J. C. Nemesh, R. E. Poplin, S. C. Yoon, J. Lihm, V. Makarov, S. Gottipati, A. Keinan, J. L. Rodriguez-Flores, T. Rausch, M. H. Fritz, A. M. Stütz, K. Beal, A. Datta, J. Herrero, G. R. S. Ritchie, D. Zerbino, P. C. Sabeti, I. Shlyakhter, S. F.

Schaffner, J. Vitti, D. N. Cooper, E. V. Ball, P. D. Stenson, B. Barnes, M. Bauer, R. K. Cheetham, A. Cox, M. Eberle, S. Kahn, L. Murray, J. Peden, R. Shaw, E. E. Kenny, M. A. Batzer, M. K. Konkel, J. A. Walker, D. G. MacArthur, M. Lek, R. Herwig, L. Ding, D. C. Koboldt, D. Larson, K. Ye, S. Gravel, A. Swaroop, E. Chew, T. Lappalainen, Y. Erlich, M. Gymrek, T. F. Willems, J. T. Simpson, M. D. Shriver, J. A. Rosenfeld, C. D. Bustamante, S. B. Montgomery, F. M. De La Vega, J. K. Byrnes, A. W. Carroll, M. K. DeGorter, P. Lacroute, B. K. Maples, A. R. Martin, A. Moreno-Estrada, S. S. Shringarpure, F. Zakharia, E. Halperin, Y. Baran, E. Cerveira, J. Hwang, A. Malhotra, D. Plewczynski, K. Radew, M. Romanovitch, C. Zhang, F. C. L. Hyland, D. W. Craig, A. Christoforides, N. Homer, T. Izatt, A. A. Kurdoglu, S. A. Sinari, K. Squire, C. Xiao, J. Sebat, D. Antaki, M. Gujral, A. Noor, K. Ye, E. G. Burchard, R. D. Hernandez, C. R. Gignoux, D. Haussler, S. J. Katzman, W. J. Kent, B. Howie, A. Ruiz-Linares, E. T. Dermitzakis, S. E. Devine, H. M. Kang, J. M. Kidd, T. Blackwell, S. Caron, W. Chen, S. Emery, L. Fritsche, C. Fuchsberger, G. Jun, B. Li, R. Lyons, C. Scheller, C. Sidore, S. Song, E. Sliwerska, D. Taliun, A. Tan, R. Welch, M. K. Wing, X. Zhan, P. Awadalla, A. Hodgkinson, Y. Li, X. Shi, A. Quitadamo, G. Lunter, J. L. Marchini, S. Myers, C. Churchhouse, O. Delaneau, A. Gupta-Hinch, W. Kretzschmar, Z. Iqbal, I. Mathieson, A. Menelaou, A. Rimmer, D. K. Xifara, T. K. Oleksyk, Y. Fu, X. Liu, M. Xiong, L. Jorde, D. Witherspoon, J. Xing, B. L. Browning, S. R. Browning, F. Hormozdiari, P. H. Sudmant, E. Khurana, C. Tyler-Smith, C. A. Albers, Q. Ayub, Y. Chen, V. Colonna, L. Jostins, K. Walter, Y. Xue, M. B. Gerstein, A. Abyzov, S. Balasubramanian, J. Chen, D. Clarke, Y. Fu, A. O. Harmanci, M. Jin, D. Lee, J. Liu, X. J. Mu, J. Zhang, Y. Zhang, C. Hartl, K. Shakir, J. Degenhardt, S. Meiers, B. Raeder, F. P. Casale, O. Stegle, E. W. Lameijer, I. Hall, V. Bafna, J. Michaelson, E. J. Gardner, R. E. Mills, G. Dayama, K.

Chen, X. Fan, Z. Chong, T. Chen, M. J. Chaisson, J. Huddleston, M. Malig, B. J. Nelson, N. F. Parrish, B. Blackburne, S. J. Lindsay, Z. Ning, Y. Zhang, H. Lam, C. Sisu, D. Challis, U. S. Evani, J. Lu, U. Nagaswamy, J. Yu, W. Li, L. Habegger, H. Yu, F. Cunningham, I. Dunham, K. Lage, J. B. Jespersen, H. Horn, D. Kim, R. Desalle, A. Narechania, M. A. W. Sayres, F. L. Mendez, G. D. Poznik, P. A. Underhill, D. Mittelman, R. Banerjee, M. Cerezo, T. W. Fitzgerald, S. Louzada, A. Massaia, F. Yang, D. Kalra, W. Hale, X. Dan, K. C. Barnes, C. Beiswanger, H. Cai, H. Cao, B. Henn, D. Jones, J. S. Kaye, A. Kent, A. Kerasidou, R. Mathias, P. N. Ossorio, M. Parker, C. N. Rotimi, C. D. Royal, K. Sandoval, Y. Su, Z. Tian, S. Tishkoff, M. Via, Y. Wang, H. Yang, L. Yang, J. Zhu, W. Bodmer, G. Bedoya, Z. Cai, Y. Gao, J. Chu, L. Peltonen, A. Garcia-Montero, A. Orfao, J. Dutil, J. C. Martinez-Cruzado, R. A. Mathias, A. Hennis, H. Watson, C. McKenzie, F. Qadri, R. LaRocque, X. Deng, D. Asogun, O. Folarin, C. Happi, O. Omoniwa, M. Stremlau, R. Tariyal, M. Jallow, F. S. Joof, T. Corrah, K. Rockett, D. Kwiatkowski, J. Kooner, T. T. Hien, S. J. Dunstan, N. ThuyHang, R. Fonnie, R. Garry, L. Kanneh, L. Moses, J. Schieffelin, D. S. Grant, C. Gallo, G. Poletti, D. Saleheen, A. Rasheed, L. D. Brooks, A. L. Felsenfeld, J. E. McEwen, Y. Vaydylevich, A. Duncanson, M. Dunn, and J. A. Schloss. 2015. A global reference for human genetic variation. Nature 526:68–74.

Barroso, G. V., N. Puzović, and J. Y. Dutheil. 2019. Inference of recombination maps from a single pair of genomes and its application to ancient samples. PLoS Genet. 15:1–21.

Beichman, A. C., E. Huerta-Sanchez, and K. E. Lohmueller. 2018. Using Genomic Data to Infer Historic Population Dynamics. Annu. Rev. Ecol. Evol. Syst. 49:433–456.

Beichman, A. C., P. Kalhori, C. C. Kyriazis, A. A. DeVries, S. Nigenda-Morales, G. Heckel, Y. Schramm, A. Moreno-Estrada, D. J. Kennett, M. Hylkema, J. Bodkin, K. Koepfli, K. E.

Lohmueller, and R. K. Wayne. 2022. Genomic analyses reveal range-wide devastation of sea otter populations. Mol. Ecol. 1–18.

Beissinger, S. R., and M. I. Westphal. 1998. On the Use of Demographic Models of Population Viability in Endangered Species Management. J. Wildl. Manage. 62:821–841.

Bertorelle, G., F. Raffini, M. Bosse, C. Bortoluzzi, A. Iannucci, E. Trucchi, H. E. Morales, and C. van Oosterhout. 2022. Genetic load: genomic estimates and applications in non-model animals. Nat. Rev. Genet., doi: 10.1038/s41576-022-00448-x.

Bittles, A. H., and J. V. Neel. 1994. The costs of human inbreeding and their implications for variations at the DNA level. Nat. Genet. 8:117–121.

Boyko, A. R., S. H. Williamson, A. R. Indap, J. D. Degenhardt, R. D. Hernandez, K. E. Lohmueller, M. D. Adams, S. Schmidt, J. J. Sninsky, S. R. Sunyaev, T. J. White, R. Nielsen, A. G. Clark, and C. D. Bustamante. 2008. Assessing the evolutionary impact of amino acid mutations in the human genome. PLoS Genet. 4.

Brook, B. W., J. J. O'Grady, A. P. Chapman, M. A. Burgman, H. Resit Akçakaya, and R. Frankham. 2000. Predictive accuracy of population viability analysis in conservation biology. Nature 404:385–387.

Caballero, A., and P. D. Keightley. 1994. A pleiotropic nonadditive model of variation in quantitative traits. Genetics 138:883–900.

Castellano, D., M. C. Macià, P. Tataru, T. Bataillon, and K. Munch. 2019. Comparison of the full distribution of fitness effects of new amino acid mutations across great apes. Genetics 213:953–966.

Charlesworth, B. 1994. Evolution in age-structured populations. Cambridge University Press.

Charlesworth, D., and J. H. Willis. 2009. The genetics of inbreeding depression. Nat. Rev.

Genet. 10:783–796.

Chen, J., S. Glémin, and M. Lascoux. 2017. Genetic diversity and the efficacy of purifying selection across plant and animal species. Mol. Biol. Evol. 34:1417–1428.

Choi, Y., G. E. Sims, S. Murphy, J. R. Miller, and A. P. Chan. 2012. Predicting the Functional Effect of Amino Acid Substitutions and Indels. PLoS One 7.

Cingolani, P., A. Platts, L. L. Wang, M. Coon, T. Nguyen, L. Wang, S. J. Land, X. Lu, and D. M. Ruden. 2012. A program for annotating and predicting the effects of single nucleotide polymorphisms, SnpEff. Fly (Austin). 6:80–92.

Clark, D. W., and et al. 2019. Associations of autozygosity with a broad range of human phenotypes. Nat. Commun. 10:1–17.

Cooper, G. M., and J. Shendure. 2011. Needles in stacks of needles: Finding disease-causal variants in a wealth of genomic data. Nat. Rev. Genet. 12:628–640. Nature Publishing Group.

Cooper, G. M., E. A. Stone, G. Asimenos, E. D. Green, S. Batzoglou, and A. Sidow. 2005. Distribution and intensity of constraint in mammalian genomic sequence. Genome Res. 15:901–913.

Cotto, O., M. Schmid, and F. Guillaume. 2020. Nemo-age: spatially explicit simulations of eco-evolutionary dynamics in stage-structured populations under changing environments. Methods Ecol. Evol. 2020:1–10.

Cotto, O., J. Wessely, D. Georges, G. Klonner, M. Schmid, S. Dullinger, W. Thuiller, and F. Guillaume. 2017. A dynamic eco-evolutionary model predicts slow response of alpine plants to climate warming. Nat. Commun. 8.

Davies, E. K., A. D. Peters, and P. D. Keightley. 1999. High frequency of cryptic deleterious

mutations in Caenorhabditis elegans. Science (80-.). 285:1748–1751.

Díez-del-Molino, D., F. Sánchez-Barreiro, I. Barnes, M. T. P. Gilbert, and L. Dalén. 2018. Quantifying Temporal Genomic Erosion in Endangered Species. Trends Ecol. Evol. xx:1–10. Elsevier Ltd.

Dukler, N., M. R. Mughal, R. Ramani, Y.-F. Huang, and A. Siepel. 2022. Extreme purifying selection against point mutations in the human genome. Nat. Commun. 13:1–12. Springer US.

Dussex, N., T. van der Valk, H. E. Morales, C. W. Wheat, D. Díez-del-Molino, J. von Seth, Y. Foster, V. E. Kutschera, K. Guschanski, A. Rhie, A. M. Phillippy, J. Korlach, K. Howe, W. Chow, S. Pelan, J. D. Mendes Damas, H. A. Lewin, A. R. Hastie, G. Formenti, O. Fedrigo, J. Guhlin, T. W. R. Harrop, M. F. Le Lec, P. K. Dearden, L. Haggerty, F. J. Martin, V. Kodali, F. Thibaud-Nissen, D. Iorns, M. Knapp, N. J. Gemmell, F. Robertson, R. Moorhouse, A. Digby, D. Eason, D. Vercoe, J. Howard, E. D. Jarvis, B. C. Robertson, and L. Dalén. 2021. Population genomics of the critically endangered kākāpō. Cell Genomics 100002.

Eyre-Walker, A., and P. D. Keightley. 2007. The distribution of fitness effects of new mutations. Nat. Rev. Genet. 8:610–618.

Eyre-Walker, A., M. Woolfit, and T. Phelps. 2006. The Distribution of Fitness Effects of New Deleterious Amino Acid Mutations in Humans. Genetics 173:891–900.

Fu, W., R. M. Gittelman, M. J. Bamshad, and J. M. Akey. 2014. Characteristics of neutral and deleterious protein-coding variation among individuals and populations. Am. J. Hum. Genet. 95:421–436. The American Society of Human Genetics.

Gao, Z., D. Waggoner, M. Stephens, C. Ober, and M. Przeworski. 2015. An estimate of the

average number of recessive lethal mutations carried by humans. Genetics 199:1243–1254.

Gibson, A. K. 2022. Genetic diversity and disease: The past, present, and future of an old idea. Evolution (N. Y). 76:20–36.

Grossen, C., F. Guillaume, L. F. Keller, and D. Croll. 2020. Purging of highly deleterious mutations through severe bottlenecks in Alpine ibex. Nat. Commun. 11:1001. Springer US.

Grummer, J. A., T. R. Booker, R. Matthey-Doret, P. Nietlisbach, A. T. Thomaz, and M. C. Whitlock. 2022. The immediate costs and long-term benefits of assisted gene flow in large populations. Conserv. Biol. 1–11.

Guillaume, F., and J. Rougemont. 2006. Nemo: An evolutionary and population genetics programming framework. Bioinformatics 22:2556–2557.

Haldane, J. 1937. The effect of variation on fitness. Am. Nat. 71:337–349.

Haller, B. C., and P. W. Messer. 2016. SLiM 2: Flexible, interactive forward genetic simulations. Mol. Biol. Evol. 34:230–240.

Haller, B. C., and P. W. Messer. 2019. SLiM 3: Forward Genetic Simulations Beyond the Wright–Fisher Model. Mol. Biol. Evol. 36:632–637.

Halligan, D. L., and P. D. Keightley. 2009. Spontaneous mutation accumulation studies in evolutionary genetics. Annu. Rev. Ecol. Evol. Syst. 40:151–172.

Harris, K., and R. Nielsen. 2016. The genetic cost of neanderthal introgression. Genetics 203:881–891.

Hedrick, P. W. 2002. Lethals in Finite Populations. Evolution (N. Y). 56:654–657.

Hedrick, P. W. 2012. What is the evidence for heterozygote advantage selection? Trends Ecol. Evol. 27:698–704. Elsevier Ltd.

Hedrick, P. W., and A. Garcia-Dorado. 2016. Understanding Inbreeding Depression, Purging,

and Genetic Rescue. Trends Ecol. Evol. 31:940–952. Elsevier Ltd.

Henn, B. M., L. R. Botigué, C. D. Bustamante, A. G. Clark, and S. Gravel. 2015. Estimating the mutation load in human genomes. Nat. Rev. Genet. 16:333–343. Nature Publishing Group.

Henn, B. M., L. R. Botigué, S. Peischl, I. Dupanloup, M. Lipatov, B. K. Maples, A. R. Martin, S. Musharoff, H. Cann, M. P. Snyder, L. Excoffier, J. M. Kidd, and C. D. Bustamante. 2016. Distance from sub-Saharan Africa predicts mutational load in diverse human genomes. Proc. Natl. Acad. Sci. 113:E440–E449.

Hoban, S., G. Bertorelle, and O. E. Gaggiotti. 2012. Computer simulations: Tools for population and evolutionary genetics. Nat. Rev. Genet. 13:110–122. Nature Publishing Group.

Huber, C. D., A. Durvasula, and A. M. Hancock. 2018. Gene expression drives the evolution of dominance. Nat. Commun. 9:1–11. Springer US.

Huber, C. D., B. Y. Kim, and K. E. Lohmueller. 2020. Population genetic models of GERP scores suggest pervasive turnover of constrained sites across mammalian evolution. PLoS Genet. 16:1–26.

Huber, C. D., B. Y. Kim, C. D. Marsden, and K. E. Lohmueller. 2017. Determining the factors driving selective effects of new nonsynonymous mutations. Proc. Natl. Acad. Sci. 114:4465–4470.

Jones, M. R., L. Scott Mills, J. D. Jensen, and J. M. Good. 2020. The origin and spread of locally adaptive seasonal camouflage in snowshoe hares. Am. Nat. 196:316–332.

Kalinowski, S. T., and P. W. Hedrick. 1999. Detecting inbreeding depression is difficult in captive endangered species. Anim. Conserv. 2:131–136.

Kardos, M., E. E. Armstrong, S. W. Fitzpatrick, S. Hauser, P. W. Hedrick, J. M. Miller, D. A. Tallmon, and W. Chris Funk. 2021. The crucial role of genome-wide genetic variation in

conservation. Proc. Natl. Acad. Sci. U. S. A. 118:1–10.

Kardos, M., H. R. Taylor, H. Ellegren, G. Luikart, and F. W. Allendorf. 2016. Genomics advances the study of inbreeding depression in the wild. Evol. Appl. 9:1205–1218.

Keller, L., and D. M. Waller. 2002. Inbreeding effects in wild populations. Trends Ecol. Evol. 17:19–23.

Kim, B. Y., C. D. Huber, and K. E. Lohmueller. 2017. Inference of the Distribution of Selection Coefficients for New Nonsynonymous Mutations Using Large Samples. Genetics 206:345–361.

Kircher, M., D. M. Witten, P. Jain, B. J. O'roak, G. M. Cooper, and J. Shendure. 2014. A general framework for estimating the relative pathogenicity of human genetic variants. Nat. Genet. 46:310–315. Nature Publishing Group.

Kruglyak, L., A. Beyer, J. S. Bloom, J. Grossbach, D. Tami, C. P. Mancuso, M. S. Rich, G. Sherlock, E. Van, and C. D. Kaplan. 2022. No evidence that synonymous mutations in yeast genes are mostly deleterious. bioRxiv 1–11.

Kumar, P., S. Henikoff, and P. C. Ng. 2009. Predicting the effects of coding non-synonymous variants on protein function using the SIFT algorithm. Nat. Protoc. 4:1073–1082.

Kutschera, V. E., J. W. Poelstra, F. Botero-Castro, N. Dussex, N. J. Gemmell, G. R. Hunt, M. G. Ritchie, C. Rutz, R. A. W. Wiberg, and J. B. W. Wolf. 2020. Purifying Selection in Corvids Is Less Efficient on Islands. Mol. Biol. Evol. 37:469–474.

Kyriazis, C. C., A. C. Beichman, K. E. Brzeski, S. R. Hoy, R. O. Peterson, J. A. Vucetich, L. M. Vucetich, K. E. Lohmueller, and R. K. Wayne. 2022. Genomic underpinnings of population persistence in Isle Royale moose. bioRxiv 1–33.

Kyriazis, C. C., R. K. Wayne, and K. E. Lohmueller. 2021. Strongly deleterious mutations are a

primary determinant of extinction risk due to inbreeding depression. Evol. Lett. 5:33–47.

Lacy, R. C. 2019. Lessons from 30 years of population viability analysis of wildlife populations. Zoo Biol. 38:67–77.

Lacy, R. C. 2000. Structure of the VORTEX simulation model for population viability analysis. Ecol. Bull. 48:191–203.

Lacy, R. C. 1993. Vortex Computer Simulation Model for Population Viability Analysis. Wildl. Res. 20:45–65.

Lynch, M., M. S. Ackerman, J. F. Gout, H. Long, W. Sung, W. K. Thomas, and P. L. Foster. 2016. Genetic drift, selection and the evolution of the mutation rate. Nat. Rev. Genet. 17:704–714. Nature Publishing Group.

Lynch, M., I. J. Conery, and R. Burger. 1995a. Mutation accumulation and the extinction of small populations. Am. Nat. 146:489–518.

Lynch, M., J. Conery, and R. Burger. 1995b. Mutational Meltdowns in Sexual Populations. Evolution (N. Y). 49:1067–1080.

Ma, X., J. L. Kelley, K. Eilertson, S. Musharoff, J. D. Degenhardt, A. L. Martins, T. Vinar, C. Kosiol, A. Siepel, R. N. Gutenkunst, and C. D. Bustamante. 2013. Population Genomic Analysis Reveals a Rich Speciation and Demographic History of Orang-utans (Pongo pygmaeus and Pongo abelii). PLoS One 8.

Marjoram, P., and P. Donnelly. 1994. Pairwise comparisons of mitochondrial DNA sequences in subdivided populations and implications for early human evolution. Genetics 136:673–683.

Marsden, C. D., D. Ortega-Del Vecchyo, D. P. O'Brien, J. F. Taylor, O. Ramirez, C. Vilà, T. Marques-Bonet, R. D. Schnabel, R. K. Wayne, and K. E. Lohmueller. 2016. Bottlenecks and selective sweeps during domestication have increased deleterious genetic variation in

dogs. Proc. Natl. Acad. Sci. 113:152–157.

Mathur, S., and J. A. DeWoody. 2021. Genetic load has potential in large populations but is realized in small inbred populations. Evol. Appl. 14:1540–1557.

Matthey-Doret, R. 2021. SimBit: A high performance, flexible and easy-to-use population genetic simulator. Mol. Ecol. Resour. 21:1745–1754.

McCune, A. R., R. C. Fuller, A. A. Aquilina, R. M. Dawley, J. M. Fadool, D. Houle, J. Travis, and A. S. Kondrashov. 2002. A low genomic number of recessive lethals in natural populations of bluefin killifish and zebrafish. Science (80-.). 296:2398–2401.

Morton, N. E., J. F. Crow, and H. J. Muller. 1956. An Estimate of the Mutational Damage in Man From Data on Consanguineous Marriages. Proc. Natl. Acad. Sci. 42:855–863.

Mukai, T. 1964. The genetic structure of natural populations of Drosophila melanogaster. I. Spontaneous mutation rate of polygenes controlling viability. Genetics 50:1–19.

Muller, H. J. 1950. Our load of mutations. Am. J. Hum. Genet. 2:111–176.

Murphy, D., E. Elyashiv, G. Amster, and G. Sella. 2021. Broad-scale variation in human genetic diversity levels is predicted by purifying selection on coding and non-coding elements. bioRxiv 1–18.

Nei, M. 1968. The frequency distribution of lethal chromosomes in finite populations. Proc. Natl. Acad. Sci. 60:517–524.

Nietlisbach, P., S. Muff, J. M. Reid, M. C. Whitlock, and L. F. Keller. 2018. Nonequivalent lethal equivalents: Models and inbreeding metrics for unbiased estimation of inbreeding load. Evol. Appl. 1–14.

O'Grady, J. J., B. W. Brook, D. H. Reed, J. D. Ballou, D. W. Tonkyn, and R. Frankham. 2006. Realistic levels of inbreeding depression strongly affect extinction risk in wild populations.

Biol. Conserv. 133:42–51.

Oosterhout, C. Van. 2019. Mutation load is the spectre of species. Nat. Ecol. Evol. 16–18. Springer US.

Pérez-Pereira, N., A. Caballero, and A. García-Dorado. 2022. Reviewing the consequences of genetic purging on the success of rescue programs. Conserv. Genet. 23:1–17. Springer Netherlands.

Pérez-Pereira, N., R. Pouso, A. Rus, A. Vilas, E. López-Cortegano, A. García-Dorado, H. Quesada, and A. Caballero. 2021. Long-term exhaustion of the inbreeding load in Drosophila melanogaster. Heredity (Edinb). 1–11. Springer US.

Pierson, J. C., S. R. Beissinger, J. G. Bragg, D. J. Coates, J. G. B. Oostermeijer, P. Sunnucks, N. H. Schumaker, M. V. Trotter, and A. G. Young. 2015. Incorporating evolutionary processes into population viability models. Conserv. Biol. 29:755–764.

Ragsdale, A. P., C. Moreau, and S. Gravel. 2018. Genomic inference using diffusion models and the allele frequency spectrum. Curr. Opin. Genet. Dev. 53:140–147. Elsevier Ltd.

Ralls, K., J. D. Ballou, A. Templeton, K. Ralls, and J. D. Ballou. 1988. Estimates of Lethal Equivalents and the Cost of Inbreeding in Mammals. Soc. Conserv. Biol. 2:185–193.

Ramachandran, S., O. Deshpande, C. C. Roseman, N. A. Rosenberg, M. W. Feldman, and L. L. Cavalli-Sforza. 2005. Support from the relationship of genetic and geographic in human populations for a serial founder effect originating in Africa. Proc. Natl. Acad. Sci. U. S. A. 102:15942–15947.

Robinson, J. A., C. Brown, B. Y. Kim, K. E. Lohmueller, and R. K. Wayne. 2018. Purging of Strongly Deleterious Mutations Explains Long-Term Persistence and Absence of Inbreeding Depression in Island Foxes. Curr. Biol. 28:3487-3494.e4. Elsevier Ltd.

Robinson, J. A., C. C. Kyriazis, S. F. Nigenda-Morales, A. C. Beichman, L. Rojas-Bracho, K. M. Robertson, M. C. Fontaine, R. K. Wayne, K. E. Lohmueller, B. L. Taylor, and P. A. Morin. 2022. The critically endangered vaquita is not doomed to extinction by inbreeding depression. Science (80-.). 639:635–639.

Robinson, J. A., J. Räikkönen, L. M. Vucetich, J. A. Vucetich, R. O. Peterson, K. E. Lohmueller, and R. K. Wayne. 2019. Genomic signatures of extensive inbreeding in Isle Royale wolves, a population on the threshold of extinction. Sci. Adv. 5:1–13.

Sandell, L., and N. P. Sharp. 2022. Fitness Effects of Mutations: An Assessment of PROVEAN Predictions Using Mutation Accumulation Data. Genome Biol. Evol. 14:1–15.

She, R., and D. F. Jarosz. 2018. Mapping Causal Variants with Single-Nucleotide Resolution Reveals Biochemical Drivers of Phenotypic Change. Cell 172:478-490.e15. Elsevier Inc.

Siepel, A., G. Bejerano, J. S. Pedersen, A. S. Hinrichs, M. Hou, K. Rosenbloom, H. Clawson, J. Spieth, L. D. W. Hillier, S. Richards, G. M. Weinstock, R. K. Wilson, R. A. Gibbs, W. J. Kent, W. Miller, and D. Haussler. 2005. Evolutionarily conserved elements in vertebrate, insect, worm, and yeast genomes. Genome Res. 15:1034–1050.

Simmons, M. J., and J. F. Crow. 1977. Mutations affecting fitness in Drosophila populations. Ann. Rev. Genet. 11:49–78.

Sletvold, N., M. Mousset, J. Hagenblad, B. Hansson, and J. Ågren. 2013. Strong inbreeding depression in two scandinavian populations of the self-incompatible perennial herb arabidopsis lyrata. Evolution (N. Y). 67:2876–2888.

Stoffel, M. A., S. E. Johnston, J. G. Pilkington, and J. M. Pemberton. 2021a. Genetic architecture and lifetime dynamics of inbreeding depression in a wild mammal. Nat. Commun. 12:1–10. Springer US.

Stoffel, M. A., S. E. Johnston, J. G. Pilkington, and J. M. Pemberton. 2021b. Mutation load decreases with haplotype age in wild Soay sheep. Evol. Lett. 5:187–195.

Swindell, W. R., and J. L. Bouzat. 2006. Reduced inbreeding depression due to historical inbreeding in Drosophila melanogaster: Evidence for purging. J. Evol. Biol. 19:1257–1264.

Takou, M., T. Hämälä, E. M. Koch, K. A. Steige, H. Dittberner, L. Yant, M. Genete, S. Sunyaev, V. Castric, X. Vekemans, O. Savolainen, and J. de Meaux. 2021. Maintenance of Adaptive Dynamics and No Detectable Load in a Range-Edge Outcrossing Plant Population. Mol. Biol. Evol., doi: 10.1093/molbev/msaa322.

Tataru, P., M. Mollion, S. Glémin, and T. Bataillon. 2017. Inference of Distribution of Fitness Effects and Proportion of Adaptive Substitutions from Polymorphism Data. Genetics 207:1103–1119.

Torgerson, D. G., A. R. Boyko, R. D. Hernandez, A. Indap, X. Hu, T. J. White, J. J. Sninsky, M. Cargill, M. D. Adams, C. D. Bustamante, and A. G. Clark. 2009. Evolutionary processes acting on candidate cis-regulatory regions in humans inferred from patterns of polymorphism and divergence. PLoS Genet. 5.

Uricchio, L. H., N. A. Zaitlen, C. J. Ye, J. S. Witte, and R. D. Hernandez. 2016. Selection and explosive growth alter genetic architecture and hamper the detection of causal rare variants. Genome Res. 26:863–873.

Van Der Valk, T., M. De Manuel, T. Marquez-Bonet, and K. Guschanski. 2019. Estimates of genetic load suggest extensive genetic purging in mammalian populations. bioRxiv.

Wade, E. E., C. C. Kyriazis, M. I. A. Cavassim, and K. E. Lohmueller. 2022. Quantifying the fraction of new mutations that are recessive lethal. bioRxiv 1–24.

Xie, H. X., X. X. Liang, Z. Q. Chen, W. M. Li, C. R. Mi, M. Li, Z. J. Wu, X. M. Zhou, and W.

G. Du. 2022. Ancient Demographics Determine the Effectiveness of Genetic Purging in Endangered Lizards. Mol. Biol. Evol. 39:1–14.